

**NOVEL ANALYTICAL APPROACHES IN THE DETERMINATION OF  
EMERGING CONTAMINANTS**

**MARYAM LASHGARI**

(M.Sc., Analytical Chemistry, Iran University of Science & Technology, Iran)

**A THESIS SUBMITTED  
FOR THE DEGREE OF DOCTOR OF PHILOSOPHY**

**DEPARTMENT OF CHEMISTRY  
NATIONAL UNIVERSITY OF SINGAPORE**

**2016**

## DECLARATION

I hereby declare that this thesis is my original work and it has been written by me in it's entirely. I have duly acknowledged all the sources of information which have been used in the thesis. This thesis has also not been submitted for any degree in any university previously.

Some contents of this thesis have been published in:

- [1] M. Lashgari, H.K. Lee, Micro-solid phase extraction of perfluorinated carboxylic acids from human plasma, Journal of Chromatography A, 1432 (2016), 7-16.
- [2] M. Lashgari, C. Basheer, H.K. Lee, Application of surfactant-templated ordered mesoporous material as sorbent in micro-solid phase extraction followed by liquid chromatography-triple quadrupole mass spectrometry for determination of perfluorinated carboxylic acids in aqueous media, Talanta, 141(2015) 200–206.
- [3] M. Lashgari, H.K. Lee, Determination of perfluorinated carboxylic acids in fish fillet by micro-solid phase extraction, followed by liquid chromatography–triple quadrupole mass spectrometry, Journal of Chromatography A, 1369 (2014) 26–32.

Maryam Lashgari

M. Lashgari  
27/02/2016

NOVEL ANALYTICAL APPROACHES IN THE DETERMINATION OF  
EMERGING CONTAMINANTS

**DEDICATED TO MY BELOVED PARENTS FOR THEIR ENDLESS LOVE  
THORUGH MY LIFE**

## ACKNOWLEDGEMENTS

Firstly, I would like to express my profound appreciation and sincere thanks to my supervisor, Professor Hian Kee Lee. I cordially confess that it was my great honor to do my PhD under supervision of such a respectful and knowledgeable personality. He taught me to be an independent researcher and have an exploring and patient attitude. He encouraged me to keep going with passion and persistence. Prof. Lee, thank you very much for your support, goal-oriented guidance, and encouragement. Thank you for being patient with me at every step.

I gratefully acknowledge the Agency for Science, Technology and Research (A\*STAR), for the “Singapore International Graduate Award (SINGA)”.

I profoundly thank the thesis committee for their insightful and constructive comments which greatly helped to improve my thesis.

During my PhD journey, I had a chance to conduct some part of my projects in the NUS-Environmental Research Institute (NERI). I would like to express my appreciation to the NERI’s staff especially Professor Ong Choon Nam, Mdm Frances Lim, Ms. Per Poh Geok, and Mr. Adam Tan for being so efficient and friendly, creating such a perfect and superlative research environment.

I also conducted some parts of my projects in the Shimadzu Asia Pacific Laboratory. I would like to sincerely thank their staff for their friendly help, especially Ms. Hui-Loo Lai Chin, and Ms. Cynthia Lahey for being welcoming all the time.

I would also like to thank my colleagues Hong Zhang, Guo Liang Guo, Yufeng Zhang, Dandan Ge, Seyed Mohammad Majedi, Ruyi Xu, Nyi Nyi Naing, Zhenzhen Huang, Claire Anne Taylor, Sheng Tang, and many other staff and laboratory technologists at the Department of Chemistry, for their kind help and assistance.

Heartfelt thanks to all my friends in Singapore. Doing a PhD in Singapore was an opportunity to build such priceless friendships that I am sure will stay forever. It was a great achievement indeed. Thank you for being with me at every step.

Last but not the least; I would like to express my profound and deepest thanks to my family for their unwavering love, and endless support. You always believed in me. You never let my faith fade away. I am richly blessed to have such a family. You always filled my life with happiness and joy with your pure love. Mom and Dad, my loveliest ones, you both truly are my heroes. You always worked hard to provide the best for your family. There are no words to express my sincere love to you. You are my inspiration, forever.

## TABLE OF CONTENTS

<b>ABSTRACT.....</b>	<b>xiii</b>
<b>LIST OF TABLES.....</b>	<b>xv</b>
<b>LIST OF FIGURES.....</b>	<b>xvii</b>
<b>LIST OF PUBLICATIONS.....</b>	<b>xix</b>
<b>NOMENCLATURE.....</b>	<b>xx</b>
<b>CHAPTER 1: Introduction.....</b>	<b>1</b>
1.1. Introduction .....	1
1.2. Emerging contaminants.....	1
1.3. Sample preparation.....	2
1.4. Microextraction based on sorbent enrichment.....	3
1.4.1. Micro-solid phase extraction ( $\mu$ -SPE) .....	4
1.4.2. Advantageous of $\mu$ -SPE.....	5
1.4.3. The role of the sorbent in $\mu$ -SPE.....	6
1.5. Nanoporous materials as sorbent.....	7
1.5.1. Ordered mesoporous silica (OMS) .....	9
1.5.2. Ordered mesoporous carbon (OMC) .....	12
1.5.3. Surface modification of OMC.....	14
1.6. Scope, significance, and structure of thesis.....	16
<b>CHAPTER 2: Introduction to perfluorinated compounds.....</b>	<b>19</b>

2.1.	Introduction.....	19
2.2.	Perfluorinated compounds (PFCs) .....	19
2.3.	Importance of the determination of PFCs.....	20
2.4.	Perfluorinated carboxylic acids (PFCAs) .....	20
2.5.	Challenges in the analysis of PFCs.....	21

**CHAPTER 3: Analysis and determination of perfluorinated carboxylic acids  
in water samples.....26**

3.1.	Introduction.....	26
3.2.	Experimental.....	26
3.2.1.	Chemicals and materials.....	26
3.2.2.	Synthesis of mesoporous silica.....	27
3.2.3.	Characterization of mesoporous materials.....	28
3.2.4.	Preparation of $\mu$ -SPE device.....	28
3.2.5.	Sample preparation and extraction procedure.....	28
3.2.6.	Instrumental analysis.....	29
3.2.7.	Control of the background contamination.....	31
3.3.	Results and discussion.....	32
3.3.1.	Characterization of CTAB-MCM-41 and MCM-41.....	32
3.3.2.	Extraction optimization.....	34
3.3.3.	Method validation.....	39



3.3.4. Analysis of real samples.....	41
3.3.5. Evaluation of matrix effects.....	42
3.4. Conclusion .....	43

**CHAPTER 4: Analysis and determination of perfluorinated carboxylic acids  
in human plasma .....45**

4.1. Introduction .....	45
4.2. Experimental.....	46
4.2.1. Chemicals and materials.....	46
4.2.2. Plasma sample collection.....	46
4.2.3. Synthesis of sorbent and extraction procedure.....	47
4.2.4. Instrumental analysis .....	47
4.2.5. RSM and data processing.....	48
4.3. Results and discussion.....	48
4.3.1. Optimization of extraction.....	48
4.3.2. Method validation.....	56
4.3.3. Analysis of real samples.....	57
4.4. Conclusion .....	58

**CHAPTER 5: Analysis and determination of perfluorinated carboxylic acids  
in fish fillet .....61**

5.1. Introduction .....	61
5.2. Experimental.....	61

5.2.1. Chemicals and materials.....	61
5.2.2. Sample collection.....	62
5.2.3. Synthesis and characterization of mesoporous silica.....	62
5.2.4. Sample preparation and extraction.....	62
5.2.5. Instrumental analysis.....	63
5.3. Results and discussion.....	64
5.3.1. Evaluation of the protective role of the membrane.....	64
5.3.2. Evaluation of extraction and concentration step.....	64
5.3.3. Method validation .....	65
5.3.4. Analysis of real samples.....	67
5.4. Conclusion.....	67
<b>CHAPTER 6: Introduction to N-nitrosamines.....</b>	<b>71</b>
6.1. Introduction .....	71
6.2. Definition and properties of N-nitrosamines.....	71
6.3. Toxicity of NAs.....	72
6.4. Sources of NAs in different environmental matrices.....	76
6.5. Regulatory responses to NAs.....	78
6.6. Analytical challenges faced in determination of NAs.....	80
6.7. Sorbents for extraction of NAs.....	81
6.8. Current gaps in the determination of NAs.....	82

**CHAPTER 7: Introducing surface-modified ordered mesoporous carbon as a promising sorbent for simultaneous extraction of N-nitrosamines.....85**

7.1. Introduction .....	85
7.2. Experimental.....	86
7.2.1. Safety considerations and pollution prevention.....	86
7.2.2. Chemicals and solutions.....	87
7.2.3. Preparation of the sorbents.....	88
7.2.4. Characterization of the sorbents.....	91
7.2.5. Evaluation of the adsorptive performance of the sorbents .....	92
7.2.6. Instrumental analysis.....	93
7.3. Results and discussion.....	94
7.3.1. Characterization of the sorbent.....	94
7.3.2. Evaluation of the extraction behaviour of sorbents.....	99
7.4. Conclusion.....	103

**CHAPTER 8: Analysis and determination of N-nitrosamines in wastewater and swimming pool water.....104**

8.1. Introduction.....	104
8.2. Experimental.....	104
8.2.1. Chemicals and solutions.....	104
8.2.2. Sample collection.....	105
8.2.3. Safety considerations and pollution prevention.....	106

8.2.4. Instrumental analysis.....	106
8.2.5. Identification and quantitation.....	107
8.2.6. Extraction procedure.....	109
8.2.7. Extraction optimization.....	110
8.3. Results and discussion.....	111
8.3.1. Optimization of the extraction.....	111
8.3.2. Study of the $\mu$ -SPE mechanism.....	114
8.3.3. Method validation.....	116
8.3.4. Analysis of the real samples.....	118
8.4. Conclusion.....	122

**CHAPTER 9: Analysis and determination of N-nitrosamines in beverages.....128**

9.1. Introduction.....	128
9.2. Experimental.....	129
9.2.1. Chemicals and materials.....	129
9.2.2. Instrumental analysis.....	129
9.2.3. Sample preparation and extraction.....	129
9.2.4. Effect of alcohol concentration on the extraction process.....	130
9.3. Results and discussion.....	130
9.3.1. Effect of ethanol concentration on the extraction process.....	130

9.3.2. Method validation.....	132
9.3.3. Analysis of real samples.....	135
9.4. Conclusion.....	137
<b>CHAPTER 10: Conclusions and future work.....</b>	<b>138</b>
<b>BIOBLOGHRAPHY.....</b>	<b>143</b>
<b>APPENDICES.....</b>	<b>152</b>
Appendix 1.....	152
Appendix 2.....	153
Appendix 3.....	154
Appendix 4.....	155
Appendix 5.....	156
Appendix 6.....	157
Appendix 7.....	161

## ABSTRACT

Over the past few decades, there have been a lot of efforts to address the immense challenge posed by emerging contaminants in different matrices. Many of these are ubiquitous, and are released as a consequence of different anthropogenic activities. They include a diverse group of chemicals such as pharmaceuticals, surfactants, disinfection byproducts (DBPs), personal care products (PCPs), perfluorinated compounds (PFCs), hormones, industrial additives and agents. These xenobiotic compounds may potentially be health hazards to the ecosystem; necessitates their monitoring and determination. However from an analytical point of view, there are two fundamental difficulties associated with the monitoring and determination of these compounds. First, most of the time these compounds are present in the complex matrices, and there are many factors and species which can interfere with their analysis. Second, the target analytes are usually found at trace levels in these samples. A combination of a powerful sample preparation method to isolate target analytes from the matrix, with a highly sensitive and reliable instrumental analysis compatible with target species, is thus highly important. In addition, the demand for routine monitoring of these compounds necessitates the development of easy-to-use, time- and cost-effective methodologies. Those methodologies must be safe and eco-friendly with minimal use of hazardous substances and waste materials generation. Considering all the above concerns, the work described in this thesis is designed and organized as given below: Two classes of emerging contaminants, perfluorinated carboxylic acids (PFCAs) as an important group of PFCs and N-nitrosamines (NAs) as an important group of DBPs are chosen.

Considering present challenges in the determination of PFCAs, simple, fast, and efficient approaches for the determination of PFCAs in water samples, human plasma, and fish fillet are reported. The methodologies are combination of micro-solid phase extraction ( $\mu$ -SPE) by use of ordered mesoporous silica, with liquid chromatography-triple quadrupole tandem mass spectrometry with negative ion electrospray ionization (LC-ESI-MS/MS).

As for NAs, since there are in a wide range of polarity and hydrophobicity/hydrophilicity, simultaneous extraction of NAs by conventional sorbents is challenging. Hence the current thesis introduces oxidative surface-modified ordered mesoporous carbon (OMC) as a promising sorbent used for successful extraction of eight NAs with different polarity and hydrophobicity/hydrophilicity. To the best of our knowledge, this is the first attempt to modify the surface chemistry of the carbonaceous sorbent to enhance the efficiency of the surface for both polar and non-polar NAs simultaneously. Subsequently, the sorbent is used in  $\mu$ -SPE followed by gas chromatography electron ionization triple quadrupole mass spectrometry (GC-EI-MS/MS) for analysis and determination of NAs from water samples and wide ranges of beverage.

## LIST OF TABLES

Table 2-1 List and characterization of PFCAs, have been chosen to study.....	21
Table 3-1 LC-MS/MS conditions for the analysis of PFCAs.....	30
Table 3-2 Experimental conditions of ESI-MS/MS.....	31
Table 3-3 Analytical parameters of the proposed method.....	41
Table 3-4 Analytical results for the determination of PFCAs.....	43
Table 4-1 Experimental conditions of negative ion ESI-MS/MS.....	47
Table 4-2 Experimental factors, levels, and design matrix .....	51
Table 4-3 ANOVA for CCD.....	52
Table 4-4 Coefficients of the regression equation .....	52
Table 4-5 Obtained figures of merit .....	56
Table 4-6 Performance of the analytical methods used to quantify PFCAs .....	59
Table 4-7 Determination of PFCAs in different plasma samples.....	60
Table 5-1 Analytes and optimized LC-MS/MS parameters.....	63
Table 5-2 Comparison of figures of merits in direct analysis, DSPE, and $\mu$ -SPE.....	65
Table 5-3 Validation parameters for the analytes.....	69
Table 5-4 Average relative recovery, standard deviation, and detected concentration of the analyte .....	69
Table 6-1 Properties of NAs (US EPA) .....	74
Table 7-1 GC-MS/MS analytical conditions.....	93
Table 7-2 Adsorption isotherm parameters for CMK-3 and O-CMK-3.....	98
Table 7-3 Name and the surface area of used carbonaceous sorbents.....	100
Table 8-1 Information on the analytes, standards and MS/MS optimized conditions.....	108
Table 8-2 Factors, their symbols and levels for CCD.....	112
Table 8-3 Design matrix (actual) with responses.....	112



Table 8-4 ANOVA for CCD.....	113
Table 8-5 Evaluation of the mechanism of the $\mu$ -SPE.....	115
Table 8-6 Instrumental quality parameters.....	117
Table 8-7 Method quality parameters.....	118
Table 8-8 Analytical parameters of NAs in swimming pool water samples.....	125
Table 8-9 Analytical parameters of NAs in wastewater samples.....	126
Table 9-1 Method quality parameters for analysis of NAs in beverages.....	134
Table 9-2 Detected concentration and spiked recovery of NAs in beverages.....	134

## LIST OF FIGURES

Figure 1-1 The $\mu$ -SPE bag.....	4
Figure 1-2 Schematic of LCT mechanism.....	10
Figure 1-3 Schematic of the hard template method for the synthesis of ordered mesoporous carbon (CMK-3) from SBA-15.....	14
Figure 1-4 Hexagonal pattern of CMK-3 with connecting bridges.....	14
Figure 1-5 Different carboxylic groups at the surface of the carbonaceous sorbents after oxidative treatment.....	16
Figure 3-1 Powder XRD patterns of (a) MCM-41, (b) CTAB-MCM-41, and (c) CTAB-MCM-41 after exposure to aqueous solution of PFCAs.....	33
Figure 3-2 FT-IR spectra of the CTAB-MCM-41 and MCM-41.....	34
Figure 3-3 Effect of sorbent type on $\mu$ -SPE.....	35
Figure 3-4 Influence of the different parameters on $\mu$ -SPE, (a): desorption solvent, (b): extraction time, (c): desorption time, (d): salt concentration.....	39
Figure 3-5 LC-ESI-MS/MS traces of rain water extracted by the developed method. (A) Unspiked rain water sample. (B) rain water sample spiked at 10 ngL <sup>-1</sup> . Peaks: (1) PFPA, (2) PFHpA, (3) PFOA, (4) PFNA, (5) PFDA.....	42
Figure 4-1 Influence of desorption solvent on $\mu$ -SPE.....	49
Figure 4-2 Linear effect of changing of the each variable on the extraction efficiency: (a) Extraction time, (b) desorption time, (c) salt concentration.....	54
Figure 4-3 3D response surfaces with contour plots of responses against different operating variables: (a) extraction time-desorption time, (b) extraction time-salt concentration, (c) salt concentration-desorption time.....	55
Figure 4-4 LC-ESI-MS/MS trace of plasma sample extracted by the developed method: (A) unspiked plasma sample, (B) plasma sample spiked at 3000 ngL <sup>-1</sup> . Peaks: (1) PFPA, (2) PFHpA, (3) PFOA, (4) PFNA, (5) PFDA, (6) PFDoDA.....	60
Figure 5-1 LC-ESI-MS/MS of analytes extracted from fish fillet by the developed method. (a) Unspiked sample, (b) sample spiked at 50 ng/ml. <sup>13</sup> C mass labelled PFOA ( <sup>13</sup> C8-PFOA) was used as internal standard.....	70
Figure 7-1 XRD pattern for O-CMK-3.....	94
Figure 7-2 FT-IR spectra of (a) CMK-3 and (b) O-CMK-3.....	95

Figure 7-3 Nitrogen adsorption desorption isotherm of (a) CMK-3, (b) O-CMK-3.....	97
Figure 7-4 Pore size distribution of CMK-3 and O-CMK-3.....	97
Figure 7-5 SEM images of (a) SBA-15, (B) CMK-3, and (C) O-CMK-3.....	99
Figure 7-6 Efficiency of the different carbonaceous sorbents in the extraction of NAs.	100
Figure 7-7 Increase in the hydrophilic character of a carbon surface as a consequence of the presence of oxygen-containing surface group.....	102
Figure 8-1 Effect of different solvents in desorption of the analytes in $\mu$ -SPE.....	111
Figure 8-2 GC-EI-MS/MS of analytes extracted from wastewater by the developed method: (1) Unspiked sample, (2) spiked sample at 100 ng/ml. $^{13}\text{H}$ mass labelled NDMA (NDMA-D6) was used as internal standard.....	127
Figure 9-1 Effect of the alcohol content in the sample media on the extraction process.....	131
Figure 9-2 GC-EI-MS/MS of analytes extracted from wine by the developed method. (1) Unspiked sample, (2) spiked sample at 100 ng/ml. $^2\text{H}$ mass labelled NDMA (NDMA-D6) was used as internal standard.....	136

## LIST OF PUBLICATIONS

1. M. Lashgari, H.K. Lee, Micro-solid phase extraction of perfluorinated carboxylic acids from human plasma, *Journal of Chromatography A*, 1432 (2016), 7-16.
2. M. Lashgari, C. Basheer, H.K. Lee, Application of surfactant-templated ordered mesoporous material as sorbent in micro-solid phase extraction followed by liquid chromatography-triple quadrupole mass spectrometry for determination of perfluorinated carboxylic acids in aqueous media, *Talanta*, 141 (2015) 200–206.
3. M. Lashgari, H.K. Lee, Determination of perfluorinated carboxylic acids in fish fillet by micro-solid phase extraction, followed by liquid chromatography–triple quadrupole mass spectrometry, *J. Chromatogr. A*, 1369 (2014) 26–32.
4. M. Lashgari, H.K. Lee, Introducing surface-modified ordered mesoporous carbon as a promising sorbent for extraction and concentration of N-nitrosamines, The 8<sup>th</sup> Singapore International Chemistry Conference, Singapore, 2014.
5. M. Lashgari, H.K. Lee, Application of mesoporous material as sorbent in micro-solid phase extraction, The 12<sup>th</sup> Asian Conference on Analytical Sciences, Japan, 2013.
6. M. Lashgari, H.K. Lee, Application of mesoporous material as sorbent in micro-solid phase extraction of perfluorinated compounds from aqueous media, The 7<sup>th</sup> Singapore International Chemical Conference, Singapore, 2012.

## NOMENCLATURE

APS	Ammonium Persulfate
ANOVA	Analysis Of Variance
BJH	Barrett–Joyner–Halenda
BET	Brunauer-Emmett-Teller
13C8-PFOA	Carbon mass isotopic label Perfluorooctanoic Acid
CCD	Central Composite Design
DEA	Diethylamine
DMA	Dimethylamine
DPA	Dipropylamine
DBPs	Disinfection By-Product
DSPE	Dispersive Solid Phase Extraction
ESI	Electrospray Interface
EHHA	Environmental Health Hazard Assessment
HCOOH	Formic Acid
FT-IR	Fourier Transform Infrared
GC-EI-MS/MS	Gas Chromatography Electron Ionization Tandem Mass Spectrometry
HAAs	Haloacetic Acids
HLB	Hydrophilic Lipophilic Balanced
NDMA-D6	Hydrogen mass isotopic label N-Nitrosodimethylamine
NPYR-D8	Hydrogen mass isotopic label N-Nitrosopyrrolidine
IMPs	Imprinted Molecular Polymers
IDL	Instrumental Detection Limit
IQL	Instrumental Quantification Limit
MAC	Interim Maximum Acceptable
IUPAC	International Union of Pure and Applied Chemistry
LOD	Limits Of Detection
LOQ	Limits Of Quantification
LC-MS/MS	Liquid Chromatography Tandem Mass Spectrometry
LCT	Liquid Crystal Template
LLE	Liquid Liquid Extraction
ME	Matrix Effect
MEPS	Microextraction in Packed Syringe
μ-SPE	Micro Solid Phase Extraction
MCM	Mobil Crystalline Material
MRM	Multiple Reaction Monitoring
DMS	N,N-dimethylsulfamide
NOM	Natural Organic Matter
NDEA	N-Nitrosodiethylamine
NDMA	N-Nitrosodimethylamine
NDBA	N-Nitroso-di-n-butylamine
NDPA	N-Nitroso-di-n-propylamine
NDPhA	N-Nitroso-di-phenylamine
NMOR	N-Nitrosomorpholine
NPIP	N-Nitrosopiperidine
NPYR	N-Nitrosopyrrolidine
CTAB-MCM-41	Non calcined MCM-41
ORS	Office of Research and Standards
OMEE	Ontario Ministry of Environmental and Energy
OMC	Ordered Mesoporous Carbon
OMS	Ordered Mesoporous Silica
PFCAs	Perfluorinated Carboxylic Acids
PFCs	Perfluorinated Compounds
PFDA	Perfluorodecanoic Acid
PFDoA	Perfluorododecanoic Acid
PFHpA	Perfluoroheptanoic Acid

PFH <sub>x</sub> A	Perfluorohexanoic Acid
PFNA	Perfluorononanoic Acid
PFOS	Perfluorooctanesulfonic Acid
PFOA	Perfluorooctanoic Acid
PFPA	Perfluoropentanoic Acid
PFTeDA	Perfluorote-tradecanoic Acid
PFTrDA	Perfluorotridecanoic Acid
PFUdA	Perfluoroundecanoic Acid
POPs	Persistent Organic Pollutants
PCPs	Personal Care Products
PSD	Pore Size Distribution
PHG	Public Health Goal
RRP	Relative Response Parameter
RSM	Response Surface Methodology
SEM	Scanning Electron Microscopy
SPE	Solid Phase Extraction
SPME	Solid Phase Microextraction
SBSE	Stir Bar Sorptive Extraction
TEOS	Tetraethyl Orthosilicate

## **CHAPTER 1: Introduction**

### **1.1. Introduction**

The current chapter introduces emerging contaminants and describes the importance of their monitoring and determination in environmental samples. Significant roles of sample preparation in the monitoring and determination of emerging contaminants are discussed. Microextraction methodologies which are based on sorbent enrichment, with particular attention to micro-solid phase extraction ( $\mu$ -SPE) are described. The important roles of sorbents in  $\mu$ -SPE are discussed and ordered mesoporous materials as potentially ideal sorbents are introduced. Eventually the scope, significance, and structure of the thesis are presented.

### **1.2. Emerging contaminants**

For several decades, chemicals deemed priority pollutants in different legislations have garnered the attention of environmentalists. Developments of more sensitive analytical approaches have led to the detection and identification of new unregulated emerging contaminants that were unrecognized or not considered as risks before. These include anthropogenic compounds such as disinfection byproducts (DBPs), personal care products (PCPs), perfluorinated compounds (PFCs), hormones, pharmaceuticals, gasoline additives, plasticizers etc. Some of these newly identified emerging contaminants lack comprehensive data related to their occurrence, ecotoxicology, and risk assessment. Therefore, their analysis and monitoring in different matrices are of paramount importance. As a result, there has been a trend in analytical chemistry to

develop rapid, cost-effective, and efficient procedures for the detection of trace levels of emerging contaminants in different matrices[1, 2].

The development of hyphenated chromatography-mass spectrometry techniques has improved sensitivity of the analytical methodologies, making these the method of choice for determination of trace levels of contaminants in environmental and biological samples. However, possibly due to the complexity of the matrices and very low concentration levels of target compounds, substantial sample preparation and analyte enrichment are required for the isolation of target compounds from the matrix before instrumental analysis.

### **1.3. Sample preparation**

As mentioned, despite technological advances in instrumental analysis, most instruments cannot directly handle and analyze complex matrix, and a sample preparation step before instrumental analysis is required to clean up, concentrate, extract, and present the target analytes in a compatible form to the analytical instrument.

In recent years, there is expanding interest and demand to offer and develop sample preparation techniques that are simplified and easy to manipulate. In addition, absence or minimized usage of organic solvents is one of the important requirements for successful sample preparation, and promoting green chemistry approaches [3].

Given its potential usefulness in achieving the above mentioned requirements, in the following section, the focus is on microextraction based on sorbent enrichment.



#### **1.4. Microextraction based on sorbent**

Many of the currently used sample preparation techniques rely on the entrapment of the analyte from the sample into adsorbent material. Adsorbents are porous material with a high surface area and analytes are temporarily stored at their surface. After analyte trapping and matrix removal, the trapped analytes can be released by extraction with a small amount of organic solvent, and aliquot of this extract is subsequently injected to the analytical instrument [3]. This is the basic idea behind microextraction based on sorbent. These methodologies have been demonstrated to be one of the best choices enabling to direct microextraction and trace level analysis. These approaches have been illustrated to enhance selectivity and sensitivity prior to the application of chromatographic or hyphenated techniques [4]. In general, they offer two potential advantages. 1) Selection of proper sorbent which can have specific or/and particular affinity for the target analytes, and 2) targeted selection of the eluting solvent. These two advantages could lead to the selective purification of the target analytes from interferences.

A wide range of commercially methodologies or those prepared in-house are available for microextraction based on sorbent enrichment. Some of the most important and well-defined methods include solid phase-microextraction (SPME) [5, 6], in-tube SPME [7, 8], stir-bar sorptive extraction (SBSE), microextraction by packed sorbent (MEPS) [9], and  $\mu$ -SPE [9]. All these methodologies have their own advantages and drawbacks. However, each of these methods has successful applications for specific analysis. Taking into account the advantages associated with  $\mu$ -SPE, this methodology was chosen in the current thesis.

#### 1.4.1. Micro-solid phase extraction ( $\mu$ -SPE)

In 2006,  $\mu$ -SPE as an extraction and pre-concentration technique based on the packing of sorbent material in a sealed porous polypropylene membrane envelope, was reported by our group [9].

The extraction procedure using  $\mu$ -SPE is quite simple. The  $\mu$ -SPE device called as bag, consists of polypropylene membrane envelope (usual dimensions less than 3 cm) enclosed with sorbent (usual weight of the sorbent is less than 50 mg). The edges of the bag are heat sealed to secure the contents (Figure 1-1).



Figure 1-1 The  $\mu$ -SPE bag.

Briefly,  $\mu$ -SPE consists of three steps:

1. Conditioning: In this step the bag is sonicated in pure organic solvent such as methanol or acetonitrile for about 10 min followed by drying with lint-free tissue.
2. Extraction: The bag is placed in the sample solution and stirred or agitated for a specified extraction time.

3. Desorption: After extraction, the bag is taken out of the sample solution using a pair of tweezers, dried thoroughly with lint-free tissue, and placed in a vial for desorption. The analytes are desorbed by ultra-sonication using a small volume (in hundred microliters) of desorption solvent, and a small volume of the extract (in few microliters) is injected into the instrument.

#### **1.4.2. Advantageous of $\mu$ -SPE**

$\mu$ -SPE is relatively inexpensive and uses only a few milligrams of sorbent. The bag is reusable for several times after ultra-sonication in organic desorption solvent (carry-over effect must be checked), saving the expensive. In addition,  $\mu$ -SPE offers acceptable sensitivity, selectivity, precision, and reproducibility with no particular requirement of commercial accessories. Besides, it is easy to make and very affordable for many of the laboratories [10-13].

From a practical point of view, extraction and concentration of the analyte in one single step is one of the significant benefits of  $\mu$ -SPE. In  $\mu$ -SPE, the bag can be quickly isolated from the sample after extraction using a pair of tweezers. It has additional practical advantages that it does not face some of the difficulties commonly encountered with other sorption-based methods, including: high back pressure required when the samples are passed through the SPE cartridge, blockage of the SPE column, need for frits to confine the sorbent in conventional SPE, relatively longer sample loading time in SPE (either by gravity flow or pressure/vacuum-assisted flow), isolation and collection of the sorbent as in dispersive solid-phase extraction (DSPE), need for

evaporation of solvent or solvent exchange (which leads to analyte loss), and fragility of the extraction device as in SPME.

From a performance point of view, the protective role of the membrane prevents interferences in the extraction. Thereby, it minimizes matrix effects. This property makes  $\mu$ -SPE very useful for the analysis of analytes from complex matrices such as aqueous samples, food products, and biological tissues which are the matrices of our interest.

#### **1.4.3. The effects of the sorbent in $\mu$ -SPE**

The same as other microextraction based on sorbent, the type of sorbent used for  $\mu$ -SPE is one the most important factors influencing the extraction process since it occurs a dynamic partitioning of analytes between the sorbent material and the sample solution. Silica-based sorbents (such as C8, C2, and C18), carbonaceous materials (such as carbon nanotube (CNTs), multiwall carbon nanotubes (MWCNTs) and graphite fiber), and molecularly imprinted polymer (MIPs) are some of the materials used as sorbents in  $\mu$ -SPE [8-13]. However, a trend of developing new and ideal sorbents has been seen for  $\mu$ -SPE. Some of the characteristics of an ideal sorbent are given below [14].

**High adsorption capacity:** An ideal sorbent must possess high adsorption capacity. There are many factors related to this feature, including specific surface area, surface chemistry of the sorbent, pore size, and its distribution.

High selectivity: This property is highly desirable when the separation of a specific target analyte from groups of compounds is needed or when the matrix is complex (multicomponent mixture). High selectivity depends on the pore size, shape, and pore size distribution, as well as the surface chemistry of the sorbent.

Good stability and durability: Adsorbents might be subjected to harsh chemical and thermal environments as well as high pressure. Hence, good stability is one of the essential requirements for an ideal sorbent.

Desirable adsorption kinetics: Desirable adsorption kinetic means that the rate of the adsorption is fast or favorable for a particular application. This feature depends on many factors such as the particle (crystallite) size, the macro-, meso- and microporosity of the sorbent, and interaction between analytes and surface of the sorbent (weak or strong interaction).

Current commercial sorbents may not have all these properties. Hence, there is an unmet need for the development, design, and synthesis of ideal sorbents that meet the above requirements and be cost-effective. In the current study, for the first time we aimed to investigate the applicability of the ordered mesoporous material as a sorbent in  $\mu$ -SPE. Hence, following sections describe their properties and usefulness.

### **1.5. Nanoporous materials as sorbent**

As an ever-growing multidisciplinary field of study, nanostructured materials are indispensable topic of research in many areas of modern science and technology. Nanoporous materials, a subset of nanostructured materials, have gathered interest and

attention for researchers due to their potential applications in water and air purification, gas separation, catalysis, energy storage, optics, sensors, and nano-reactors [15].

According to the International Union of Pure and Applied Chemistry (IUPAC), nonporous materials are categorized based on their pore size into three classes: microporous material with a pore size less than 2 nm, mesoporous material with intermediate pore size between 2.0 nm and 50 nm, and macroporous material with a pore size greater than 50 nm [16, 17].

Although there are many existing applications of microporous such as zeolites and molecular sieves, expanding the pore dimensions of the sorbent to mesopore range will increase the scope of their applications as adsorbent. In fact, in microporous materials such as zeolite, a number of physical factors such as the size of the adsorbing molecules, the pore diameter of the specific zeolite, and the length of the diffusion path limit their adsorption potential. Hence, the total surface area of microporous may not be utilized in adsorption process and it may not be useful for larger molecules [18]. In addition, for some cases relatively narrow pore size distribution is desirable for adsorption. However, amorphous nanoporous materials such as silica gels, alumina, and activated carbons are limited in shape selectivity because of their broad pore size distribution and fixed pore geometries.

On the contrary, mesoporous materials have these properties as following: potentially uniform pores, tunable pore size and pore size distribution, highly ordered structures, adjustable morphologies, large surface area, high surface to volume ratio, various wall compositions, non-toxicity, inertness, large porosity, fluid permeability,

and chemical and thermal stability. Although not all mesoporous materials possess above features, some mesoporous materials with above mentioned properties have been identified and reported [16]. Thus they would meet the above mentioned requirements of an ideal sorbent.

From the various mesoporous material types, two basic groups, ordered mesoporous silica (OMS), and ordered mesoporous carbon (OMC) were chosen. The following section describes these two groups.

### **1.5.1. Ordered mesoporous silica (OMS)**

In 1990, OMS materials were introduced for the first time after the discovery of MCM-41 (Mobil Crystalline Material) by Mobil scientists. Later, it was considered as a large family called M41S. Three well-known members of this family with different structures have been identified: lamellar (MCM-50), hexagonal (MCM-41), and cubic (MCM-48) phases [17].

OMS materials are synthesized via a cooperative assembly of organic surfactants and inorganic silicate species. The latter allows solidification of diverse flexible liquid crystal structures by hard materials [19]. Instead of using small organic molecules as templating compounds (as in cases of zeolites), long-chain surfactant molecules were employed as the structure-directing agent during the synthesis of these highly ordered materials. The structure, composition, and pore size of these materials can be tailored during synthesis by variation in the reactant stoichiometry, the nature of the surfactant molecule, auxiliary chemicals, reaction conditions, or by post-synthesis functionalization techniques [17].

There are some practical benefits offered by MCM-41 as a sorbent: MCM-41 is stable, economically cheap, the synthesis is quite simple and reproducible, and the pore size of the material is tunable during synthesis [20]. Considering all the features of MCM-41 explain here, we chose MCM-41 as a sorbent for some part of the present study. MCM-41 is synthesized via a mechanism called as liquid-crystal templating (LCT) [21]. The schematic model of LCT has been shown in Figure 1-2.

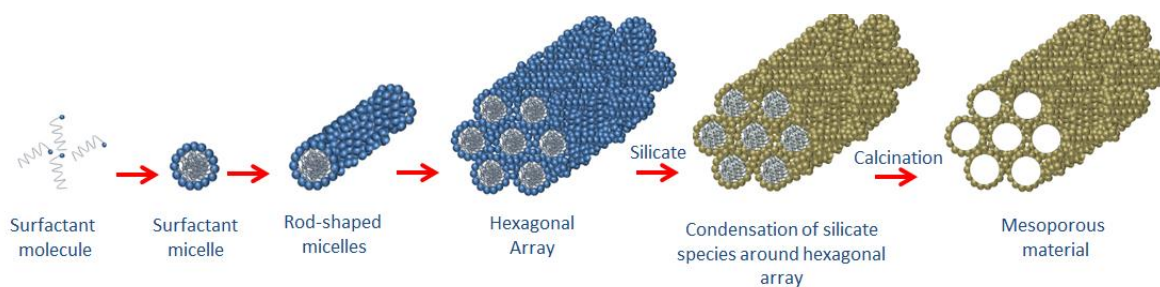


Figure 1-2 Schematic of LCT mechanism

As seen from Figure 1-2, the formation of a composite hexagonal mesophase is accomplished by the condensation of silicate species (formation of a sol-gel) around a preformed hexagonal surfactant array. Moreover, it can be accomplished through the adsorption of silicate species at the external surfaces of randomly ordered rod-like micelles through coulombic or other types of interactions. Through the second pathway, these randomly ordered composite species spontaneously pack into a highly ordered mesoporous phase with an energetically favorable hexagonal arrangement, accompanied by silicate condensation [22-24]. Eventually, the process would be completed by a calcination step, in which the surfactant template is removed either through chemical or thermal treatment, giving high porosity to the final product. The hexagonal mesophase, denoted as MCM-41, possesses highly regular arrays of uniform-sized channels with a diameter ranging from 1.5 nm–10 nm, depending on the



templates used and the reaction parameters such as pH, ionic strength, temperature, and the addition of auxiliary organic compounds. The wall of the channel is amorphous SiO<sub>2</sub> and the porosity can be as high as 80% of its total volume [15].

The preparation of MCM-41 type materials can be considered by an S<sup>+</sup>I<sup>-</sup> pathway (in the basic media, using the cationic surfactant and anionic silica source), in which strong electrostatic interactions exist between rod-like micelles of surfactants (S<sup>+</sup>) and inorganic network of anionic silicate species (I<sup>-</sup>) [25]. These surfactant-containing mesoporous silica synthesized under alkaline conditions were suitable for use as an adsorbent [18, 26, 27]. Non-calcined mesoporous materials have been used extensively in previous studies as sorbents successfully and ordered structure conceivably enforced and use as helping points. For instance, Bruzzoniti and coworkers investigated the possibility of absorbing hydrophobic organic molecules and trichloroacetic acid from aqueous solution into non-calcined (i.e, surfactant-containing) and calcined mesoporous silica [28]. During synthesis using TMOS, MCM-41 materials dried at 90 °C were used as sorbents to remove 3-chlorophenol from water [29]. Another study by Zhao et al [30] used non-calcined MCM-41 materials dried at 70 °C as an adsorbent for removal of trichloroethylene and tetrachloroethylene from water. They observed that MCM-41 without surfactant template (calcined) showed weaker adsorption as compared to non-calcined MCM-41. Ghiaci and co-workers performed equilibrium isotherm studies for the adsorption of benzene, toluene, and phenol onto organo-zeolites and non-calcined MCM-41 [26], while Rayalu studied adsorption of o-chlorophenol and phenol onto non-calcined MCM-41 [18]. Interestingly, the ordered structure in non-calcined mesoporous material is used by the surfactant to enhance the adsorptive behavior of the sorbent.

Hence the investigation of the adsorptive properties of non-calcined mesoporous materials is in interest.

### **1.5.2. Ordered mesoporous carbon (OMC)**

The other important group of ordered mesoporous material is ordered mesoporous carbon (OMC). In general, there is an increasing demand for porous carbon materials due to their wide applications. Accordingly, different approaches have been used to synthesize porous carbon materials [31]. However, the synthesis of uniform porous carbon material as a sorbent is demanding.

One of the ways to achieve the uniform porous carbonic material is hard template approach in which pre-designed and rigid templates are used to create porosity and structure. This idea for the first time was introduced by Knox and co-workers [20]. Briefly, the process is similar to the fabrication of ceramic jar. To make a jar, firstly a hard template with desirable shape is carved. Then clay is applied for covering the surface of the template. Eventually, through the heating process the template is removed and the clay is transformed to ceramic.

By considering similar strategy as ceramic jar fabrication, in hard template approach various inorganic materials as template, such as zeolite, anodic alumina membranes, silica nanoparticles, and OMS are employed, thereby producing different types of porous carbon material each with its own unique characteristics. Using mesoporous silica material as a template, an OMC is formed, which is the focus of our study. The synthesis of OMC using this method involves four separate steps: (1) preparation of ordered mesoporous silica with controlled pore structure; (2)

impregnation/infiltration of the silica template with carbon precursors; (3) cross-linking and carbonization of the carbon precursors; (4) dissolution of the silica template.

Historically, MCM-48 (as mesoporous ordered silica) was used for the first time by two different groups in Korea separately as a hard template for the synthesis of OMCs [32, 33]. Since then, different OMC types were synthesised using different OMS [31]. In our study, we focus on Carbon Microstructures from Korea (CMK-3); a highly ordered structured mesoporous carbon produced by Ryoo's group in 2000 using hexagonally structured mesoporous silica SBA-15 as a template and sucrose as a carbon source [34]. These two basic materials made the synthesis procedure very cost-effective.

SBA-15 belongs to Santa Barbara Amorphous (SBA) materials, synthesized using triblock polyethylene oxide—poly propylene oxide—poly ethylene oxide ( $\text{EO}_n\text{PO}_m\text{EO}_n$ ) copolymers. SBA-15 is synthesized under acidic condition using the triblock copolymer,  $\text{EO}_{20}\text{PO}_{70}\text{EO}_{20}$  (Pluronic P-123) as structure-directing agents (such as the surfactant in M41S), and tetraethyl orthosilicate (TEOS) as a silica source. SBA-15 is an excellent choice as a template, attributable to its high quality structure regularity, thick inorganic walls, excellent thermal and hydrothermal stability, economically cheap synthesis, non-toxicity, simplicity and reproducibility of synthesis, and tuneable pore size through hydrothermal treatment.

Figure 1-3 shows the hard template approach for the synthesis of CMK-3. CMK-3 is the first ordered mesoporous carbon that is a faithful replica of SBA-15, without the

structural transformation during the removal of the template; in the other word the ordered structure of the CMK-3 is the exact inverse of SBA-15.

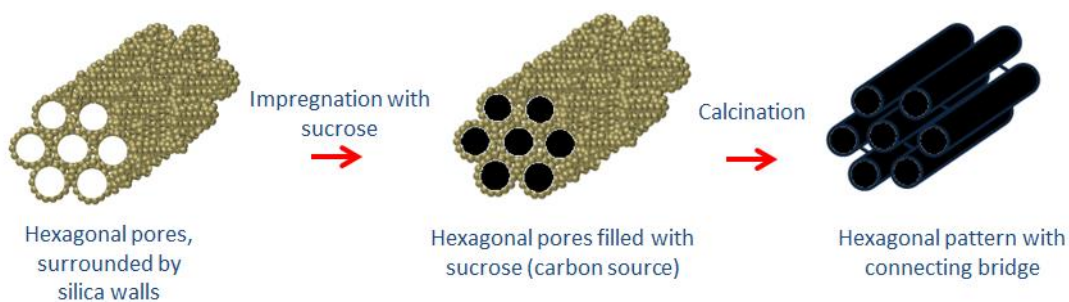


Figure 1-3 Schematic of the hard template method for the synthesis of ordered mesoporous carbon (CMK-3) from SBA-15

This material is composed of hexagonally packed amorphous carbon nano-rods arranged in a hexagonal pattern with connecting bridges between them ( ) with uniform meso-pores and highly ordered long-range regularity which exhibit uniform mesopore size, high BET-specific surface area, and large total pore volume. All these make it a promising material in many modern-day scientific applications [31, 35].

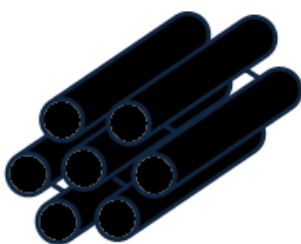


Figure 1-4 Hexagonal pattern of CMK-3 with connecting bridges

### 1.5.3. Surface modification of OMC

Studies have proved that both surface chemistry and textural properties affect the adsorption behavior of a sorbent. High surface area, adequate pore size distribution, and

porous texture are essential, but not sufficient factors for a sorbent to perform ideal in particular applications. There are many examples of sorbents with similar characteristics but different surface chemistry which having a very different adsorption capacity with the same analyte. Hence, the nature and composition of the groups present at the surface of the sorbent also play an important role.

With OMC, the inert and hydrophobic nature with poor wettability of the carbon surface might limit some of its applications as a sorbent. Hence, surface modification seems to be a critical requirement in the development of successful adsorptive applications of OMC with specific and/or selective affinity. In this direction, it is important to know how surface features are engaged in specific adsorptive applications.

Significant efforts have been devoted to the functionalization of the surface of the mesoporous carbon material which leads to enhanced or reduced adsorption capacity and selectivity of certain targets as the case may be. By considering that the chemical modification for the carbon surface with functionalized groups is difficult process due to low reactivity of the carbon, oxidative treatment is one of the most commonly appropriate used approaches. The surface oxidation of the carbonaceous material by oxidative reagents such as ozone or acids leads to introduce the carbonyl functional group at the surface (Figure 1-5) [36]. At the nano-scale level, the edges of the carbonic layer are very active sites for some atoms, because they are associated with high density of unpaired electron. Therefore, they have a strong tendency to adsorb heteroatoms such as hydrogen, nitrogen, sulfur, and oxygen. It needs to be mentioned that the nature and amount of the different surface oxygen-containing carbon groups at the carbon surface may vary depending on the oxidation conditions [37].

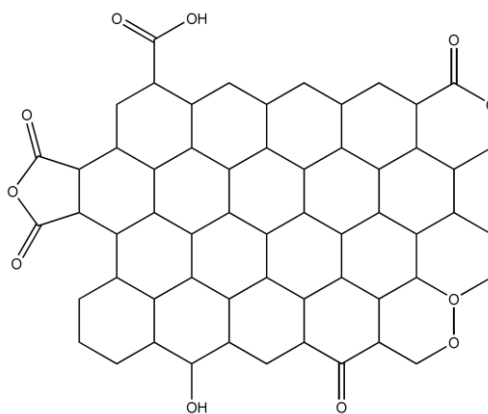


Figure 1-5 Different carboxylic groups at the surface of the carbonaceous sorbents after oxidative treatment

Oxidative treatment can help to change the inert and hydrophobic nature of carbon materials and enhance the wettability for polar solvents making the surface active for immobilization of organic compounds via adsorption [38]. Although the surface sites associated with functional groups represent a small proportion of the total surface area, small variations in the chemical nature of a sorbent in the nano-scale may produce important changes in its adsorption capacity. Moreover, the oxidative treatment process not only attaches oxygen-containing groups at the surface but also modifies the surface by creating hydrophobic/hydrophilic balance at the surface [39, 40]. In the following chapter, (Section 7.4.) we explain how hydrophobic/hydrophilic balance on the surface can improve the adsorptive capacity for our aim.

## 1.6. Scope, significance, and structure of thesis

The primary aim of this study was to develop analytical methodologies for the monitoring and determination of two classes of emerging contaminants. Perfluorinated carboxylic acids (PFCAs) as an important group of PFCs, and N-nitrosamines (NAs) as

a challenging group of DBPs, were two classes of emerging contaminants of interest in this thesis.

In the present thesis, the basic extraction processes rely on the  $\mu$ -SPE by using ordered mesoporous materials as sorbents for extraction. Hence, our results may provide new prospective applications of ordered mesoporous materials and  $\mu$ -SPE.

The need for routine monitoring of these contaminants in many laboratories necessitates the development of affordable and safe analytical methodologies with a minimum use and production of hazardous substances. Therefore, we aimed to develop and introduce easy-to-go, cost-effective, safe, and practical methodologies.

We have described all the previously reported studies on the determination and monitoring such analytes in each matrix of interest, along with shortcomings in each section. The results of this work would pave the way for new approaches to overcome some of the current challenges in this area.

To go forward, we evaluated the applicability of each proposed method using real environmental samples.

The present thesis is divided into two broad parts. Part 1 covers Chapters 2-5 and deals with PFCs. Chapter 2 introduces PFCAs and describes the current challenges for their monitoring. Subsequently, in Chapters 3-5 a combination of  $\mu$ -SPE with liquid chromatography-triple quadrupole tandem mass spectrometry with negative ion electrospray ionization (LC-ESI-MS/MS) is introduced for the determination of PFCAs in water samples, human plasma, and fish fillet, respectively.

Part 2 consists of Chapters 6-9 and focuses on NAs. In Chapter 6, the important aspects of NAs and the current challenges and shortcomings in their analysis are described. The necessity for development of new carbonaceous sorbents for simultaneous extraction of group of is highlighted. Chapter 7 introduces new surfaced modified OMC as a promising carbonaceous sorbent for simultaneous extraction of 8 NAs. Subsequently Chapters 8 and 9 focus on the use of the designed sorbent for extraction of NAs following analysis by using triple quadrupole GC-MS/MS with electron ionization (EI) from water samples (wastewater and swimming pool water) and different beverages (alcoholic and non-alcoholic), respectively.

Chapter 10 represents the conclusion, highlighting the important achievements of our work, discussing limitations and drawbacks and possible future works.



## **Part 1**

### **CHAPTER 2: Introduction to perfluorinated compounds**

#### **2.1. Introduction**

The current chapter gives brief introduction about PFCs; their unique physico-chemical properties and their applications. The importance of the analysis of the PFCAs is explained (why this group is chosen among the other groups of PFCs). Eventually current challenges in their determination and analysis is described with details.

#### **2.2. Perfluorinated compounds (PFCs)**

PFCs as a group of emerging contaminants are anthropogenic chemicals which have been used in a wide range of applications over the past 6 decades. In PFCs, aliphatic hydrogen atoms of hydrocarbons chains are replaced by fluorine atoms leading to compounds with unique physicochemical properties, including water and oil repellency, unusual thermal and chemical stability, and unusual surfactant properties. The strong interaction between carbon and fluorine atoms as well as the weak intermolecular interactions probably accounts for the high stability of these compounds. All these properties make them very useful substances for a wide range of industrial applications [41-43]. For example these compounds repels both water and oil, hence they are ideal for surfaces one wants to keep clean and dry such as in paper packaging, as surface protectors and stain repellents [44]. This chemistry is also useful for surfactants and dispersants, leading to their widespread use as levelling agents for paints, lubricants, mist suppression, and fire fighting foams [45].

### **2.3. Importance of the determination of PFCs**

Despite the favourable properties of PFCs in manufacturing and as finished products, some of these compounds exhibit characteristics of persistent organic pollutants (POPs), as defined by the United Nations Environment Programme's Stockholm Convention [46]. Most of them are toxic, extremely resistant to degradation, and bioaccumulative in biological tissues with an extended half-life [45, 47, 48].

Many international organizations and authorities have undertaken many efforts to put pressure on the industry to limit the production and usage of some of the most harmful PFCs. This has already lead to a decreasing production and use of the chemicals in the recent years [49]. However these substances are ubiquitous and persistent, and are still widely prevalent in many environmental and biological media such as surface waters, aquatic environments, sediments, soils, human blood, and biota [50-53].

### **2.4. Perfluorinated carboxylic acids (PFCAs)**

PFCAs are one of the most important group of PFCs and topic of interest for this thesis. PFCAs are persistent against the typical environmental degradation processes (hydrolysis, photolysis, microbial degradation, and metabolism) compared to other members of PFCs, moreover, they are known to bioaccumulate [19, 20]. A comprehensive survey conducted in a wide range of geographical locations (e.g., South America, Russia, Antarctica) on monitoring of PFCs in aquatic ecosystems, has revealed a decrease in the levels of perfluorooctanesulfonic acid (PFOS)— which is the most well-defined PFCs till now—over time. In contrast, PFCAs have tended to

increase in biota at many of the locations under survey [21]. Moreover, most of the studies hitherto on monitoring of PFCs have only been focused on PFOS and perfluorooctanoic acid (PFOA)—the most well-defined toxin of PFCAs. In 2010, however, the commission recommendation 2010/161/EU document invited member states to monitor and study other similar PFOA compounds with different carbon chain lengths in food matrices [22]. Hence, in this thesis, PFCAs with different carbon chain lengths have been chosen for analysis from different media (Table 2-1).

Table 2-1 List and characterization of PFCAs, have been chosen to study

Analyte	Abbr.	Chain length	Molecular formula	Molecular mass	Cas No.
Perfluoropentanoic acid	PFPA	C5	C <sub>5</sub> HF <sub>9</sub> O <sub>2</sub>	264	2706-90-3
Perfluorohexanoic acid	PFHxA	C6	C <sub>6</sub> HF <sub>11</sub> O <sub>2</sub>	314	307-24-4
Perfluoroheptanoic acid	PFHpA	C7	C <sub>7</sub> HF <sub>13</sub> O <sub>2</sub>	364	375-85-9
Perfluorooctanoic acid	PFOA	C8	C <sub>8</sub> HF <sub>15</sub> O <sub>2</sub>	414	335-67-1
Perfluorononanoic acid	PFNA	C9	C <sub>9</sub> HF <sub>17</sub> O <sub>2</sub>	464	375-95-1
Perfluorodecanoic acid	PFDA	C10	C <sub>10</sub> HF <sub>19</sub> O <sub>2</sub>	514	335-76-2
Perfluoroundecanoic acid	PFUdA	C11	C <sub>11</sub> HF <sub>21</sub> O <sub>2</sub>	564	2058-94-8
Perfluorododecanoic acid	PFDoA	C12	C <sub>12</sub> HF <sub>23</sub> O <sub>2</sub>	614	307-55-1
Perfluorotridecanoic acid	PFTTrDA	C13	C <sub>13</sub> HF <sub>25</sub> O <sub>2</sub>	664	72629-94-8
Perfluorotetradecanoic acid	PFTeDA	C14	C <sub>14</sub> HF <sub>27</sub> O <sub>2</sub>	714	376-06-7

## 2.5. Challenges in the analysis of PFCs

Much effort has been made to develop methods for the detection and determination of harmful PFCs in different media and there are many comprehensive publications, which in particular evaluate the analytical challenges and uncertainties associated in the analysis of PFCs [49, 54]. Among all of them, matrix effects have

been considered as one of the most important sources of uncertainties in quantitative analysis of PFCs. Hence here we try to explain this phenomenon:

Due to lack of volatility of PFCs, GC rarely leads to sensitive determination of trace concentration levels of these compounds. Moreover due to the lack of a suitable chromophore, their analysis using ultraviolet detection in LC is impossible. Hence prior to instrumental analysis, chemical derivatization by methyl esters is helpful in overcoming these issues; however the results are not as sensitive as desirable. Moreover chemical derivatization imposes one extra step in their analysis [55]. Given that their analysis especially at the trace concentration level is highly and significantly affected by background contamination, the researchers are looking for straightforward methodologies with few steps to minimize these background contaminations. Hence the methodologies without need of derivatization are desirable.

After the commercialization of the electrospray interface (ESI) for liquid LC-MS/MS, it was used extensively to determine selected PFCs [44]. Although LC-MS/MS with ESI demonstrates excellent sensitivity and specificity for PFCs without the need for chemical derivatization, it brought a critical challenge. The quantitative results are often adversely affected by the phenomena commonly referred to Matrix Effect [55]. This phenomenon can have suppressive and/or enhancing effect on the results. Matrix suppression occurs in the electrospray interface when co-eluting matrix components compete with the analyte for charge, thereby reducing the number of gas-phase ions available for detection. Conversely, if a matrix component facilitates the ionization process (e.g., by reducing surface tension), an enhancement is obtained [56]. Matrix effect is especially important in the complex matrices which obtaining sufficiently

reliable quantitative data for the purposes of monitoring and government regulation of PFCs is particularly necessary and demanding. In a comprehensive review paper, Powley and coworkers have given a detailed descriptions of this phenomenon in LC-MS/MS [55]. Ideally stable isotope analogues of the analytes can be used as internal standards to compensate for matrix effects, but they are of limited availability due to the cost of their synthesis. Moreover based on the publication it cannot truly eliminate, or compensate for matrix effect [57].

Overall, there is no unique or universal strategy or solution concerning matrix effects, even though several practical suggestions have been made, and evaluated to overcome this phenomenon [52]. However, it has been confirmed that sample preparation is still the key step for minimizing the presence of interfering compounds in complex matrices before analysis. Many methodologies have been reported in determination and monitoring of PFCs in different matrices. However each approach is associated with its own advantages and disadvantages [58].

In ion pair extraction (IPE), tetrabutylammonium hydrogen sulphate is used for the ion pairing of the target compounds and subsequently extracted with methyl tert-butyl ether (MTBE) [59, 60]. This method has been widely used for biological matrices like fish, molluscs, and tissues such as those of liver, kidney, gall bladder and blood. However, this method is relatively laborious and the co-extraction of lipid and the interference of matrix have been also reported. In this method, sample clean up after extraction is necessary to remove impurities, as may severely affect the analysis [61]. Solid phase extraction (SPE) with different sorbent such as reversed phase [62], hydrophilic-lipophilic-balanced (HLB), and weak anion exchange (WAX) [63-65], is

another common method for PFCs analysis. Most of the time, an appropriate sample pretreatment to prevent clogging of SPE columns and removal of the proteins is required [58, 66]. Additionally, high background levels of PFCs (which is due to presence of the Polytetrafluoroethylene (PTFE) in the frits or the body of the extraction tube) were reported, which necessitated the use of a glass cartridge. The method based on alkaline digestion, improves the extraction of targets bound to biological tissue, and reduces interferences from the matrix [65, 67, 68]. However, it is time consuming and involves many steps. Hence it runs the risk of increased contamination during processing. Methods having as few steps as possible are preferred in order to avoid analyte losses, which is likely during practical processes such as solvent change, solvent evaporation or the transfer of extract between containers. In comparison to the previous extraction methods, extraction with organic solvents has the benefit of simplicity; however, it is not without its own problems. For example, tetrahydrofuran/water has been reported as a successful solvent mixture, with good recovery and rapid extraction rate [68-70]. However, it is necessary to control the amount of water in the sample. MTBE is another solvent which has been used for extraction [71]. However, in this case the process needs solvent reduction and solvent exchange which could lead to the loss of the analytes. A mixture of mobile phase (methanol/ammonium acetate) has also been used as a quick and cost effective screening extraction method [72], but a high matrix effect has been observed. Moreover, due to the low solubility of the long-chain compounds in this mixture, it is not possible to extract these particular compounds.

Eventually the primary aim of the first part of this thesis (Chapters 3-5 is to develop analytical methodology for the determination of PFCAs—with respect to all

above mentioned challenges in their analysis. Three important matrices are chosen: aqueous media, human plasma and fish fillet (Chapters 3-5 respectively).

## **CHAPTER 3: Analysis and determination of perfluorinated carboxylic acids in water samples**

### **3.1. Introduction**

The objective of the work reported in the present chapter is to evaluate the feasibility of  $\mu$ -SPE technique using ordered mesoporous silica as sorbents for analysis of PFCAs. To the best of our knowledge this is the first time mesoporous materials are used as sorbents in  $\mu$ -SPE, and their adsorption potential relating to the PFCAs are investigated. MCM-41 and non-calcined MCM-41 (denoted as CTAB-MCM-41) are evaluated for their adsorptive performance. Various parameters affecting the  $\mu$ -SPE, including the effect of desorption solvent, extraction time, salt concentration, and desorption time, are investigated. The performances of different commercial sorbents are compared. Under the optimized conditions, the proposed method is applied to the analysis of real world samples, including rain water and river water.

### **3.2. Experimental**

#### **3.2.1. Chemicals and materials**

The five most studied PFCAs—PFPA, PFHA, PFOA, PFNA, PFDA—were considered. PFPA (97%), PFHA (99%), PFOA (96%), PFNA (97%), and PFDA (96%) were purchased from Sigma–Aldrich (Louis, MO, USA). Accurel polypropylene flat sheet membrane (200  $\mu\text{m}$  wall thickness, 0.2  $\mu\text{m}$  pore size) was purchased from Membrana (Wuppertal, Germany). Commercial sorbents, including HayeSep-A (divinylbenzene ethylene glycodimethyl acrylate), HayeSep-B (divinylbenzene



polyethyleneimine), and Porapak-R (divinylbenzene-vinyl pyrrolidinone), were purchased from Alltech (Waukegan, Illinois, USA), and C18 was purchased from Waters (Milford, MA, USA). HPLC grade methanol, acetone, and dichloromethane were purchased from Fisher Scientific (Loughborough, UK). Hexane and acetonitrile were obtained from Fisher Scientific (Fair Lawn, NJ, USA). Ammonium acetate was obtained from Fluka (Wageningen, Netherland). Tetraethyl orthosilicate (TEOS, 98%) was purchased from Aldrich Chemistry (Steinheim, Germany). Cetyltrimethylammonium bromide (CTAB) as cationic organic surfactant for synthesis of MCM-41 was purchased from Sigma-Aldrich (Milwaukee, WI, USA). Sodium chloride (NaCl) and sodium hydroxide (NaOH) were obtained from Goodrich Chemical Enterprise (Singapore). Ultrapure water was used for all experiments.

### **3.2.2. Synthesis of mesoporous silica**

MCM-41 silica was prepared using a low surfactant concentration at ambient temperature. TEOS was chosen as source of silica and CTAB as the structure directing agent. Briefly [73], an aqueous solution containing 1.01 g of CTAB, 0.34 g of NaOH and 30 ml of deionized water was added to 5.78 g of TEOS. The mixture was stirred for 1h at ambient temperature and the resulting homogeneous mixture was crystallized under static hydrothermal conditions at 110 °C in a autoclave for 96 h. The molar composition of the initial gel is one important factor and to ensure the stability of the resulting mesoporous product, it should be 1.0:0.10:0.30:60 TEOS/CTAB/NaOH/water. After crystallization, the mixture was filtered. The white precipitate was washed with deionized water at room temperature until foam due to the surfactant was no longer present. This was done to ensure elimination of the surfactant weakly retained on

the material. The white powder was denoted as CTAB-MCM-41. To remove the CTAB completely, dried CTAB-MCM-41 was placed in a furnace under air at a heating rate of 10 °Cmin<sup>-1</sup> from 25 to 550 °C and held at the latter temperature for an additional 12 h. This calcined sorbent was denoted as MCM-41.

### **3.2.3. Characterization of mesoporous materials**

The XRD patterns were obtained with a CuK $\alpha$  radiation source (40 kV, 40 mA) by using a X-ray diffractometer (D5005, Siemens, Karlsruhe, Germany) at 0.02° step size and 1 s step time over a 1.5° < 2 $\theta$  < 10° range. Fourier transform infrared (FT-IR) spectra (Varian Excalibur 3100, Palo Alto, CA, USA) was used to confirm the presence of the functional groups on the surface of the mesoporous silica, and were measured at a resolution of 4 cm<sup>-1</sup> with a scan range of between 400 and 4000 cm<sup>-1</sup>.

### **3.2.4. Preparation of $\mu$ -SPE device**

The polypropylene sheet membrane was used to prepare the  $\mu$ -SPE device. Briefly, 5 mg sorbent was packed inside an envelope made of two pieces of polypropylene sheet membrane (tried dimensions of 0.8 cm length  $\times$  0.5 cm width), with their edges heat-sealed to secure the contents. Before use, each  $\mu$ -SPE device was conditioned (by ultrasonication for 10 min in methanol) and dried in air.

### **3.2.5. Sample preparation and extraction procedure**

Stock solutions containing 10 mgL<sup>-1</sup> of each PFCA were prepared in methanol and stored in methanol-rinsed and air-dried polypropylene bottles at 4 °C. Working solutions containing all the PFCAs at different concentrations were prepared by spiking

the appropriate stock solutions into ultrapure water. Environmental water samples (river water and rain water) for the experiments were collected locally in September 2012. Samples were collected into methanol-rinsed and air-dried polypropylene bottles. Before use, samples were filtered to remove any suspended solids using Whatman filter paper (Maidstone, England) (Grade 1, 11  $\mu\text{m}$ , cellulose filters). The samples were stored at 4  $^{\circ}\text{C}$  until analysis and processed within 1 week of collection. pH adjustment or sample dilution was not carried out on samples.

For extraction,  $\mu\text{-SPE}$  device was placed in 10 mL of the sample solution and the solution was shaken at 300 revolutions per minute (rpm) (KS 4000i control orbital shaker incubator, IKA, Germany), at a temperature of 30  $^{\circ}\text{C}$  for a specified extraction time. After extraction, the device was taken out of the sample solution using pair of tweezers, dried thoroughly with lint-free tissue and placed in a vial for desorption. The analytes were desorbed by ultrasonication with 200  $\mu\text{L}$  of solvent, and 10  $\mu\text{L}$  of the extract was injected into the LC–MS/MS system [74]. The final results were as an average value from 3 repeated parallel experiments in the absolutely same conditions. The  $\mu\text{-SPE}$  device could be reused after ultrasonication in methanol, with no carryover effect observed (Result not shown).

### **3.2.6. Instrumental analysis**

Samples were analyzed by using a Model 8030 LC-triple quadrupole MS system (Shimadzu, Kyoto, Japan) with electrospray ionization, equipped with an autosampler (CTC Analytics AG, Zwingen, Switzerland), LC-30AD binary pumps, DGU-20A degasser, and a CTO-30A column oven. The mobile phase comprised of 50 mM

ammonium acetate and methanol. The LC was operated under gradient mode with the following program: 72% methanol from 0 to 0.1 min, linear increase to 95% in 4 min, maintained at 95% for 7 min, linear decrease to 72% in 0.1 min and maintained at 72% for 10 min. The flow rate of the mobile phase was 1 mL/min. A Luna C18 column (5 $\mu$ m particle diameter, 150 mm  $\times$  4.6 mm, Phenomenex, Torrance, USA) was used. Analysis conditions have been summarized in Table 3-1.

Table 3-1 LC-MS/MS conditions for the analysis of PFCAs

LC	
Column	Luna C18 column (5 $\mu$ m particle diameter, 150 mm $\times$ 4.6 mm)
Mobile phase	Ammonium acetate (50 mM) Pure Methanol
Mobile phase gradient	0-0.1 Min $\rightarrow$ 72% methanol, 28% Ammonium acetate (50 mM) 0.1-4 min $\rightarrow$ linear increase to 95% MeOH, 5% Ammonium acetate (50 mM) 4-7 min $\rightarrow$ maintained with 95% MeOH, 5% Ammonium acetate (50 mM) 7- 7.1 min $\rightarrow$ linear decrease to 72% methanol, 28% Ammonium acetate (50 mM) 7.1-17.1 min $\rightarrow$ maintained with 72% methanol, 28% Ammonium acetate (50 mM)
Flow rate of the mobile phase	1 mL/min
Oven temp.	40 $^{\circ}$ C
Total program time	10 min
MS	
Ionization mode	Electrospray ionization (Negative)
Detector voltage	Relative to the tuning result
Interface temp.	250 $^{\circ}$ C
DL temp.	250 $^{\circ}$ C
Heat block temp.	300 $^{\circ}$ C
Acquisition mode	MRM
CID gas	Argon
Nebulizing gas	N <sub>2</sub>
Nebulizing gas flow	3 l/min
Drying gas	N <sub>2</sub>
Drying gas flow	15 l/min
Loop time	0.399 (ms)
Event time	11 (ms)
Pause time *	5 (ms)
Dwell time **	12 (ms)

\* Time required for MS instrument to change and stabilize voltages for each MRM transition

\*\* Time that target ions spent in the collision cell

Under the above mentioned conditions, PFCAs were well separated with retention time of between 2.05 and 5.46 min. Based on preliminary experiments, it was observed that the concentration of the volatile salt was an important factor affecting the shape of the LC peaks; apparently it has a suppressive effect on the analyte signals. Several

concentrations of the salt (5, 10, 20, 50, and 100 mM) were tested to identify the most favorable concentration, that provided short retention times, highest intensities (with little or no suppression), acceptable resolution and best peak shapes. Eventually 50 mM was selected. PFCA analysis was carried out in negative ESI mode and the MS/MS parameters and product ions were obtained by multiple reaction monitoring (MRM) by using a mixture of the target analytes (1 mgL<sup>-1</sup> of each standard compound) in methanol. All analytes presented several transitions. Identification of the analytes was based on the precursor ions, retention time and two most intensive product ions of each analyte. Moreover, total ion chromatography (TIC) was used for quantification analysis. As was expected, the ESI source showed a better sensitivity because of the presence of the carboxylic acid as ionisable groups. The list of the analytes and the optimized LC-MS/MS parameters are shown in Table 3-2.

Table 3-2 Experimental conditions of ESI-MS/MS

Analyte	Chain length	Molecular mass	Retention time (min)	Precursor ion (m/z)	Product ion 1			Product ion 2				
					(m/z)	DP (V)	CE (V)	CXP (V)	(m/z)	DP (V)	CE (V)	CXP (V)
PFPA	C5	264	2.09	262.80	219.05	13	10	20	119.35	13	20	19
PFHpA	C7	364	2.85	362.80	319.00	14	10	20	169.05	14	20	30
PFOA	C8	414	3.30	412.90	369.05	12	10	23	169.06	12	20	30
PFNA	C9	464	3.76	462.90	419.00	13	10	28	219.05	13	15	20
PFDA	C10	514	4.18	512.09	469.05	20	10	30	219.02	20	20	13

DP. The voltage used to select the targeted precursor ion into the Q1 section

CE. Energy used to fragment the precursor ions

CXP. The voltage used to select the targeted product ions into the Q3 section

### 3.2.7. Control of the background contamination

PFC analysis is commonly affected by background contamination and carryover effects. During this analysis, we considered some strategies to minimize these problems. Methanol-rinsed, air-dried disposable polypropylene tubes, vials, and pipettes

were used to avoid potential contamination from laboratory ware. During sampling, storage, and sample preparation, any contact with Teflon containers was avoided. To check for potential contamination, blank solutions were routinely extracted and analyzed every day and whenever a new bottle of solvent was used. No contamination was detected above the limit of detection. With a similar protocol in a previous study, no contamination was observed [75].

Carryover effects have also been reported in analysis of PFCAs. To overcome this, the syringe was washed with pure methanol using the LC-MS autosampler twice both before and after any injection. In addition, the syringe was also rinsed with the sample before any injection. Furthermore, methanol was injected after every sample. Using this washing protocol, no significant contaminant peaks or signals were observed.

### **3.3. Results and discussion**

#### **3.3.1. Characterization of CTAB-MCM-41 and MCM-41**

The powder XRD patterns and the FT-IR spectra of the CTAB-MCM-41 and MCM-41 are shown in Figure 3-1. In the XRD patterns, three diffraction peaks in the  $2\theta$  range from  $1.5^\circ$  to  $10^\circ$  are due to the hexagonal mesoporous material. The stability of the CTAB-MCM-41 after exposure with aqueous solution of PFCAs was investigated. It can be observed that the stability of the sample is retained after exposure to an aqueous solution of PFCAs.

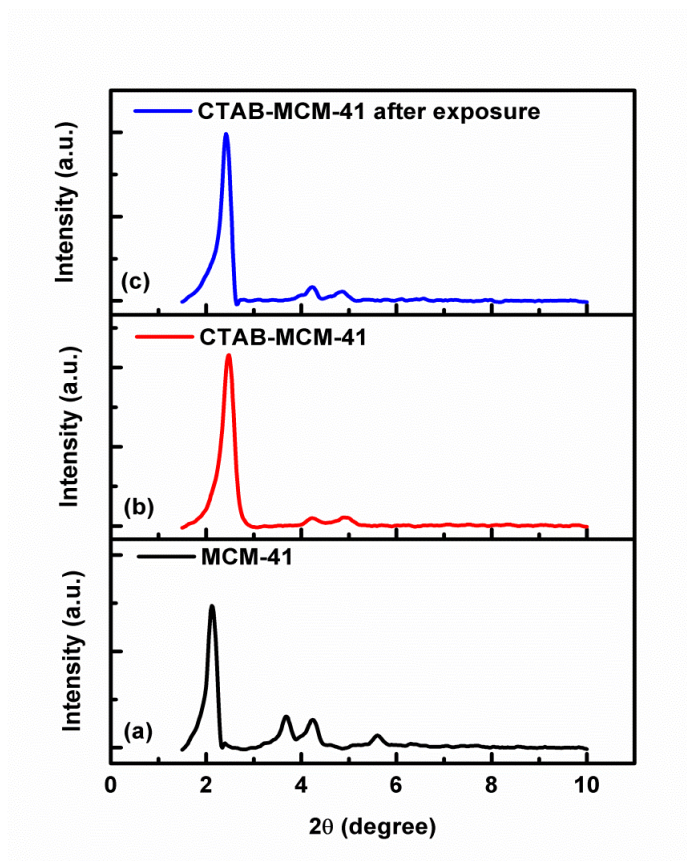


Figure 3-1 Powder XRD patterns of (a) MCM-41, (b) CTAB-MCM-41, and (c) CTAB-MCM-41 after exposure to aqueous solution of PFCAs

In the FT-IR spectra (Figure 3-2), the characteristic band for ammonium ion can be seen at  $1469.7\text{ cm}^{-1}$ , and presence of organic surfactant can be confirmed by various C-H stretching vibrations at  $2920$  and  $2850.54\text{ cm}^{-1}$ ; these peaks disappeared after removal of the surfactant. The stretching vibrations of Si-O-Si and Si-OH can be seen at  $1053\text{ cm}^{-1}$  in both samples. A broad band in the hydroxyl region between  $3700$  and  $3000\text{ cm}^{-1}$  with a maximum in the range of  $3400\text{-}3450\text{ cm}^{-1}$  was observed in both cases and can be related to the framework Si-O. These observations were corroborated by the results of previous studies, and confirmed that synthesis was preceded correctly [18, 76].

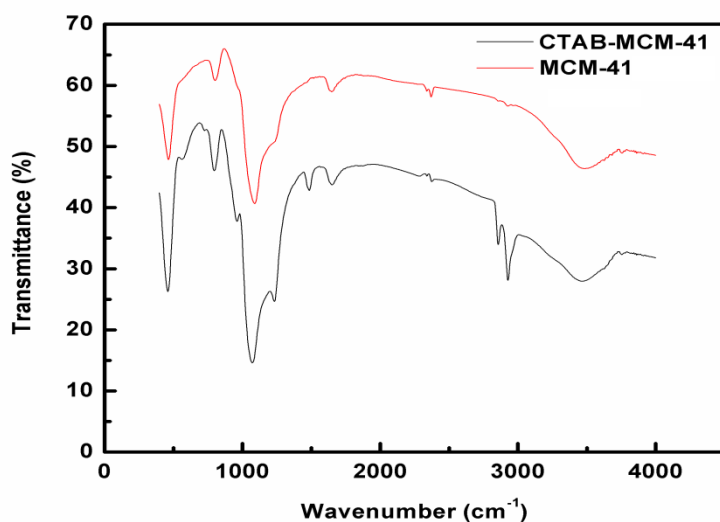


Figure 3-2 FT-IR spectra of the CTAB-MCM-41 and MCM-41

### 3.3.2. Extraction optimization

In  $\mu$ -SPE, there is dynamic partitioning of analytes between the sorbent material and the sample solution. To compare the performance of the mesoporous material for the adsorption of PFCAs with some commercial sorbents,  $\mu$ -SPE devices were packed with the commercial sorbents (C18, HayeSep-A, HayeSep-B, and Porapak-R) and evaluated against one another. All analysis was conducted under the most favorable experimental conditions obtained in the present work. The results are shown in the Figure 3-3 CTAB-MCM-41 had the highest extraction efficiency compared with the other sorbents. It is interesting that CTAB-MCM-41 had even higher adsorption efficiency than the calcined type. This may be attributed to the hydrophobicity created by the surfactant template in CTAB-MCM-41. We speculate that the surfactant template can alter the surface chemistry and population of sorption sites of the material. Therefore, both the silanol groups and cationic groups favored the adsorption of organic compounds. On the other hand, PFCAs are anionic pollutants that can be trapped by the



hydrophobic and positively charged surfaces of CTAB. The same phenomenon has also been observed in the extraction of PFACs by chitosan-coated octadecyl-functionalized magnetite nanoparticles [77, 78] and CTAB-coated silica [79]. Adsorption was thus driven by hydrophobic interactions and electrostatic attraction. The ordered structure of the CTAB-MCM-41 conceivably enforced this interaction. Many studies have also reported the higher adsorption performance of non-calcined mesoporous material sorbents for organic species [18]. Among the commercial sorbents, C18 had a higher extraction efficiency for PFACs due to hydrophobic interactions, followed by HayeSep-B due to relatively higher polarity. Porapak-R and HayeSep-A had the lowest extraction efficiencies. Hence CTAB-MCM-41 was used for the remaining of the work.

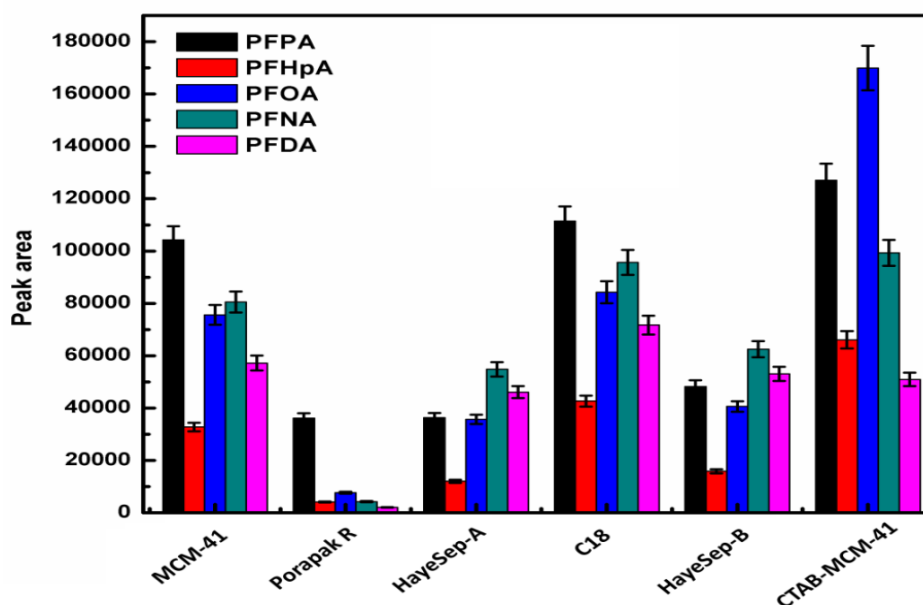


Figure 3-3 Effect of sorbent type on  $\mu$ -SPE.

Other parameters influencing extraction efficiency such as extraction time, desorption time, desorption solvent, and salt concentration were investigated as follows:

After extraction, the analytes were desorbed from the  $\mu$ -SPE device by ultrasonication with suitable common organic solvents. One nonpolar solvents (hexane), three polar aprotic solvents (acetone, acetonitrile, dichloromethane), and one polar protic solvent (methanol) were investigated (refer to Appendix 1 for more details about solvents used). The results are shown in Figure 3-4- a. Methanol and acetone gave the highest peak areas for all analytes in general, followed by acetonitrile. For all the analytes, there are no great differences in results obtained by methanol and acetone. However, only for PFHpA there is a significant difference between average peak areas; the average value obtained for PFHpA in acetone is higher than methanol. Hence eventually the acetone was chosen.

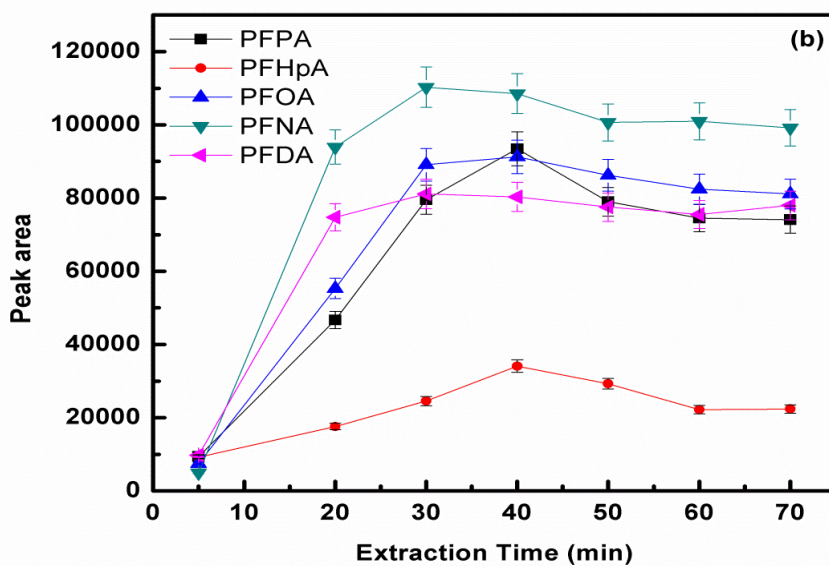
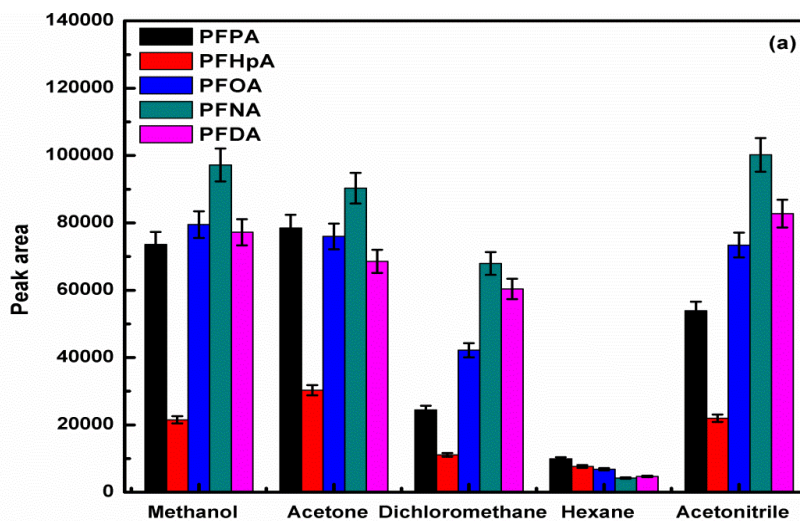
Given that  $\mu$ -SPE is an equilibrium-based and time-dependent process, the effect of extraction time was investigated. Extraction times were varied between a range of 5 and 70 min. Figure 3-4-b shows the extraction time profiles. There was a rapid increase in extraction from 5 to 20 min followed by a more gradual increase up to 40 min. Extraction after 40 min decreased slightly or remained invariant. The reason is after the proper extraction time, the active sites of the sorbent are no longer available for analytes, because they have been already occupied by analytes. Hence extraction efficiencies remained invariant. On the other hand, by adsorption of the analytes on the sorbent surface, the physical properties of the surface change and new analytes might be repelled by the surface. Hence slightly decreases in the numbers of analyte absorbed by surface might be also observed. This is a common observation in microextraction [80, 81]. As it can be seen there is no major difference in the extraction efficiencies for 30 min and 40 min, except that for PFPA 40 min gives relatively higher peak area in

comparison to 30 min. However the peak area obtained in 30min (for PFPA) is sufficient to provide desirable signals. Regarding the above observation and in order to minimize overall time of the analysis, 30 min was taken as an acceptable extraction time.

The effect of desorption time was also investigated by considering the time in the range of 5-20 min. Figure 3-4-c shows the results. Although there were no significant differences among the various desorption times, 15 min was selected to ensure complete desorption of analytes. Had the overall analysis time been a critical factor, 10 min could have been chosen as well. In order to examine the possible carryover effect, a used  $\mu$ -SPE device was further desorbed in methanol for another 20 min; however, no analytes were detected. Thus, the same  $\mu$ -SPE device could be reused for additional experiments without any concern for carryover effects. Nevertheless, in this work a fresh  $\mu$ -SPE bag was used each time.

The salting-out effect is one factor that is often studied to maximize the efficiency of extraction and microextraction. This effect was determined by adding NaCl (to give 5%-30% [w/v] salt concentration in the samples). The results (Figure 3-4-d) demonstrated that the extraction efficiency increased to a maximum at 15% NaCl concentration. This phenomenon arises from the engagement of water molecules in the hydration spheres around the ionic species and decrease in available water molecule to dissolve solute compounds which leads to decrease their solubility in the aqueous phase. However, reduced extraction was observed when the salt concentration was raised from 15% to 30%. It has been assumed that increasing the salt concentration could reduce the diffusion rate of the target analytes into the membrane and sorbent.

Moreover the salt molecules may compete with target molecules in entrapment by the surface of sorbent, which leads to reduction in the extraction results. This observation is often encountered in microextraction studies [11, 12, 82-84]



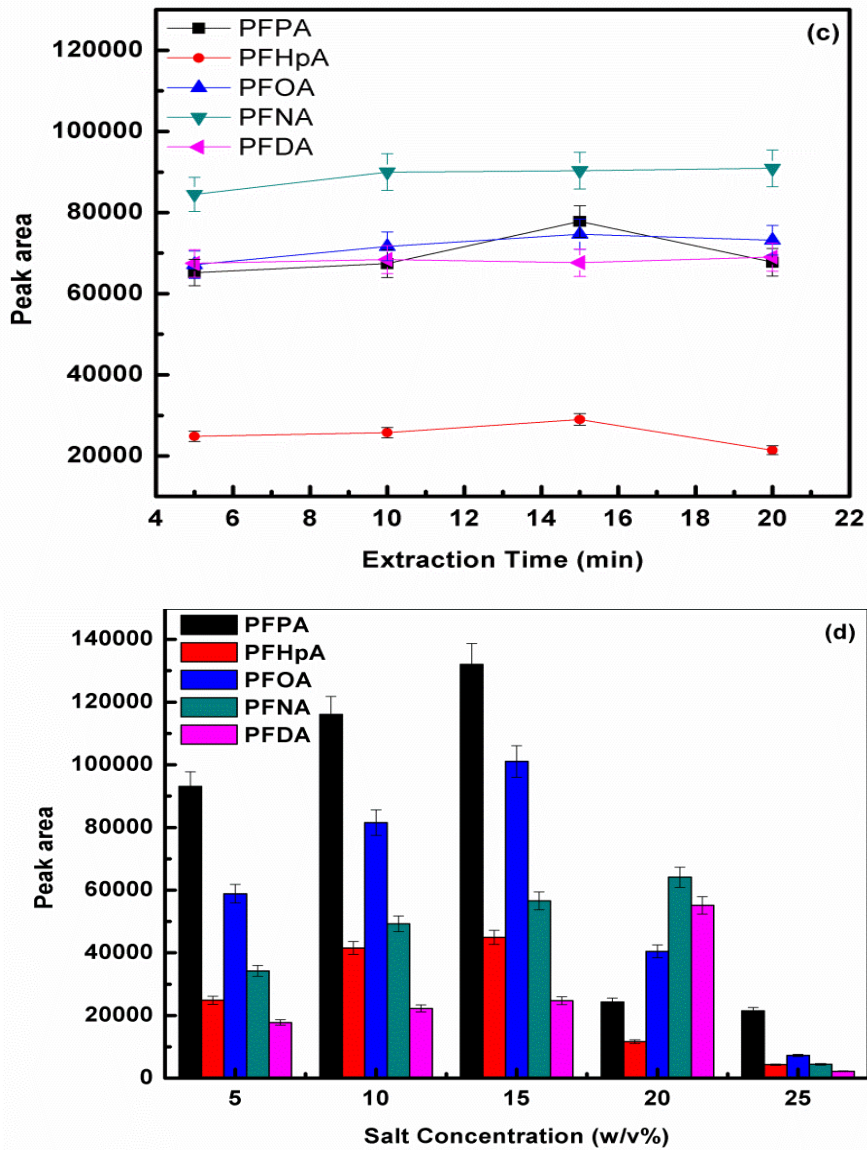


Figure 3-4 Influence of the different parameters on  $\mu$ -SPE, (a): desorption solvent, (b): extraction time, (c): desorption time, (d): salt concentration

### 3.3.3. Method validation

Under the most favorable extraction conditions (extraction time: 30 min, desorption time: 15 min, desorption solvent: acetone, salt concentration: 15% w/v, sorbent: CTAB-MCM-41), the repeatability, linearity, limits of quantification (LOQs), and limits of detection (LODs) were calculated. Using spiked ultrapure water samples,

the LODs and LOQs of the method were calculated based on the mass of each analyte such that it produced signal to noise ratios of 3 and 10, respectively, at the specific retention time. The linearity of the calibration curve was examined for each analyte using an aqueous standard solution containing a mixture of the analytes at concentrations between 1 and 50 ngL<sup>-1</sup>. Two ranges of linearity were observed: the first from 1 to 5 ngL<sup>-1</sup>, with coefficients of determination ( $r^2$ ) of between 0.987 and 0.995, and the second range related to higher analyte concentrations from 5 to 50 ngL<sup>-1</sup>, with  $r^2$  values of between 0.992 and 0.999. Two different ranges for calibration curves have been reported previously [85, 86], the plausible reason being related to equilibrium time. Probably, at very low analyte concentrations, the equilibrium time is long; however, it is reduced with increasing concentrations. The LODs, LOQs, and relative standard deviations (RSDs) of the determinations (n=3) are reported in Table 3-3. These results are in line with some previously reported studies [77-79].

These figures of merit indicate this method has excellent stability, and reliability, and satisfactory sensitivity. The obtained results were comparable with those reported in previous studies as well (Table 3-3). Possible carryover effects were addressed by a randomized injection and washing process, as described before. The accuracy and repeatability of the tests were studied by a three-replicate analysis of the same sample set.

Table 3-3 Analytical parameters of the proposed method

Analyte	r <sup>2</sup> (1-5 ngL <sup>-1</sup> )	RSD (%) (1-5 ngL <sup>-1</sup> )	r <sup>2</sup> (5-50 ngL <sup>-1</sup> )	RSD (%) (5-50 ngL <sup>-1</sup> )	LOD	LOQ	Ref. [87]		Ref.[78]		Ref. [75]		Ref. [79]	
							LOD	RSD	LOD	RSD	LOD	RSD	LOD	RSD
PFOA	0.9951	1.9	0.9933	2.1	0.02	0.07	-	-	-	-	-	-	-	-
PFHpA	0.9940	5.9	0.9970	10.5	0.02	0.08	-	-	-	-	-	-	0.28	2.3
PFOA	0.9869	2.7	0.9997	5.3	0.06	0.20	0.19	6.7	0.14	8.8	0.15	7.8	0.07	5.6
PFNA	0.9946	4.5	0.9925	8.8	0.08	0.28	0.14	3	0.31	2.7	0.11	7.0	0.1	3.9
PFDA	0.9942	5.9	0.9959	10.5	0.06	0.21	0.05	9.4	0.23	4.5	0.03	6.2	0.05	5.1

### 3.3.4. Analysis of real samples

Samples of rain water and river water were analyzed with this method to evaluate its applicability to real-world environmental aqueous samples. The concentrations and recoveries obtained for the analysis, expressed as the mean value (n=3), are listed in the Table 3-4. Given that PFCAs are ubiquitous, all samples, as expected, were found to contain PFCAs. As shown by the results, individual concentrations of PFCAs ranging between 0.52 and 1.17 ng<sup>-1</sup> in rain water, and between 1.29 and 2.03 ngL<sup>-1</sup> in river water, were detected, with RSDs ranging between 2.03% and 12.07% and between 3.39% and 7.12%, respectively. The relatively higher level of PFOA determined corroborated the results of previous studies [78, 79].

Real samples were spiked with 10 ngL<sup>-1</sup> of standards. The relative recoveries (RR%) were calculated by using the equation below [88-91]:

$$RR\% = (C_{\text{found}} - C_{\text{real}})/C_{\text{added}} \quad (3-1)$$

where C<sub>found</sub> is the concentration (ngL<sup>-1</sup>) of the analyte in the real sample which is added by known amount of the standard spiked into it (10 ngL<sup>-1</sup>); C<sub>real</sub> (ngL<sup>-1</sup>) is the concentration of the analyte in the real sample; and C<sub>added</sub> (ngL<sup>-1</sup>) is the concentration of a known amount of the standard spiked into the real sample. The results are shown in Table 3-4. The RR% values for the analytes ranged from 73.6% to 95.8 (rain water),

and 72% to 127% (river water). LC-ESI-MS/MS traces of rain water extracted by the developed method without and with spiking are shown in Figure 3-5.

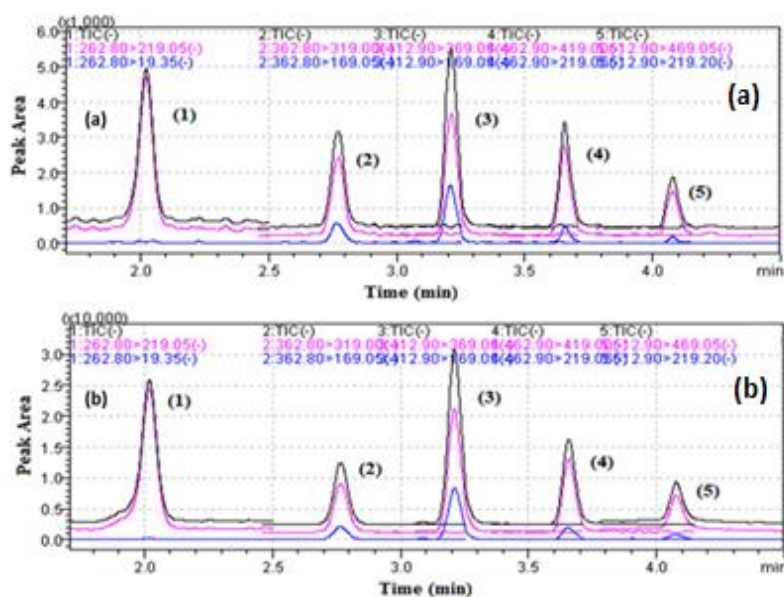


Figure 3-5 LC-ESI-MS/MS traces of rain water extracted by the developed method. (A) Unspiked rain water sample. (B) rain water sample spiked at 10 ngL<sup>-1</sup>. Peaks: (1) PFPA, (2) PFHpA, (3) PFOA, (4) PFNA, (5) PFDA.

### 3.3.5. Evaluation of matrix effects

The matrix effects posed by environmental samples on extraction efficiencies were investigated. In order to evaluate the effect of the matrix on the MS signals (either suppression or enhancement), real samples and ultrapure water were spiked with a solution (containing 10 ngL<sup>-1</sup> of each analyte) and processed as described above. The absolute ratio of signal of the analyte in the ultrapure water and samples was compared. The results are summarized in Table 3-4. A value < 1 represents signal suppression, and a value > 1 represents signal enhancement due to the co-elution of matrix compounds. Only minor effects on ionization efficiencies were observed. These observations



evidently showed that the polypropylene membrane had a significant positive impact by at least reducing matrix effects, and could offer suitable protection of the sorbent against potentially adverse interferences in complex samples. Considering the greater complexity of river water than rain water, higher matrix effects were observed for river water samples. Nevertheless, it is worthwhile to mention that neither the retention times nor the peak shapes in LC were affected by the respective matrices.

Table 3-4 Analytical results for the determination of PFCAs in river water and rain water

Analyte	Concentration (ngL <sup>-1</sup> ) detected	RSD % (n = 3)	RR (%) from spiked sample(10 ngL <sup>-1</sup> )	Matrix effect in ionization
<b>Rain Water</b>				
PFPA	0.52	2.03	95.8	1.02
PFHpA	1.11	4.75	86	0.86
PFOA	1.17	4.37	89.2	1.01
PFNA	1.12	8.05	64.7	0.93
PFDA	1.01	12.07	73.6	0.94
<b>River Water</b>				
PFPA	1.52	3.39	126	1.13
PFHpA	1.29	4.65	72	0.99
PFOA	2.03	6.53	127	1.17
PFNA	1.29	5.62	125	1.13
PFDA	1.31	7.12	127	1.19

### 3.4. Conclusion

$\mu$ -SPE followed by LC-ESI-MS/MS was developed for the determination of PFCAs at trace levels in water samples. The  $\mu$ -SPE device comprised of a porous polypropylene membrane bag containing 5 mg sorbent. The membrane bag acted as a clean-up filter and prevented matrix compounds from interfering with the extraction process. Calcined and non-calcined MCM-41, as silica-ordered mesoporous materials, were used as sorbents in  $\mu$ -SPE for the extraction of five PFCAs—PFPA, PFHpA, PFOA, PFNA, and PFDA—from aqueous media. The performances of these two sorbents were compared with other sorbents such as C18modified silica, HayaSep-A,

HayeSep-B, and Porapak-R. It was found that non-calcined MCM-41 showed better extraction performance for the analytes considered. Parameters influencing extraction efficiency, such as desorption time, extraction time, desorption solvent, and salt concentration, were investigated. The effect of the matrix on MS signals (suppression or enhancement) was also evaluated. Only minor effects on ionization efficiencies were observed. The developed method proved to be convenient and offered good sensitivity and reproducibility. The LODs ranged from 0.02 ngL<sup>-1</sup> to 0.08 ngL<sup>-1</sup>, with a relative standard deviation of between 1.9 and 10.5. It was successfully applied to the extraction of PFCAs in river and rain water samples. As expected from the ubiquitous nature of PFCAs, contamination at low levels was detected for some analytes in the samples (with the highest concentration recorded for PFOA). Satisfactory relative recoveries ranging between 64% and 127% at spiking levels of 10 ngL<sup>-1</sup> of each analyte were obtained.

## **CHAPTER 4: Analysis and determination of perfluorinated carboxylic acids in human plasma**

### **4.1. Introduction**

Unlike some of the well-defined persistent organic pollutants, which do tend to accumulate in pose tissue, amphiphilic ionic PFCs prefer to bind to blood proteins and accumulate in the blood, liver, kidney, and gallbladder [92, 93]. Thus, modes of exposure to these compounds and their levels in the body can be assessed by monitoring them in the blood. A powerful sample preparation is the most crucial issue in the analysis of PFCs in such complex matrices especially with respect to their heterogeneous nature [57]. In the current study we developed the previous method (Chapter 3) for analysis and determination of PFCAs from human plasma. The protective membrane in  $\mu$ -SPE may reduce the matrix effect.

As most of the time biological samples are not available in large amount, experimental design was used to optimize extraction conditions of the  $\mu$ -SPE. In general one of the excellent aims of experiment design is doing smarter experiments which help to obtain most data and information with the fewest experiments. Hence, in the present study central composite design (CCD) with response surface methodology (RSM) is applied to achieve the optimum condition of extraction. To the best of our knowledge, this is the first time that experimental design has been used for evaluation of experimental conditions of  $\mu$ -SPE. Under the optimized conditions, figures of merit for the proposed method are reported. The performance of the current method is compared with those reported in previous studies.

## **4.2. Experimental**

### **4.2.1. Chemicals and materials**

Five PFCAs, including PFPA, PFHpA, PFOA, PFNA, and PFDA were used as in the chapter 3 (section 3.2.1), in addition PFDoDA (96%) was purchased from Alfa-Aesar (Heysham, Lancs, UK). The other chemicals were same as those in the previous chapter (Section 3.2.1). Formic acid (HCOOH, 95%) was used for the protein precipitation and was bought from Sigma-Aldrich (Steinheim, Germany).

### **4.2.2. Plasma sample collection**

Plasma samples were supplied by the School of Medicine of National University of Singapore. The samples were lyophilized plasma, prepared in 1995 from a pool of fresh blood collected from 18 volunteers (Singaporean, male and female, aged 19-47 years). The samples were anti-coagulated with 3.8% sodium citrate and 2-[4-(2-hydroxyethyl) piperazin-1-yl] ethanesulfonic acid was added to stabilize the pH and then freeze dried and stored at -80 °C. Samples were primarily prepared by protein precipitation with HCOOH [57]. For the later one, samples were thawed at room temperature, and were diluted with ultrapure water. The mixture of 80/20 (v/v%) of 0.1% HCOOH solution in ultrapure water and 0.1% HCOOH solution in methanol were added to sample. After centrifuging, supernatant solutions were collected and kept at -31 °C. Working solutions containing all of the PFCAs at different concentrations were prepared by spiking them into the supernatant solution. pH adjustment was not carried out on samples.

### 4.2.3. Synthesis of sorbent and extraction procedure

CTAM-MCM-41 was synthesis based on procedure as explained in chapter 3 (section 3.2.2). For the extraction procedure 15mg of sorbent was packed in a 1.5 cm × 1cm polypropylene bag and extractions were carried out accordingly. Eventually 5 µL of the extract was injected into the LC-MS/MS. A blank solution of methanol were extracted and analysed frequently and whenever a new bottle of solvent was used. No contamination was detected above the limit of detection. All experiments were conducted in triplicate.

### 4.2.4. Instrumental analysis

Instrumental analysis performed were the same as mentioned in Chapter 3 (section 3.2.6). The optimized obtained parameters were similar as previous chapter (Table 3-2). PFDoA was also included in this study. The results for the instrumental optimization condition for PFDoA have been summarized in Table 4-1.

Table 4-1 Experimental conditions of negative ion ESI-MS/MS for the PFDoA

Analyte	Chain length	Molecular mass	Retention time (min)	Precursor ion (m/z)	Product ion 1			Product ion 2				
					(m/z)	DP (V)	CE (V)	CXP (V)	(m/z)	DP (V)	CE (V)	CXP (V)
PFDoA	C12	614	4.91	613.00	569.00	24	15	38	169.20	24	30	30

#### **4.2.5. RSM and data processing**

As mentioned the RSM is an effective statistical approach for responses which are influenced by different factors and this study was the first attempt of the systematic study of the optimization of effective parameters on the  $\mu$ -SPE and their interactions. Two-level design can only lead to linear models; consequently it cannot give any information about the non-linear relations. By use of the full factorial design with more than two levels, the number of experiments will increase dramatically. So, for overcoming this issue CCD is a robust choice which allows higher number of levels without an increase in experiments at every combination of factor levels. It combines two-level factorial design with star (axial) and central points [80]. Optimization of the parameters and evaluation of their interaction was performed by CCD. The software package, Design expert (version 8.0.7.1, Stat-Ease, Minneapolis, Minnesota, USA) was used for design and statistical analysis.

### **4.3. Results and discussion**

#### **4.3.1. Optimization of extraction**

Optimization of qualitative parameters: After extraction, the analytes are desorbed from the  $\mu$ -SPE device by ultrasonication with a suitable organic solvent, which should be quite compatible with polypropylene membrane as well. Five common organic solvents consisting of nonpolar solvents, polar protic solvents and polar aprotic solvents were investigated: Hexane, acetone, dichloromethane, acetonitrile, and methanol (refer to Appendix 1 for more information about the properties of used solvents). The results are shown in Figure 4-1. Hexane with

lowest dielectric constant and as the most non-polar solvent showed the lowest extraction efficiency, and methanol as the only polar protic solvents, showed the highest extraction efficiency. Hence, methanol was chosen as extraction solvent. The rest of solvents, as a group of polar aprotic solvents, showed moderate and (more or less) same results.

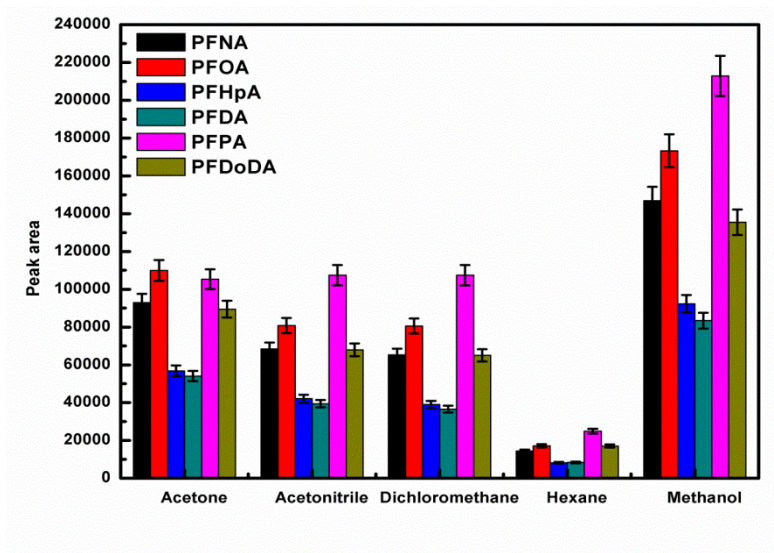


Figure 4-1 Influence of desorption solvent on  $\mu$ -SPE

Optimization of numeric parameters: Based on the previous studies in the use of the  $\mu$ -SPE, regardless of kind of sorbent and desorption solvent, other factors like extraction time, desorption time, and salt concentration are some important factors which are effective in enhancing extraction efficiency. The effect of these parameters on the extraction efficiency was studied simultaneously by CCD (Table 4-2)

As mentioned CCD is one of the most frequently used response surface designs that combine a two level factorial design with additional points to allow fitting of a full quadratic polynomial, against factorial design that uses only two levels. These points consist of factorial points ( $N_f = 2^f$ ), ( $f$  is number of factors) with additional star (axial)

points ( $N_a = 2f$ ), and the points at the center of the experimental region (central points,  $N_0$ ), which are usually repeated to get a good estimation of experimental error (pure error). The star points are located at  $+\alpha$  and  $-\alpha$  from the center of the experimental domain [94]. Orthogonally and reliability can be evaluated by  $\alpha$  and can be calculated from Eq.(4-1) [90].

$$\alpha = \sqrt[4]{Nf} \quad (4-1)$$

The total number of the experiment was equal to 20 ( $N = 2^f + 2f + N_0$ ), consisting of 6 central points and 14 non-central points. Normalized extraction efficiency (extraction efficiency being defined as a ratio of concentration after and before extraction) was chosen as an experimental response. To normalize the extraction efficiency, all of the experiments were first conducted based on Table 4-2. Then the extraction efficiency of each analyte was divided by its smallest extraction efficiency that was attained from the entire experiments. The normalized extraction efficiency for the analytes were subsequently added for each run and utilized in the calculation of the total normalized extraction efficiency (response) [90].



Table 4-2 Experimental factors, levels, and design matrix (coded) with responses

Factor	Symbol	Level				
		- $\alpha$	-1	0	+1	+ $\alpha$
Extraction time (min)	A	3.2	10	20	30	36.8
Desorption time (min)	B	6.6	10	15	20	23.4
Salt concentration (w/v%)	C	4.9	10	17.5	25	30.1

Run	A	B	C	Response
1	-1	-1	1	0.60
2	0	0	0	5.65
3	0	0	0	5.74
4	1	-1	1	2.60
5	0	0	0	5.83
6	-1	1	-1	1.31
7	1	-1	-1	3.04
8	-1	0	0	0.06
9	0	-1	0	0.71
10	-1	1	1	1.00
11	0	0	0	4.19
12	0	0	1	0.04
13	1	1	-1	4.56
14	1	1	1	1.71
15	0	0	-1	0.36
16	0	1	0	3.34
17	0	0	0	5.48
18	0	0	0	5.55
19	-1	-1	-1	0.60
20	1	0	0	5.96

The ANOVA was used to evaluate the data (Table 4-3). The F-value of 16.78, indicated that the model (quadratic) was significant. The "Lack of Fit (LOF) F-value" of 2.25 implied that it was insignificant relative to the pure error. "Adeq Precision" measured the signal to noise ratio. A ratio greater than 4 was desirable. In this case the ratio was 10.88 indicating an adequate signal, so the suggested model could be used to navigate the design space [95].

CCD is a second-order model that can be expressed as the following equation for three independent variables [90].

$$Y = a_0 + \sum_{i=1}^3 a_i x_i + \sum_{i=1}^3 \sum_{j=1}^3 a_{ij} x_i x_j + \sum_{i=1}^3 a_{ii} x_i^2 \quad (4-2)$$

where Y is the dependent variable (response);  $x_i$  is the independent variable (extraction time, desorption time and salt concentration); the  $a_i$  terms represent the regression

coefficient of the model and  $a_0$  is the deviation between the observed and predicted responses in the design point (error). Thus in this study, the second order polynomial with most logical statically parameters (higher F-value, and low standard error) were considered as the appropriate response surface model for CCD.

Table 4-3 ANOVA for CCD.

Source	Sum of squares	d.f. <sup>a</sup>	Mean square	F-value <sup>b</sup>	p-value <sup>c</sup> Prob > F	
Model	91.54	9	10.17	16.78	< 0.0001	significant
A	24.59	1	24.59	40.57	< 0.0001	
B	2.78	1	2.78	4.58	0.0579	
C	1.25	1	1.25	2.07	0.1808	
AB	0.029	1	0.029	0.048	0.8308	
AC	1.11	1	1.11	1.83	0.206	
BC	0.91	1	0.91	1.51	0.2477	
A <sup>2</sup>	8.37	1	8.37	13.81	0.004	
B <sup>2</sup>	17.75	1	17.75	29.28	0.0003	
C <sup>2</sup>	44.41	1	44.41	73.28	< 0.0001	
Residual	6.06	10	0.61			
Lack of Fit <sup>d</sup>	4.2	5	0.84	2.25	0.1967	not significant
Pure Error	1.86	5	0.37			

<sup>a</sup> Degrees of freedom

<sup>b</sup> Test for comparing model variance with residual (error) variance.

<sup>c</sup> Probability of seeing the observed F-value if the null hypothesis is true.

<sup>d</sup> The variation of the data around the fitted model.

F-value less than 0.0500 indicated the statistical significance of an effect at the 95% confidence level. So based on the results, extraction time was one of the significant model terms. The magnitudes of coefficients in the regression equation in terms of the coded factors (Table 4-4) were used to evaluate statistical significance. The absolute value of the coefficient showed the amount of the effectiveness of the term.

Table 4-4 Coefficients of the regression equation for simultaneous determination of PFCAs.

Parameters	Coefficients of the regression
Constant ( $a_0$ )	+5.40
A	+1.34
B	+0.45
C	-0.30
A*B	-0.060
A*C	-0.37
B*C	-0.34
A <sup>2</sup>	-0.76
B <sup>2</sup>	-1.11
C <sup>2</sup>	-1.76

Figure 4-2 shows the linear effect of changing of each variable in the extraction efficiency very clearly and logically.

From Figure 4-2-a it is clear that by increasing extraction time from 10 to 25 min, there was a rapid increase in extraction efficiency. Probably, more time was required for the analyte to diffuse through the porous membrane, and onto the sorbent material. Extraction efficiency is highly depends on the mass transfer of the target molecules from the sample solutions to the sorbent. There was no meaningful increase after 25 min.

The optimum desorption time was set at between 15-17 min (Figure 4-2-b) and after this time extraction began to decrease. This is a common observation that has been reported in other microextraction studies [96-98].

Figure 4-2-c demonstrates the effect of salt concentration on the extraction efficiency. It is clear from the plot that the extraction efficiency increased to a maximum when NaCl concentration was in the range between 14 and 19%. Addition of the salt usually decreased solubility of organic compounds in water (salting out effect). This phenomenon is due to the engagement of the water molecule in the hydration spheres around the ionic species which leads to decrease in the available water molecules to dissolve organic compounds. However, when the salt concentration was raised from 19%, the mass transfer process from sample solution to the sorbent was conceivably inhibited, probably due to increased viscosity of the solution, leading to changes in the physical properties of the diffusion layer near organic film, which could

reduce the diffusion rate of the target analyte into the membrane and sorbent [99]. All these observations are in accordance with sorbent based extraction methods.

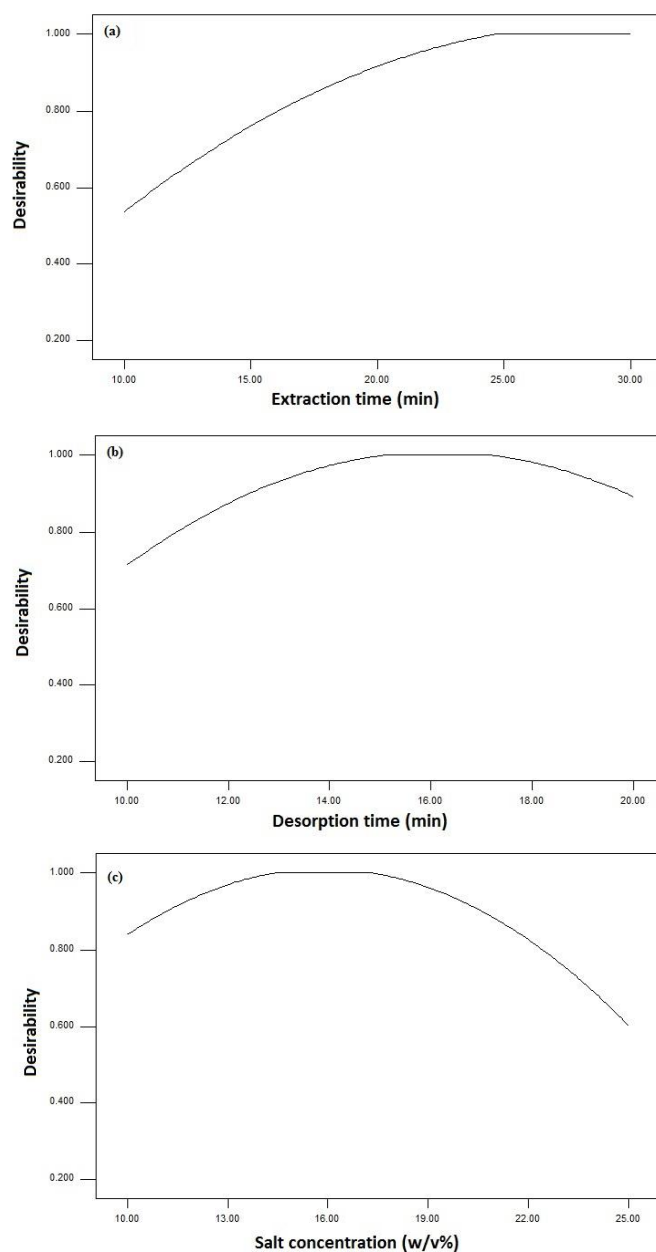


Figure 4-2 Linear effect of changing of the each variable on the extraction efficiency: (a) Extraction time, (b) desorption time, (c) salt concentration.

Figure 4-3 shows the three dimensional (3D) and contour plots of the model based on the variables. The responses were mapped against two experimental factors while the third one was kept constant.

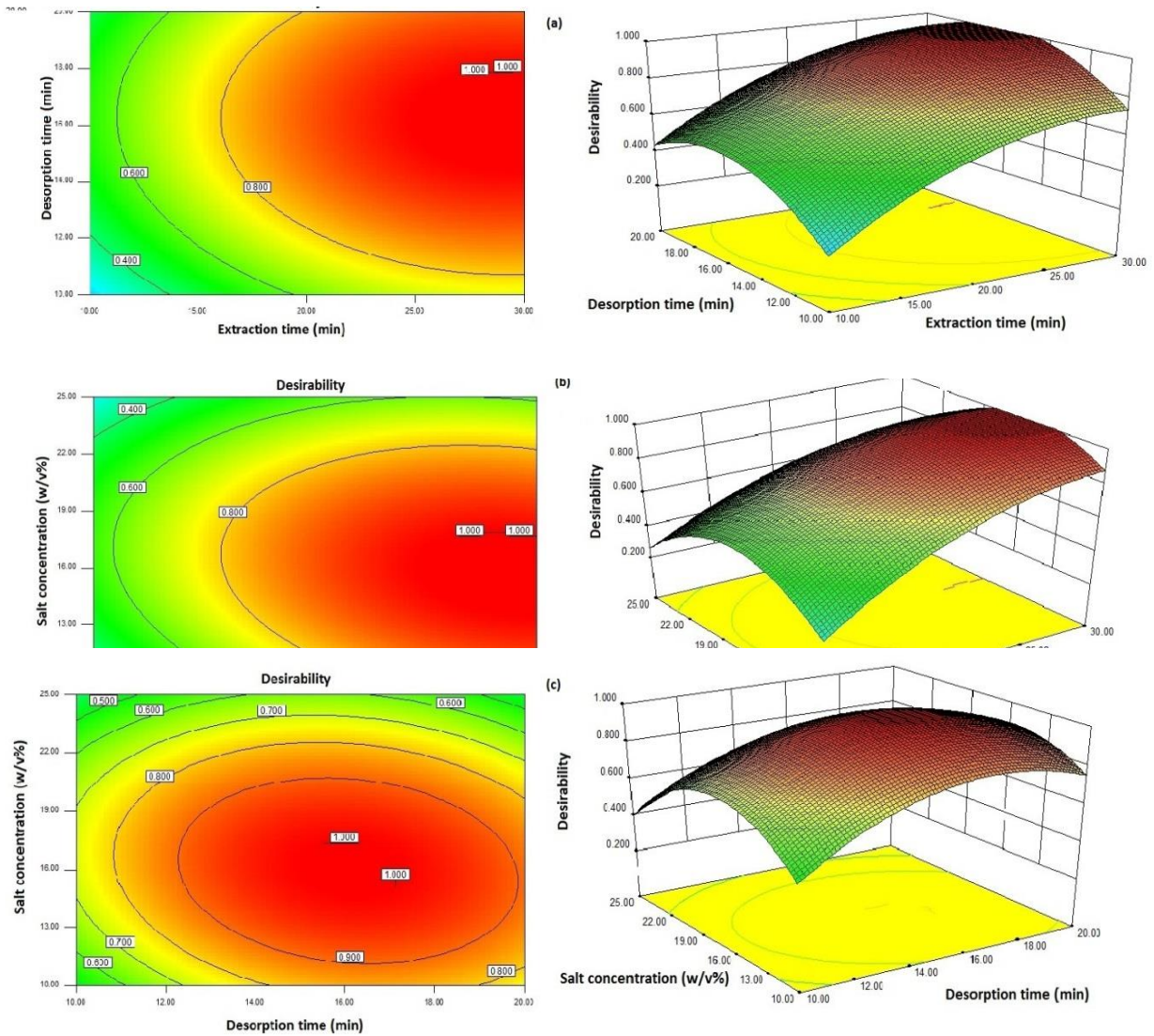


Figure 4-3 3D response surfaces with contour plots of responses against different operating variables:

- (a) extraction time-desorption time, (b) extraction time-salt concentration, (c) salt concentration-desorption time.

Eventually the optimization mode of Design-Expert 8.0.7.1 was used to obtain the optimum conditions.

#### 4.3.2. Method validation

Under the optimal conditions, the figures of merit of the proposed method were investigated according to recommendations of the US Food and Drug Administration (USFDA) guidelines [100].

For each PFCA, a calibration plot was prepared. The linearity of the calibration curve was examined in concentration ranges between 100 and 5000 ngL<sup>-1</sup>. A good linearity of the response with R<sup>2</sup> value of between 0.986 and 0.995 were obtained for all analysts.

The LODs at signal to noise ratio of 3 were in the range of between 21.23 and 65.07ngL<sup>-1</sup>. The LOQs at signal to noise ratio of 10, were in the range of between 70.77 and 216.91 ngL<sup>-1</sup> (Table 4-5). The results of the developed method in comparison with other analytical techniques for determination of same analytes from human plasma showed that the developed method not only offered acceptable efficiency, but also it used beneficial with respect to simplicity, low cost, short time, and easy manipulation (Table 4-6).

Table 4-5 Obtained figures of merit of the proposed method

Analyte	LOD (ngL <sup>-1</sup> )	LOQ (ngL <sup>-1</sup> )	R <sup>2</sup>	Linear range (ngL <sup>-1</sup> )	RSD %
PFPA	23.94	79.80	0.995	100-5000	6.66
PFHpA	65.07	216.91	0.986	100-5000	15.22
PFOA	27.24	90.82	0.988	100-5000	6.34
PFNA	30.48	101.62	0.992	100-5000	5.75
PFDA	49.09	163.66	0.991	100-5000	5.68
PFDoDA	21.23	70.77	0.993	100-5000	6.24

The precision of the analysis, defined as the RSD%, was determined for intra-day and inter-day (3 days) assay to evaluate effect of time on the analysis. The results show that the average RSD% of the concentration were 2.9 and 13.1 for intra-day and inter day analysis respectively. Thus, the analysis of samples in the same day of extraction is recommended for more reliable results.

#### 4.3.3. Analysis of real samples

The quantification data for different real samples are reported in Table 4-7. As was expected from ubiquities nature of FCAs, the samples were contaminated with some analytes. The highest concentration of contamination was related to PFOA. Contamination with PFDA and PFDoDA were not observed in any of the samples.

In order to determine the method accuracy (error %), and relative recovery (RR %), each sample was spiked at 3000 ngL<sup>-1</sup> of the mixture of analytes and analysis was carried out. RR% and error% were calculated by the following equations:

$$RR\% = (C_{\text{found}} - C_{\text{real}}) / (C_{\text{added}}) \quad (4-3)$$

$$\text{Error \%} = \text{Relative recovery \%} - 100 \quad (4-4)$$

Where  $C_{\text{found}}$ ,  $C_{\text{real}}$  and  $C_{\text{added}}$  are concentration (ngL<sup>-1</sup>) of the analyte addition to the given amount of standard into the real sample, the concentration of the analyte in the real sample, and the concentration of a known amount of standard spiked into the real sample, respectively. As shown in the table, proposed method showed good RR% (87.58-102.45). The amounts of RR% are comparable with those reported in some previous methods (Table 4-7) and showed evidently that polypropylene membrane had

a positive impact on the elimination of the matrix effect. It is worthwhile to mention that neither the retention time, nor the signal shape in LC was effected by the presence of matrix components in the extract. Chromatograms obtained for sample 1 are shown in Figure 4-4.

#### **4.4. Conclusion**

The identification and quantification of PFCs in biological complex matrices is affected by matrix effects (ion suppression and/or enhancement). In the present study,  $\mu$ -SPE has been developed for the determination of trace levels PFCAs from human plasma by fabricating a small polypropylene made bag, containing mesoporous silica sorbent. Extraction time, desorption time and salt concentration were chosen as the most effective parameters and were optimized simultaneously by use of CCD. Under the optimized extraction conditions, good linearity in the range between 100 and 5000  $\text{ngL}^{-1}$  was obtained with the coefficient of determination between 0.986 and 0.995. The LODs (were obtained in the range between 21.23 and 65.07  $\text{ngL}^{-1}$ , and LOQs were obtained in the range between 70.77 and 216.92  $\text{ngL}^{-1}$ . The relative recoveries of spiked PFCAs in different samples were in the range between 87.58 and 102.45%. Regardless of the easy manipulation, the obtained results verified the reliability and feasibility of the developed method.



Table 4-6 Performance of the analytical methods used to quantify PFCAs in blood sam

Extraction technique	Instrument	Analyte	Matrix	Linear range (ngL <sup>-1</sup> )	LOD (ngL <sup>-1</sup> )	LOQ (ngL <sup>-1</sup> )	RSD%	R <sup>2</sup>	Mean recovery	Ref.
Anion exchange-SPE	LC-MS	PFNA	Human blood						95.9	[51]
Anion exchange-SPE	LC-MS	PFOA	Human blood						93.7	[51]
Ion pair –SPE	LC-MS	PFHA	Human blood	500-58000	100	500	24.3			[101]
Ion pair –SPE	LC-MS	PFOA	Human blood	800-136000	500	800	6.4			[101]
Ion pair –SPE	LC-MS	PFNA	Human blood	500-86000	100	500	10			[101]
Ion pair –SPE	LC-MS	PFDA	Human blood	500-137000	100	500	15.4			[101]
Ion pair –SPE	LC-MS	PFDoDA	Human blood	90-116000	300	900	25.8			[101]
Ion pair –SPE	LC-ESI-MS/MS	PFOA	Human serum						97	[102]
Ion pair –SPE	LC-ESI-MS/MS	PFOAH	Human serum						110	[102]
Ion pair –SPE	LC-ESI-MS/MS	PFOA	Human serum						84	[102]
Ion pair –SPE	LC-ESI-MS/MS	PFOA	Human serum						99	[102]
On-line SPE	LC-MS/MS	PFHpA	Human serum		600				114	[103]
Off-Line SPE	LC-MS/MS	PFHpA	Human serum		3200				60	[103]
On-line SPE	LC-ESI-MS/MS	PFOA	Human serum		105				200	[103]
Off-Line SPE	LC-ESI-MS/MS	PFOA	Human serum		91				100	[103]
On-line SPE	LC-ESI-MS/MS	PFNA	Human serum		109				200	[103]
Off-Line SPE	LC-ESI-MS/MS	PFNA	Human serum		82				100	[103]
On-line SPE	LC-ESI-MS/MS	PFDA	Human serum		96				200	[103]
Off-Line SPE	LC-ESI-MS/MS	PFDA	Human serum		70				300	[103]
On-line SPE	LC-ESI-MS/MS	PFDoDA	Human serum		75				200	[103]
Off-Line SPE	LC-ESI-MS/MS	PFDoDA	Human serum		30				100	[103]
Direct protein precipitation*	UHPLC-MS/MS	PFHA	Cord blood plasma		240	780				[50]
Direct protein precipitation*	UHPLC-MS/MS	PFOA	Cord blood plasma		1230	1580				[50]
Direct protein precipitation*	UHPLC-MS/MS	PFNA	Cord blood plasma		67	840				[50]
Direct protein precipitation*	UHPLC-MS/MS	PFDA	Cord blood plasma		42	140				[50]
Direct protein precipitation*	UHPLC-MS/MS	PFDoDa	Cord blood plasma		63	210				[50]
on-line SPE	UHPLC-MS/MS	PFHpA	Human Plasma	10-1000	3	10	1.9	0.995		[52]
on-line SPE	UHPLC-MS/MS	PFOA	Human Plasma	10-1000	3	10	3.2	0.994		[52]
on-line SPE	UHPLC-MS/MS	PFDA	Human Plasma	10-1000	3	10	1.7	0.994		[52]
on-line SPE	UHPLC-MS/MS	PFPPA	Human Plasma	50-1000	15	50	3.2	0.995		[52]
Ion-pair SPE	LC-MS	PFDoDA	Human blood						102	[57]
Ion-pair SPE	LC-MS	PFNA	Human blood						110	[57]
Ion-pair SPE	LC-MS	PFOA	Human blood						118	[57]
Ion-pair SPE	LC-MS	PFDA	Human blood						112	[57]
Ion-pair SPE	LC-MS	PFHpA	Human blood						85	[57]

Table 4-7 Determination of PFCAs in different plasma samples

Sample	Analyte	C <sub>real</sub> (ngL <sup>-1</sup> )	C <sub>added</sub> (ngL <sup>-1</sup> )	C <sub>found</sub> (ngL <sup>-1</sup> )	RR%	Error%
Sample 1	PFPA	135.16	3000	3001.24	95.53	-5.47
	PFHpA	nd	3000	2961.55	98.71	-1.28
	PFOA	196.35	3000	2881.19	89.49	-10.51
	PFNA	162.85	3000	3140.40	99.25	-0.75
	PFDA	nd	3000	2986.12	99.54	-0.47
	PFDoDA	nd	3000	2643.48	88.12	-11.89
Sample 2	PFPA	109.20	3000	2750.73	88.05	-11.95
	PFHpA	nd	3000	2797.69	93.26	-6.74
	PFOA	165.11	3000	2910.41	91.51	-8.50
	PFNA	117.18	3000	2901.88	92.82	-7.18
	PFDA	nd	3000	3073.47	102.45	2.50
	PFDoDA	nd	3000	2927.45	97.58	-2.41
Sample 3	PFPA	119.45	3000	2862.05	91.42	-8.58
	PFHpA	nd	3000	2862.27	95.41	-4.59
	PFOA	168.78	3000	2796.12	87.58	-12.42
	PFNA	129.42	3000	2834.00	90.15	-9.84
	PFDA	nd	3000	3039.73	101.32	1.32
	PFDoDA	nd	3000	2968.94	98.96	-2.42

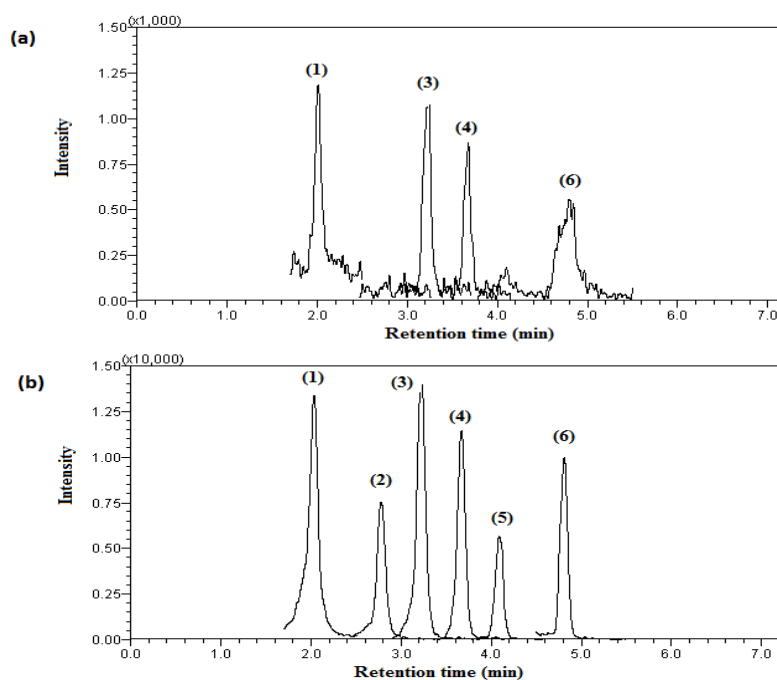


Figure 4-4 LC-ESI-MS/MS trace of plasma sample extracted by the developed method: (A) unspiked plasma sample, (B) plasma sample spiked at 3000 ngL<sup>-1</sup>. Peaks: (1) PFPA, (2) PFHpA, (3) PFOA, (4) PFNA, (5) PFDA, (6) PFDoDA

## **CHAPTER 5: Analysis and determination of perfluorinated carboxylic acids in fish fillet**

### **5.1. Introduction**

The relative importance of different routes of human exposure to PFCs is not yet well established; however, it has been suggested that water, food and dietary intake are potentially significant routes. In 2008, the European Food Safety Authority professed that considering human exposure assessment, exclusive data related to the PFCs levels in food is needed [6]. In this chapter, we report a simple protein precipitation with consequent extraction and concentration by  $\mu$ -SPE followed by LC-ESI-MS/MS analysis (as chapter 3,4) for the determination of 10 PFCAs including PFPA, PFHxA, PFHpA, PFOA, PFNA, PFDA, PFUdA, PFDoA, PFTrDA, and PFTeDA, in fish fillet. This protein precipitation sorption based assisted extraction method is used for the extraction of analytes and reducing interferences and matrix effects. A stable-isotopic internal standard (IS) is used for calibration. The method is then applied to the analysis of PFCAs in different local fish fillet samples.

### **5.2. Experimental**

#### **5.2.1. Chemicals and materials**

PFPA, PFHpA, PFOA, PFNA, PFDA, and PFDoA were the same analytes mentioned in chapters 4 and 5. In addition for the current study PFUdA (95%), PFTrDA (97%), PFTeDA (97%), and PFHxA (97%) were purchased from Sigma–Aldrich (St. Louis, MO, USA).  $^{13}\text{C}_8$ -PFOA was purchased from Cambridge Isotope Laboratories

(Tewksbury, MA, USA) and used as isotopic IS. Rest of the chemicals were same as reported before.

### **5.2.2. Sample collection**

Fresh fish fillets (Salmon, Toman, Red Snapper, Wolf-Herring, and White Snapper) were purchased from local wet markets (Singapore) in the period August - September 2013. All samples were purchased in fresh condition and were de-skinned. Fillets were cut to small sizes and homogenized with ultrapure water (50% weight) in a blender (Bullet blender 50-DX, Next Advance Inc, Averill Park, NY, USA) with stainless steel (4.8 mm) beads, and stored in polypropylene tubes at -30 °C, prior to processing.

### **5.2.3. Synthesis and characterization of mesoporous silica**

CTAB-MCM-41 was synthesized and characterized as methods described in chapter 3 (3.2.2 & 3.2.3).

### **5.2.4. Sample preparation and extraction**

One gram of each homogenized sample (after refreezing) was weighted accurately (0.1 mg), in a polypropylene centrifuge tube. IS and PFCAs standards were then added. After incubation for 24 hours at 4 °C, 1 ml acetonitrile was added, and the sample was thoroughly homogenized at 300 revolutions per minute (rpm) (KS 4000i control orbital shaker incubator, IKA, Germany) for 1 hour. Finally the obtained milky suspension was centrifuged (Model 5430R, Eppendorf, Hamburg, Germany) at 20,000 rpm for 20 min to clarify the supernatant; any drop in the temperature was prevented to avoid analyte

loss. The clarified supernatant was separated in a propylene tube. Then the  $\mu$ -SPE was carried out with 25 mg of CTAB-MCM-41 in a polypropylene bag (1.0  $\times$  2.0 cm). The extraction time was chosen as 30 min and desorption solvent was MeOH. Eventually 5  $\mu$ l of extract was injected to the LC-ESI-MS/MS. For DSPE, 25 mg of sorbent were dispersed in 1 ml of supernatant solution; the mixture was mixed for 30 min at 300 rpm. After simultaneously centrifuging and drying of solvent under nitrogen stream (Centrivap, Labconco, Kansas City, MO, USA) 200 $\mu$ l of methanol was added to the sorbent and the analytes were desorbed by ultrasonication for 10 min. After centrifugation, 5  $\mu$ L of the supernatant was injected into the LC-MS/MS system. Moreover, in order to study the adsorptive performance of the CTAB-MCM-41, and its role in concentrating of the analytes, direct analysis of the solution that resulted from the protein precipitation, was also carried out.

### 5.2.5. Instrumental analysis

The quantification of PFCAs by LC-MS/MS was using the same methodology that was described in Chapter 3 (section 3.2.6). The list of the rest of the analytes which had not been analysis in previous chapters and their optimized LC-MS/MS parameters are shown in Table 5-1.

Table 5-1 Analytes and optimized LC-MS/MS parameters

Analyte	Molecular mass	Retention time (min)	Precursor ion (m/z)	Product ion 1			Product ion 2				
				(m/z)	DP (V)	CE (V)	CXP(V)	(m/z)	DP (V)	CE (V)	CXP (V)
PFHxA	314	2.42	313.00	269.05	15	10	28	119.15	15	25	22
PFUdA	564	4.57	563.00	519.00	40	10	36	269.10	40	20	28
PFTTrDA	664	5.20	663.00	619.00	32	15	28	169.15	32	30	30
PFTeDA	714	5.46	713.00	668.90	36	15	32	169.10	36	35	30
<sup>13</sup> C8-PFOA	422	3.30	421.00	376.05	20	10	25	172.15	20	20	16

### **5.3. Results and discussion**

#### **5.3.1. Evaluation of the protective role of the membrane**

In order to evaluate the protective role of the polypropylene membrane, DSPE was conducted in parallel with  $\mu$ -SPE under the same extraction conditions. Toman fillets were used for these experiments. When  $\mu$ -SPE was used instead of DSPE, the average RSD for all analytes significantly decreased from 24% to 9% in the concentration range between of 1 to 100 ng/ml, and the average peak areas of all the analytes in the mentioned concentration range, increased at least 3 times for  $\mu$ -SPE. Additionally, the use of nitrogen flow during solvent evaporation in DSPE (which was unnecessary in  $\mu$ -SPE) could lead to loss of analytes. Furthermore, the linearity of the calibration curve for the all analytes was improved (average coefficients of determination of 0.8669 for DSPE, and 0.9972 for  $\mu$ -SPE).

#### **5.3.2. Evaluation of extraction and concentration step**

In order to study the role of the CTAB-MCM-41 in extraction, results of the direct analysis of the extract, after protein precipitation, were compared with those of  $\mu$ -SPE. The use of  $\mu$ -SPE had a positive effect on the extraction efficiency and removal of the interferences (i.e., clean-up). In the concentration range of between 1 and 100 ng/ml, the average peak areas for all analytes increased by 8 times. The average RSD for all analyses significantly decreased from 16% to 9% and linearity of the calibration curves also improved (average coefficients of determination of 0.9426 for direct analysis, and 0.9972 for  $\mu$ -SPE). Thus it was demonstrated that CTAB-MCM-41, particularly when protected by a membrane, could be used as an effective sorbent for the concentration of

PFCAs. Table 5-2 shows the results of this comparison between direct analysis of protein precipitation, DSPE, and  $\mu$ -SPE.

Table 5-2 Comparison of the linearity of the calibration curves and RSD% of the analysis, in direct analysis of the extract, DSPE, and  $\mu$ -SPE

Analyte	Protein precipitation		DSPE		$\mu$ -SPE	
	RSD%	R <sup>2</sup>	RSD%	R <sup>2</sup>	RSD%	R <sup>2</sup>
PFPA	13.26	0.9657	5.72	0.8856	8.25	0.9985
PFHxA	11.80	0.9311	19.23	0.8819	5.40	0.9985
PFHpA	11.70	0.9143	60.60	0.8231	5.67	0.9987
PFOA	23.73	0.9807	19.18	0.8947	12.40	0.9904
PFNA	11.20	0.7965	20.83	0.8602	13.50	0.9975
PFDA	18.47	0.9731	14.56	0.8515	6.47	0.9975
PFUdA	23.29	0.9403	32.12	0.8068	9.66	0.9977
PFDoA	12.51	0.9756	12.59	0.9000	7.41	0.9967
PFTrDA	18.01	0.982	9.83	0.8786	10.03	0.9968
PFTeDA	20.12	0.9672	10.51	0.8868	10.03	0.9979
Avg.	16.41	0.94265	23.78	0.8669	8.88	0.9972

### 5.3.3. Method validation

For each analyte and each sample, 12-point calibration curves was prepared for the concentration range between 1 and 100 ng/ml by plotting the ratio of analyte peak areas to IS peak area, against analyte concentrations in the fish extract. The LODs and LOQs, and RSDs were calculated from the extracts of a real sample with the lowest concentrations of contaminants, and are reported in Table 5-3. All coefficients of determination indicated satisfactory linearity. The LOD of the method (at signal to noise ratio of 3) ranged between 0.97 and 2.40 ng/g, with a maximum RSD of 14% for PFNA. The LOQ of the method (at signal to noise ratio of 10) ranged between 3.2 ng/g and 9.0 ng/g. The LODs and LOQs obtained were comparable with those reported in previous publications, and would be suitable for the analysis of fish fillet [69, 72, 104]. Possible carryover effects were addressed by a randomized injection and washing process, as described before. It is worthwhile to mention that each analytical set

consisted of a blank sample for contamination control. The accuracy and repeatability of the tests was studied by three repeated analyses of the same sample set.

In order to evaluate the effect of the matrix on the MS signals (either suppression or enhancement), standard solutions with equal analyte concentrations were prepared in the extract of the unspiked fish fillet and in pure methanol. The samples were analyzed and the absolute signal ratios of the analyte were compared. The results are summarized in Table 5-3 (column 9). In the table, a value of  $< 1$ , representing signal suppression, and  $> 1$  representing signal enhancement due to the co-elution of matrix compounds, are shown. Only minor effects on ionization efficiencies were observed. This would be considered as evidence for the successful reduction of matrix effects, during sample preparation. The same observation has been previously reported [72]. Moreover it is worthwhile to mention that neither the retention times, nor the peak shapes in LC were affected by the presence of matrix components in the extract.

RR% and their possible dependence on analyte concentrations were studied. Each sample was spiked at 40, 80, and 100 ng/ml of each analyte. As shown in Table Table 5-3, the proposed method showed an acceptable RR% (77.5%-121.2%). Typical chromatograms are shown in Figure 5-1.

In order to verify the dependence of the RR on concentration, a statistical test was used for the analysis of the data (using IBM SPSS Statistics, version 20). The P value for each analyte at different concentration levels (40, 80, and 100 ng/ml) are reported in Table 5-3. A P-value higher than 0.05 means that the observed difference was not statistically significant. Based on the ANOVA at 95% confidence level, for all analytes,



the difference among the RR% values obtained for the three mentioned concentration levels, were not statistically significant. Hence it may be concluded that RR% is independent of analyte concentration. A similar observation has been reported previously [52]. Data related to this statistical test are summarized in Appendix 2 and 3.

#### **5.3.4. Analysis of real samples**

The quantification data for real fish samples obtained by described method are reported in Table 5-4 Recoveries have been considered in the amount of the final concentration. Fish fillet samples were not contaminated by most of the PFCAs. Only PFHxA, PFTrDA, and PFTeDA were detected in some samples, at low concentration levels. The results were in conformity with those of previous reports [69, 105, 106]. Based on the recovery, it can be concluded that the lowest RR% is related to the analyte with the shortest carbon chain. It is conceivable that the longer the carbon chain of the analyte, the more efficiently it can be trapped by CTAB. This observation confirmed our belief that PFCAs as anionic pollutants could be trapped by the hydrophobic and positively charged surfaces of CTAB. The same phenomenon has also been observed in the extraction of PFCs by chitosan-coated octadecyl-functionalized magnetite nanoparticles [77], and CTAB-coated silica [79].

#### **5.4. Conclusion**

In the current study, a simple, fast and efficient combination of protein precipitation and  $\mu$ -SPE followed by LC-ESI-MS/MS was developed for the determination of PFCAs in fish fillet. Ten PFCAs with different hydrocarbon chain lengths (C5-C14) were analyzed simultaneously using this method. Protein precipitation

by acetonitrile and  $\mu$ -SPE by surfactant-incorporated ordered mesoporous silica were applied to the extraction and concentration of the PFCAs as well as for removal of interferences. Determination of the PFCAs was carried out by LC–MS/MS in negative electrospray ionization mode. MS/MS parameters were optimized for multiple reaction monitoring of the analytes.  $^{13}\text{C}$  mass labelled PFOA as a stable-isotopic internal standard, was used for calibration. The detection limits of the method ranged from 0.97 ng/g to 2.7 ng/g, with a relative standard deviation of between 5.4 and 13.5. The recoveries were evaluated for each analyte and were ranged from 77% to 120%. The t-Test at 95% confidence level showed that for all the analytes, the relative recoveries did not depend on their concentrations in the explored concentration range. The effect of the matrix on MS signals (suppression or enhancement) was also evaluated. Contamination at low levels was detected for some analytes in the fish samples. The protective role of the polypropylene membrane used in  $\mu$ -SPE in the elimination of matrix effects was evaluated by parallel experiments in classical dispersive solid phase extraction. The results evidently showed that the polypropylene membrane was significantly effective in reducing matrix effects.

Table 5-3 Validation parameters for the analytes

Analyte	LOD* (ng/g)	LOQ* (ng/g)	Calibration range (ng/ml)	R <sup>2</sup>	RSD%	RR%	Error %	Matrix effect in ionization	Total Mean of RR%	P value**
PFPA	1.62	5.43	1-100	0.99	8.25	77.52	-22.48	1.02	77.14	0.77
PFHxA	2.09	6.98	1-100	0.99	5.4	87.53	-12.47	1.07	87.53	0.81
PFHpA	1.06	3.50	1-100	0.99	5.67	97.57	-2.43	1.01	97.11	0.95
PFOA	1.85	6.16	1-100	0.99	12.40	97.23	-2.43	1.04	95.07	0.46
PFNA	1.52	5.06	1-100	0.99	13.50	94.72	-2.77	1.07	94.80	0.60
PFDA	0.99	3.29	1-100	0.99	6.47	107.33	-5.28	1.07	98.66	0.05
PFUdA	2.70	8.99	1-100	0.99	9.66	100.44	7.33	1.04	99.67	0.81
PFDoA	2.40	7.67	1-100	0.99	7.41	91.03	0.44	1.02	91.84	0.51
PFTTrDA	0.97	3.21	1-100	0.99	10.03	119.93	-8.97	1.07	117.23	0.35
PFTeDA	0.99	3.34	1-100	0.99	10.03	121.24	19.93	1.02	120.91	0.38

\*Calculated on the basis of recovery

\*\*At 95% confidence level

Table 5-4 Average relative recovery (RR%), relative standard deviation, and detected concentration of the analyte (ng/g) in samples

Analyte	Salmon		Red Snapper		Toman		Wolf-Herring		White Snapper	
	Avg. RR% (± RSD)	Conc. (ng/g)	Avg. RR% (± RSD)	Conc. (ng/g)	Avg. RR% (± RSD)	Conc. (ng/g)	Avg. RR% (± RSD)	Conc. (ng/g)	Av. RR% (± RSD)	Conc. (ng/g)
PFPA	87.83± 14.55	n.d.	92.99± 14.13	n.d.	77.52± 8.25	n.d.	96.81± 9.24	n.d.	94.14 ± 5.66	n.d.
PFHxA	83.69± 16.81	<LOQ	94.44± 5.2	n.d.	87.53± 5.4	<LOQ	90.21± 13.10	1.22	96.81± 15.5	1.06
PFHpA	95.45± 18.20	n.d.	94.44± 6.21	n.d.	97.57± 5.67	n.d.	96.49± 9.80	n.d.	110.88± 6.79	n.d.
PFOA	93.81± 17.54	n.d.	92.91± 6.27	n.d.	97.23± 12.40	n.d.	94.81± 11.77	n.d.	92.88± 8.56	n.d.
PFNA	91.26± 18.40	n.d.	97.12± 7.76	n.d.	94.72± 13.50	n.d.	94.22± 11.47	n.d.	94.13± 9.46	n.d.
PFDA	106.97± 13.81	n.d.	107.44± 8.69	n.d.	107.33± 6.47	n.d.	110.16± 16.25	n.d.	111.42± 14.31	n.d.
PFUdA	107.93± 13.47	n.d.	108.50± 18.19	n.d.	100.44± 9.66	n.d.	122.86± 9.31	n.d.	125.31± 15.51	n.d.
PFDoA	107.64± 19.64	n.d.	108.12± 13.46	<LOQ	91.03± 7.41	n.d.	102.41± 6.80	n.d.	106.14± 8.23	n.d.
PFTTrDA	109.79± 13.23	n.d.	111.77± 13.78	n.d.	119.93± 10.03	1.27	107.55± 9.00	n.d.	107.43± 14.21	n.d.
PFTeDA	99.40± 11.53	1.93	110.30± 15.29	2.72	121.24± 10.03	n.d.	108.95± 8.64	4.30	101.71± 7.65	2.49

n.d. Non-detected

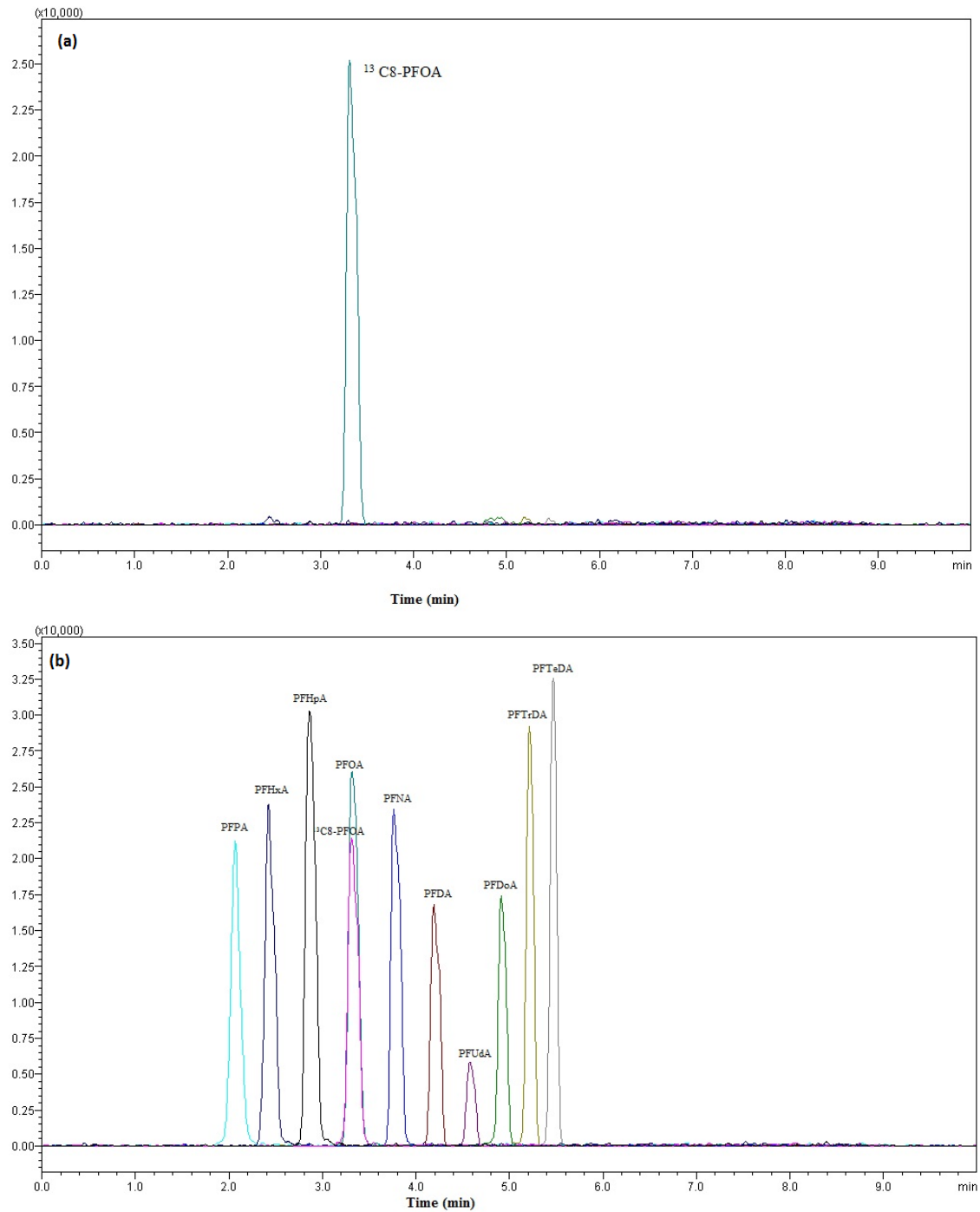


Figure 5-1 LC-ESI-MS/MS of analytes extracted from fish fillet by the developed method. (a) Unspiked sample, (b) sample spiked at 50 ng/ml.  $^{13}\text{C}_8$  mass labelled PFOA ( $^{13}\text{C}_8\text{-PFOA}$ ) was used as internal standard.

## **CHAPTER 6: Introduction to N-nitrosamines**

### **6.1. Introduction**

In the second part of this thesis (Chapters 6-9), we choose eight NAs as a second group of emerging environmental contaminants for analysis from different water samples and beverages.

The current chapter summarizes the important aspects of NAs. It gives a brief introduction of these compounds, and highlights their physicochemical properties, toxicity, established regulations for their monitoring, and their original sources in different environmental samples. Furthermore, it focuses on the efforts devoted for their analysis and determination in various matrices. Eventually, the current challenges and shortcomings in their analysis and determination are described.

### **6.2. Definition and properties of N-nitrosamines**

Currently, there is an increasing demand for safe drinking water. According to a survey conducted in 2010, an estimate of 780 million people around the world still do not have access to clean and safe drinking water [107]. More than 2.2 million people are dying every year because of waterborne diarrheal diseases [108]. Hence, disinfection of drinking water has been considered as one of the most important measures for public health protection and for reducing morbidity rate associated with waterborne diseases such as cholera and typhoid. However, it also leads to the formation of unintended chemicals called as disinfection byproducts (DBPs). DBPs are results of the reactions between oxidants such as chlorine,

chloramine, ozone, and chlorine-dioxide used for the disinfection process and a wide and diverse group of precursors within the water source. Over 35 years ago, DBPs were detected for the first time in drinking water, and today more than 600 individual DBP species from diverse chemical classes have been identified [1, 109].

To comply with the universally increasingly stringent DBP regulations, in the last decade many water treatment plants switched to alternative disinfectants to reduce formation of some regulated DBPs such as trihalomethanes (THMs) and haloacetic acids (HAAs); however, ironically this resulted in formation of compounds such as NAs as new unregulated emerging DBPs [1].

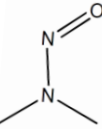
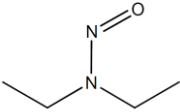
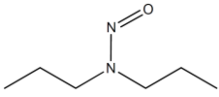
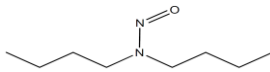
Generally, NAs are formed through nitrosation of secondary and higher degree amines and have a basic structure of  $R_1R_2N-NO$  [110]. The structures and some important properties of NAs have been summarized in Table 6-1. These compounds bio-accumulate and are hardly biodegradable. Moreover, their degradation occurs by treatment with radiations in UV-VIS range. In general, these exhibit high water solubility and relatively low partition coefficients in octanol/water ( $K_{O/W}$ ). Moreover, NAs are in a wide range of hydrophobicity/hydrophilicity.

### **6.3. Toxicity of NAs**

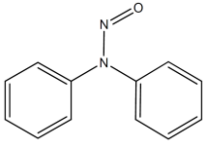
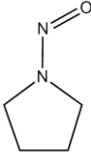
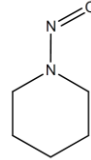
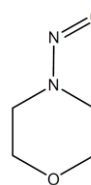
The toxicity of the NAs has been relatively well studied. The NAs are known rodent carcinogens and suspected human carcinogens and they have been categorized in a class to cause cancer in every major tissue in laboratory animals. Historically the US EPA was classified N-Nitrosodimethylamine (NDMA) as a probable human carcinogen based on the estimation of  $10^{-6}$  carcinogenic risk being 0.7 ng/l [96]. Lifetime cancer risk estimates of 8

identified NAs have been summarized in Table 6-1. The potency of B as in cancer causing reflected by upper bound one-in-a million lifetime cancer risk, which estimated from consumption of NAs in drinking water—which are typically in the low ng/L range. This means that they might able to cause health effects even if they are present in at very low ng/L concentrations. Approximately 90% of nitrosamine compounds are deemed to be carcinogenic [111]. From a DBPs research points of view, NAs are much more potent compared to THMs and HAAs (2 to 4 order of magnitude) [1].

Table 6-1 Properties of NAs (US EPA) [112, 113]

N-nitrosamines	Abbrev.	Molecular formula	Structure	Log <sup>*</sup> K <sub>ow</sub>	Standard US EPA cancer classification group	10 <sup>-6</sup> upper bound lifetime cancer risk from drinking water consumption (ng/L)	Water solubility (g/100ml)
N-Nitrosodimethylamine	NDMA	C <sub>2</sub> H <sub>6</sub> N <sub>2</sub> O		-0.57	B <sub>2</sub>	0.7	∞
N-Nitrosodiethylamine	NDEA	C <sub>4</sub> H <sub>10</sub> N <sub>2</sub> O		0.48	B <sub>2</sub>	0.2	10.6
N-Nitroso-di-n-propylamine	NDPA	C <sub>6</sub> H <sub>14</sub> N <sub>2</sub> O		1.36	B <sub>2</sub>	5	0.98
N-nitroso-di-n-butylamine	NDBA	C <sub>8</sub> H <sub>18</sub> N <sub>2</sub> O		2.63	B <sub>2</sub>	6	1.92



N-Nitroso-di-phenylamine	NDPhA	$C_{12}H_{10}N_2O$		3.13	B <sub>2</sub>	7000	0.003
N-Nitrosopyrrolidine	NPYR	$C_4H_8N_2O$		-0.19	2B (IARC)	20	∞
N-Nitrosopiperidine	NPIP	$C_5H_{10}N_2O$		0.36	B <sub>2</sub>	NA**	7.7
N-Nitrosomorpholine	NMOR	$C_4H_8N_2O_2$		-0.44	2B (IARC)	NA	∞

\*Log octanol/water coefficient

\*\* not applicable

#### 6.4. Sources of NAs in different environmental matrices

Historically, NAs were first detected in a wide ranges of food items (meats products and cheese), beverages, cigarettes, and cosmetics [112].

In beer, the nitrosating reagent is nitrite. Nitrite is produced by bacterial reduction of nitrate naturally present in water. The bacteria originate from the yeast used for fermentation. Hence, formation of nitrite can be reduced significantly by ensuring that the yeast used contains low levels of bacteria. The secondary amine source is dimethylamine produced from gramine<sup>1</sup> present in barley [114]. The economic impact of NAs has been very significant, as it has affected industries producing beer, whisky, and cured meats. Fortunately, recent modifications in production processes have significantly reduced their levels in food products and beverages[115].

In drinking water, NDMA was first detected in Ontario in 1989 [116]. Subsequent experiments indicated that it was contributed by water disinfection process rather than any anthropogenic process; therefore, it was introduced as a first nitrosamine type of DBP. Later, in 1998 it was detected at very high concentration in drinking water in California [117]. Although their very high levels were associated with contamination of water source by rocket fuels, it encouraged studies and surveys on regulation of NAs in drinking water sources. Later, NAs were detected in water sources of many other locations such as the UK [118], China [119], Japan [120], and Canada [121].

---

<sup>1</sup> Gramine (also called donaxine) is a naturally occurring indole alkaloid present in several plant species.

In general, there are two basic sources of NAs in drinking waters. First is related to the contamination of surface water and groundwater by industrial discharge, or wastewater used for aquifer [122]. Second, is drinking water disinfection process, where in NAs are formed by reactions between disinfection reagents and NA precursors inside the source water [123]. Studies have suggested that precursors of NAs, which are compounds containing organic nitrogen such as secondary and tertiary amines (dimethylamine [DMA], diethylamine [DEA], dipropylamine [DPA], etc) and other organic amino compounds such as natural organic matter (NOM), nitrite, bromides, pesticides, and pharmaceuticals, are associated with disinfection reagents in the formation of NDMA [124, 125]. Moreover, these precursors may be introduced by ion-exchange resins and (or) cationic polymeric coagulants (poly-DADMAC type) in drinking water treatment plans. It is worth mentioning that the operational conditions of the process, such as the dose of the disinfectant, pH, temperature, and water retention time, are important factors determining the concentration of NAs formed [121, 122].

In wastewater, NAs can originate from some industrial sources such as food and cosmetics processing, dye and rubber manufacturing, as well as leather tanning and metal casting [126]. Many pharmaceuticals (for both human and livestock) and pesticides are secondary or tertiary amines. These compounds may act as precursors for nitrosamine formation in the wastewater treatment processes [110]. Urine also appears to be an important source of NAs, and high concentrations of NAs have been observed in sewage. Moreover, NAs are excreted in urine of tobacco consumers at higher rates [127]. Given that wastewater and drinking water treatment efficiencies for these tobacco-specific NAs are unknown, there is a rising concern that these sources may increase human exposure to NAs [110]. In addition,

amine-based herbicides—often employed along with nitrogen fertilizers—may be particularly vulnerable to nitrosation [110] and can also be present as impurities in nitrogenous pesticides [128]. For example, Schmidt et al. reported that N,N-dimethylsulfamide (DMS), a degradation product of fungicide tolyfluanid, can be found widely in wastewater and converted around 30%–50% into NDMA after ozonation process [114]. Consequently, NAs can appear in sewage treatment plant effluents, and wastewater is a potential source matrix of NAs with high concentrations [129].

NAs occurrence in water from swimming pools has been reported widely as a result of disinfection process. Additional precursors such as those from sweat, urine, sunscreen, and other sources further contribute to NAs in swimming pool water [130].

## **6.5. Regulatory responses to NAs**

Strict regulations on the presence of NDMA and other NAs have been adopted, owing to the serious risk on human health. The US EPA included six NAs (NDMA, NDEA, NDPA, NPyr, NMEA, and NDBA) in Unregulated Contaminants Monitoring Rule-2 (UCMR-2) that required these NAs to be monitored in US drinking-water systems between 2007 and 2010 [131]. These NAs represent six of 26 compounds included in the UCMR-2 list, highlighting the importance of monitoring required for this class of compounds in drinking water. UCMR-2 monitoring results have revealed that a significant portion of USA is exposed to NDMA levels above the health reference level for cancer and that chlorination is responsible for the highest levels of nitrosamines produced [132]. Five nitrosamines (NDMA, NDEA, NDPA, NPyr, and NDPhA) were also added to the third version of the Candidate Contaminant List that proposes water contaminants for possible future regulation [44].

Eventually in 2010, the US EPA administrator announced that nitrosamines were among a set of drinking water contaminants that are considered for regulation as a group. The following regulations have been reported for the matrices of interest for this thesis. Certainly, the regulatory responses to NAs are varied depending on the jurisdiction.

Drinking water: Health Canada has proposed permissible limit of 40 ng/L for NDMA [29]. In North America, the Ontario Ministry of Environmental and Energy (OMEE) issued an interim maximum acceptable (MAC) of 9 ng/L for NDMA in 2003 [116]. The state of the Massachusetts Office of Research and Standards (ORS) has set a level of 10 ng/L for NDMA [79]. California has set maximum levels (notification level) of 10 ng/L for NDMA, NDEA, and NDPA and a public health goal of 3 ng/L for NDMA [74]. In the US, the Office of Environmental Health Hazard Assessment (OEHHA) released a public health goal (PHG) of 3 ng/L of NDMA in 2006. The Australian National Health and Medical Research Council considered NDMA guideline of 100 ng/L in drinking water [133]. In Germany, the recommendation by the federal environmental agency gives an admissible health-based precautionary value of 10 ng/L for life-long oral NDMA exposure through drinking water. Based on our knowledge, there is no such regulatory value from the health organizations of Singapore.

Wastewater: In the early 1990s, a regulatory level of 200 ng/L in effluents was established for NDMA by the OMEE [134]. Based on our knowledge, there is no new and/or other version of such regulations for different wastewater sample types [135].

Swimming pool water: To the best of our knowledge, there is no such regulation for the swimming pool water.

Beverages: In case of beverage industries, there are no clear regulations related to NAs, even though there is a significant consumption. Regulations limiting the levels of NAs in food are very rare, and those imposed depend on the country practicing them. For instance, the maximum contaminant level for NAs is 5 µg/kg in beer and bacon in the US; 0.5 µg/kg for beer in Italy, Switzerland, and Germany; and 2–15 µg/kg for meat, beer, and smoked products in Russia [136].

Evidently, these levels established by the authorities are in low concentration range that necessitates great efforts for their analysis and determination. Hence there is a pressing need for development as well as improvement of sensitive and reliable analytical methods.

#### **6.6. Analytical challenges faced in determination of NAs**

Regardless of common and acceptable issues in the determination and analysis of emerging contaminations from the environmental matrices, owing to physicochemical characteristics of NAs, some specific and unique difficulties exist in the extraction of these compounds.

The most important NAs such as NDMA are polar, with a high level of solubility in water and low partition coefficient in octanol/water (Table 6-1). Therefore, regardless of the common shortcomings and defects in the LLE (use of excessive volume of hazardous solvents; labour, time and cost intensive, and etc), LLE is basically an insufficient and unsuccessful extraction method for this group of compounds [112, 137]. This issue limits the use of extraction methodologies for NAs, and currently their extraction and pre-concentration rely on sorbent-based extraction methods. SPME [138, 139], DSPE [140], and more extensively SPE are extraction methods which have been used for the pre-treatment of

samples before NAs analysis. Boyd et al. overviewed those extraction methods for NAs [112].

The second problem is the urgent need for simultaneous extraction and analysis of NAs as a group. As evident from Table 6-1, NAs are found in wide ranges of hydrophilicity/hydrophobicity and polarity. For instance, if we consider  $K_{o/w}$  as a scale for hydrophobicity, NDPHA is about 363 times more hydrophobic than NDMA. This acts as an obstacle for successful simultaneous extraction to achieve acceptable recoveries for all NAs at the same time.

### **6.7. Sorbents for extraction of NAs**

Until now, the choice of an appropriate sorbent for extraction of NAs solely depended on the sorbent's ability to extract polar NAs, particularly NDMA. In fact, the amount of obtained recovery for NDMA by an extraction method is an index to assess the efficiency of the method. Keeping this in mind, the use of the polymeric reversed phase type sorbents (such as C18, phenyl modified silica gel, Oasis HLB [divinylbenzene/N-vinylpyrrolidone])—which are some of the most applicable and commercially available sorbents in the extraction process—was not successful for extraction of NAs. This is because NDMA are weakly retained in the reversed phase type sorbents and low extraction recoveries for polar NAs are obtained [121, 141].

Therefore, currently most sorbents used for extraction of NAs are non-polar carbonaceous adsorbents. From the variety of carbonaceous sorbent, Ambersorb 572 was one of the most commonly used SPE sorbents. Ambersorb 572 was a spherical carbonaceous resin which works well for polar NAs, particularly for NDMA. However, despite its

extensive use in NA analysis, the manufacturer (supplier is Supelco) has discontinued its production from 2007 and it is no longer available. Supelco now produces a replacement, Carboxen 572, which is more expensive. Besides, its performance has not been verified yet. Other carbonaceous sorbents such as Bakerbond carbon [142], Amborsorb 348F [143], neutralized activated charcoal [144], carboxen with different pore size [140], and coconut activated carbon have been used widely in extraction of NAs. Currently, coconut charcoal is the most widely reported sorbent in this case and has been used by the EPA 521 method for extraction of NAs [145]. Some benefits of coconut charcoal, compared to other type of graphitized carbon black or carbon disk, include higher adsorption capacity, evaluated porous surface area, controllable pore size structure, and thermal and chemical stability [40, 144, 146]. However by using the above sorbents there is still one basic unsolved problem.

#### **6.8. Current gaps in the determination of NAs**

The basic principle of a successful sorbent-based extraction methodology can be described as below. In sorbent-based extraction process a successful extraction depends upon two factors: 1) correct retention and adsorption of the analyte on the sorbent surface, and 2) successful elution of the analyte from the sorbent during the desorption process. Thus, not only that the species must have desirable retention on the sorbent but also they must elute efficiently in desorption step. Eventually resulting in high recovery is a function of balance between adsorption and desorption step.

Considering this fact, the basic problem of carbonaceous sorbent is related to the lack of such balance between adsorption and desorption processes. For instance, ENVI-carb sorbent was able to retain NDMA; however, the results of the extraction recovery were



unsuccessful, since NDMA could not be eluted from the sorbent successfully [112]. Meanwhile, to our best knowledge, when other carbonaceous sorbents are used for simultaneous extraction of a group of NAs, the extraction recoveries for non-polar analytes are not as good as those for polar analytes [112]. The plausible reason for this observation is the difficulty in achieving successful elution of non-polar or less-polar analytes using carbonaceous sorbent. Those hydrophobic compounds are strongly and irreversibly absorbed on carbonic surface and thus were strongly retained on the surface of the sorbent [126, 134]. For example, Plumlee et al. tested several activated carbons and found that neutralized activated charcoal had the best NDMA recovery. However, extraction recoveries were absolutely related to the polarity of a compounds, and non-polar analytes such as the NDBA had very low extraction efficiency while very non-polar analyte (NDPhA) could not be included in the study [144]. The same observations have been reported widely [134, 147, 148]. Lee and co-workers have developed analytical methods for the analysis of nine NAs from water samples by evaluating two kinds of activated carbon-based. They obtained a good level of recovery (up to 88%) for NDMA by the use of activated carbon sorbent; however, the recovery amount for NDPhA was low, and they stressed the need for further studies to overcome this issue [141].

In order to overcome this problem, some researchers have started using dual SPE cartridges; yet lower extraction recoveries have been reported for those analytes [141]. Krasus and coworkers coupled HLB cartridge with Bakerbond carbon. Although the method could report trace level quantification of NAs, recoveries related to non-polar analyte were still low [142]. Moreover, this approach is time consuming and expensive.

To conclude, there is still an increasing demand for the development and designing of proper sorbent for simultaneous extraction of NAs which achieve acceptable recoveries for all of them (polar and non-polar) simultaneously.

It is worth mentioning that in the analysis of NAs from complex matrices in the environment, eliminating matrix interference is important because studies have demonstrated the challenges in achieving reliable results in determination of NAs at trace levels from complex matrices due to matrix interference. In this direction, some studies have used Florisil cartridge for eliminating matrix interference from the eluent prior to analysis. However, Wang et al. reported that pre-conditioning by Florisil cartridges could result in matrix elution that interferes with NDMA [112].

In this direction, we first designed and developed surface-modified carbonaceous sorbent which could achieve acceptable recoveries for all US EPA concerned NAs simultaneously. Following this, the obtained sorbent is used to develop method for the determination and analysis of NAs from water samples and beverages.

## **CHAPTER 7: Introducing surface-modified ordered mesoporous carbon as a promising sorbent for simultaneous extraction of N-nitrosamines**

### **7.1. Introduction**

Chapter 6, explained one of the shortcomings in the simultaneous extraction of NAs. As mentioned earlier, achieving high extraction recoveries simultaneously for a group of NAs with different range of polarity is challenging. As stated before, carbonaceous sorbents lead to good extraction recovery for polar compounds because these are absorbed by the surface of the sorbent desirably and not retained at the surface of sorbent in the eluting process. However, non-polar analytes show very strong and irreversible adsorption at the surface of the sorbent, which acts as an obstacle while elution; eventually leading to low recovery rate for these compounds. However, development and designing of an ideal sorbent depends on some critical factors. The sorbent must have high surface area, accurate pore-size distribution, appropriate adsorption kinetic, and stability under correct working conditions such as pH, temperature, and chemicals (Refer to Chapter 1, Section 1.4.3). Furthermore, the adsorbent should have acceptable adsorptive behavior for a group of NAs with a wide range of polarity.

The present chapter focuses on the development and designing of new surface-modified ordered mesoporous carbon (OMC) developed to overcome this issue. For the first time, the use of OMC and surface-modified OMC as sorbents for extraction of eight UP EPA NAs is investigated.

In the present study, CMK-3 was chosen as a carbonaceous adsorbent and its surface was modified by carboxylic group through an oxidative treatment, to get what is called O-CMK-3. O-CMK-3 was extensively characterized and used for simultaneous extraction of NAs from water samples. For ease in manipulation,  $\mu$ -SPE methodology was chosen for extraction process. In order to evaluate the probable influence of the analyte at the surface of the sorbent, it was also characterized after extraction in a similar way. Eventually, the results of the extraction were compared (in a same extraction condition) with 10 different kinds of commercial carbonaceous sorbent, which have been used widely for extraction of NAs.

## **7.2. Experimental**

### **7.2.1. Safety considerations and pollution prevention**

As mentioned in Chapter 6, NAs are potential carcinogens. Extreme care must be taken at all steps such as handling, storage, and disposal. Working under fume hood with great ventilation is highly necessary all the time. Moreover, appropriate personal protective equipment (latex gloves, laboratory coat, and safety goggles) must be used at all steps of experiments. Some NAs are shown to be highly permeable; for instance, NDMA is predicted to have the same permeability ( $10^{-4}$  cm/h) as hydrocortisone<sup>1</sup> [149]. Hence, it is essential to avoid any skin contact with NAs. Proper strategy must be considered for disposal of the solutions, especially stock standards that contain high

---

<sup>1</sup> Hydrocortisone is the active ingredient in typical ointments used for skin treatment.

concentration of NAs. All glassware used for NAs analysis must be thoroughly rinsed with water and dichloromethane.

### **7.2.2. Chemicals and solutions**

NAs containing NDMA, NDEA, NDPA, NDBA, NPYR, N-nitrosopiperidine (NPIP), N-nitrosomorpholine (NMOR) (all with 99.9% purity), and NDPhA (96.58% purity) were purchased from Supelco (Bellefonte, PA, USA). Triblock copolymer P123 (EO<sub>20</sub>PO<sub>70</sub>EO<sub>20</sub>, 5800), ammonium persulfate (APS, (NH<sub>4</sub>)<sub>2</sub>S<sub>2</sub>O<sub>8</sub>, ≥98.0%), sucrose, and activated charcoal (100 mesh particle size) were purchased from Sigma–Aldrich (St. Louis, MO, USA). Tetraethyl orthosilicate (TEOS, 98%) was purchased from Aldrich Chemistry (Steinheim, Germany). Accurel polypropylene flat sheet membrane (200 μm wall thickness, 0.2 μm pore size) was purchased from Membrana (Wuppertal, Germany). Eight types of carbon molecular sieve (CMS) with different micropore diameters and surface area, including Carboxen-1016, Carboxen-569, Carboxen-1021, Carboxen 1018, Carboxen-1000, Carboxen-1012, Carbosieve S-III, Carbosieve G, and coconut charcoal SPE tubes (just the sorbent inside the tubes was used) were bought from Supelco. Sulfuric acid (H<sub>2</sub>SO<sub>4</sub>, 95%) and potassium chloride (KCL) were obtained from BDH (Poole Dorset, UK). Ultrapure water was used for all experimental purposes. Dichloromethane (DCM) purchased from Fisher Scientific (Fair Lawn, NJ, USA) and was of Liquid chromatography grade.

### 7.2.3. Preparation of the sorbents

#### Synthesis of SBA-15

Mechanism of synthesis: During synthesis, an association between the hydronium ions and hydrophilic alkylene oxide moieties through hydrogen binding leads to dissolution of the non-ionic EO-PO-EO triblock copolymers in an acidic media (HCl). Adding silica source results in the formation of cylindrical micelles due to the swelling effect of ethanol released during the hydrolysis of TEOS and dehydrating effects of HCl on the PPO block. The synthesis takes place in HCl media below the aqueous isoelectric point of silica. During this process, it is expected that the cooperative self-assembly of the inorganic and block polymer species would proceed through an intermediate of the form  $(S^0H^+)(X^-I^+)$ , where  $S^0$  is the block polymer,  $H^+$  is the hydronium ions,  $X^-$  is the halide anion, and  $I^+$  is a protonated Si-OH moiety. The overall charge balance is due to the association with an additional halide anion. Following this, inorganic species are cross-linked to form dense, continuous silica networks [150, 151]. (Further description in Chapter 1, Section 1.5.1).

Methodology of synthesis: Highly ordered mesoporous silica SBA-15 was prepared by the procedure reported by Zhao et al. [152]. Briefly, 3.2 g triblock copolymer P123 as an organic surfactant template and 4.4 g KCl as an inorganic salt additive were mixed with 120 g of 2M HCl solution. The mixture was magnetically stirred at 38 °C until the polymer was completely dissolved in the solution and clear solution obtained (about 40 min). To the solution, 8.4 g TEOS was added as a silica source. The solution was stirred for more than 10 min at the same temperature and

maintained at this temperature for 24 h with no stirring (static condition). After 24 h, the mixture was transferred to an autoclave maintained at 130 °C under static condition for another 24 h and then recovered by filtration. It was washed sequentially with deionized water and 50% water-ethanol mixture. The white powder obtained was dried in air at 60 °C for 2 h, after which it was calcined at 550 °C in the air for another 8 h in order to remove P123 template. The white powder thus obtained was SBA-15.

### Synthesis of CMK-3

Mechanism of synthesis: As explained in Chapter 1 (Section 1.5.2), the synthesis of CMK-3 is performed by hard template method using SBA-15 silica as a template and sucrose as a carbon precursor. In general, during synthesis sucrose is impregnated into the pores of SBA-15 silica using aqueous solution containing H<sub>2</sub>SO<sub>4</sub> as the carbonization catalyst [153]. The impregnated sucrose is then converted to carbon that fills the SBA-15 pores during two runs of impregnation and subsequent pyrolysis at high temperature under vacuum. After carbonization process, the silica framework is removed using aqueous solution of sodium hydroxide (NaOH). The space once occupied by the silica template is now transferred to the pores in the resulting carbon materials, and the carbon in these silica template pores forms a continuous framework. Sucrose impregnation completed in a single step would produce carbon samples with completely featureless XRD pattern, as the pore volume of SBA-15 is too small to contain a sucrose quantity sufficient enough to form a rigid carbon structure in single step. The excess sucrose would coagulate SBA-15 particles, thereby producing nonporous amorphous carbon [153]. To our advantage, carbonization starts under mild conditions at low temperature similar to sol-gel processes. Also, it is easy to achieve

uniform infiltration of carbon within the silica nanopores to generate carbon materials that retain the mesostructural order of the silica templates [34]. (Further information in Chapter 1, Section 1.5.2).

Methodology of synthesis: Mesoporous silica SBA-15 was used as a hard template for the synthesis of carbon mesoporous CMK-3, as reported by Ryoo et al. [154]. SBA-15 was impregnated with acidic aqueous solution of sucrose. 2 g SBA-15 was added to 15 mL aqueous solution containing 2.5 g sucrose and 0.3 g H<sub>2</sub>SO<sub>4</sub>, to obtain a milky sludge. The sludge was left at 70 °C for 6 hours in drying oven and subsequently the oven temperature was increased to and maintained at 150 °C for 7 h. Following thermal treatment, the mixture turned back to dark brown or black in color. At this step, silica sample gets partially polymerized and carbonized with sucrose. In order to obtain fully polymerized and carbonized sucrose inside the pores of silica template, 15 mL aqueous solution containing of 1.5 g sucrose and 0.16 g H<sub>2</sub>SO<sub>4</sub> was added to the sample and sample was subjected to same thermal treatment. Complete carbonization was achieved by pyrolysis of the sample by heating under vacuum (argon flow is also reported) at 900 °C for 6h. The carbon-silica composite obtained was calcined by washing four times with a 100 °C solution of 1M NaOH (in 50% ethanol: water) to remove silica template (studies report twice washing to be enough, we made it four times to ensure complete removal of silica template). The template-free carbonic product was filtered, washed with ethanol, and dried at 100 °C. The black powder eventually obtained was CMK-3.



## Surface modification of the CMK-3

Oxidative treatment, one of the most convenient and frequently used methods, has been used to introduce carboxylic functional groups upon oxidization of the surfaces of carbon materials by H<sub>2</sub>SO<sub>4</sub> and APS solution (refer to Chapter 1 Section 1.5.2 for more details) [36]. For this, 400 mg CMK-3 was added to a solution (10 mL) containing APS and H<sub>2</sub>SO<sub>4</sub>. The concentration of APS and H<sub>2</sub>SO<sub>4</sub> in the solution was 1.5M and 2M, respectively. The mixture was stirred at 25 °C for 20 h. The resulting O-CMK-3 material was recovered by filtration, followed by washing with ultrapure water first and eventually with ethanol and subsequent drying at 100 °C for 6 h.

### **7.2.4. Characterization of the sorbents**

Various characterization techniques were used to investigate the structural properties, morphology, and surface chemistry of the synthesized sorbents.

Low angle x-ray diffraction patterns for crystal, channel, and hexagonally ordered structure identification were obtained with a Cu K $\alpha$  radiation source (40 kV, 40 mA, small angle x-ray scanning) by using an x-ray diffractometer (D5005, Siemens, Karlsruhe, Germany) at 0.02° step size and 1 s step time over a 1.5° < 2 $\theta$  < 10° range.

FT-IR spectra (Varian Excalibur 3100, Palo Alto, CA, USA) was used to confirm the presence of the functional groups at the surface of the sorbent, measured at a resolution of 4 cm<sup>-1</sup>, with a scan range between 400 and 4000 cm<sup>-1</sup>.

The nitrogen adsorption and desorption isotherms for studies of structural properties were measured at -195.855 °C on a Micromeritics ASAP 2020 instrument

(Micromeritics Instrument Corp, Norcross, GA, USA). Specific surface area was calculated using N<sub>2</sub> adsorption-desorption isotherms in the relative pressure range from 0.06 to 0.2 using BET (Brunauer-Emmett-Teller) equation. Pore-size distribution (PSD) curves were calculated from the analysis of the adsorption branch of the isotherm using the Barrett–Joyner–Halenda (BJH) algorithm. Micropore volume was calculated with t-plot method using nitrogen adsorption data in a relative pressure of 0.00–0.65. The total pore volume was estimated from the amount of nitrogen adsorbed at a relative pressure of about 0.97.

For the Scanning electron microscopy (SEM), the copper grid with sample deposited on it was mounted on a sample stub with an adhesive double-side carbon tape and coated with gold to increase the electronic conductivity. The particle morphologies were observed on an ultra-high resolutions scanning electron microscope (JEOL 7610F Field Emission Scanning Electron Microscope, Pleasanton, CA, USA).

#### **7.2.5. Evaluation of the adsorptive performance of the sorbents**

For a reliable evaluation and comparison of the performance of synthesized carbonaceous sorbents and other different commercially available carbonaceous sorbents in the extraction of NAs, a set of experiments with different sorbent types but same extraction conditions were carried out. Briefly, different carbonaceous sorbents were filled in  $\mu$ -SPE bag and the extraction process on ultra-pure water samples spiked with mixture of NAs were carried out (initial concentration = 100 ng/mL, amount of adsorbent = 30 mg, extraction time = 30 min, desorption time = 15 min, sample volume

= 30 mL, no salt or pH adjustment, desorption time=20 min). The analytes were desorbed and analyzed by EI-GC-MS/MS.

### 7.2.6. Instrumental analysis

Analyses were carried out by gas chromatography-electron ionization tandem mass spectrometry (GC-EI-MS/MS) (GCMS-TQ8030 Triple Quadrupole Mass Spectrometer, Shimadzu, Kyoto, Japan). Chromatographic separation was achieved by using a Stabilwax®-DB Columns (polar phase; Crossbond® base deactivated Carbowax® polyethylene glycol, 30 L, 0.25 mm I.D, and 0.25 µm film thickness), along with deactivated borosilicate glass liner (3.5 mm i.d, single taper inlet, intermediate polarity), both obtained from Restek Corp. (Bellefonte, PA, USA). Separation of each of the eight NAs was performed in less than 18 min. More details about the instrumental and analytical conditions are listed in Table 7-1.

Table 7-1 GC-MS/MS analytical conditions

<b>GC</b>	
Column	DB-STABIWAX, L:30.0 m, df: 0.25µm, Id: 0.25 mm
Carrier gas	Helium
Oven program	50 °C, hold for 2min 20 °C /min to 210, hold for 15 min
Total program time	25 min
Linear	Deactivated borosilicate glass liner
Injection temp.	200 °C
Injection volume	1µl
Injection mode	Split less
Pressure	64.9 kPa
Total flow	30.0 ml/min
Column flow	1.22 ml/min
Purge flow	3.0 ml/min
Sampling time	1 min
<b>MS</b>	
Ionization mode	Electron ionization
Detector voltage	Relative to the tuning result
Ion source temp.	200 °C
Interface temp.	210 °C
CID gas	Argon
Solvent cut time	4 min
Acquisition mode	MRM

### 7.3. Results and discussion

#### 7.3.1. Characterization of the sorbent

Figure 7-1 has shown small angle XRD pattern of the O-CMK-3. Evidently, the sample exhibits narrow (100) reflection peak and the other reflection peaks (110 and 200) observed in the ordered mesoporous structure.

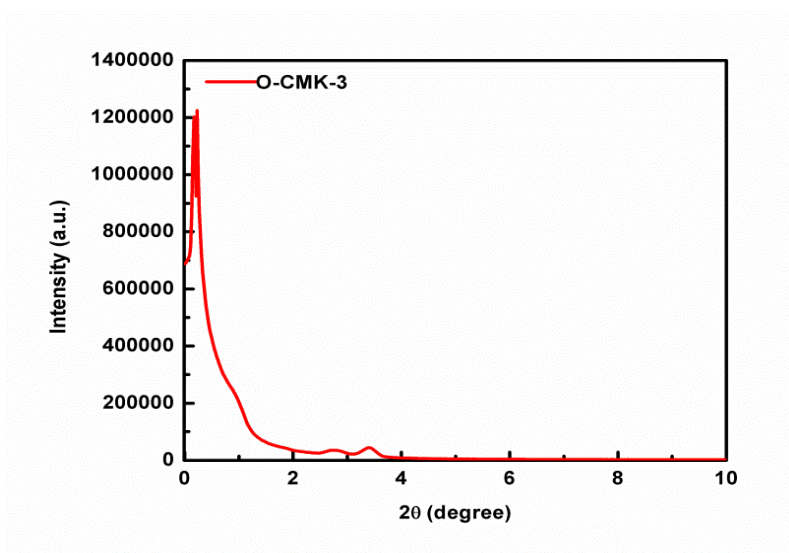


Figure 7-1 XRD pattern for O-CMK-3

FT-IR has been used to confirm the presence of different functionalized group at the surface of the sorbent. For CMK-3, the FT-IR spectrum only shows a few weak broad absorption bands (Figure 7-2-a). This observation was expected due the highly carbonized framework of CMK-3. However, after the oxidative treatment different carboxylic group have been added to the surface of the sorbent. Hence, O-CMK-3 shows different bands centered around 1097, 1226, 1460, and 1697  $\text{cm}^{-1}$ , and a broad band centered at 2970  $\text{cm}^{-1}$ (Figure 7-2-b), which are not observed for the untreated CMK-3. The strong adsorption band at 1697  $\text{cm}^{-1}$  can be attributed to the presence of carbonyl groups, 1460  $\text{cm}^{-1}$  is related to carboxyl-carbonate structures or aromatic C–C

bonds, and  $1097\text{ cm}^{-1}$  can be attributed to C–O vibrations in alcohol groups at the surface of treated mesoporous carbon. These results clearly confirmed that functional groups were created in the carbon frameworks after oxidative treatment and that the modification process was successful. Same observations have been reported before [36].

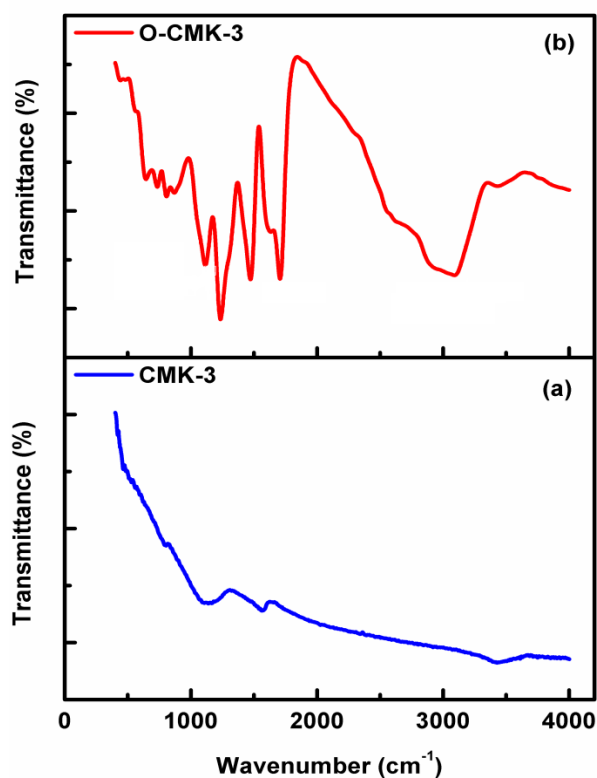
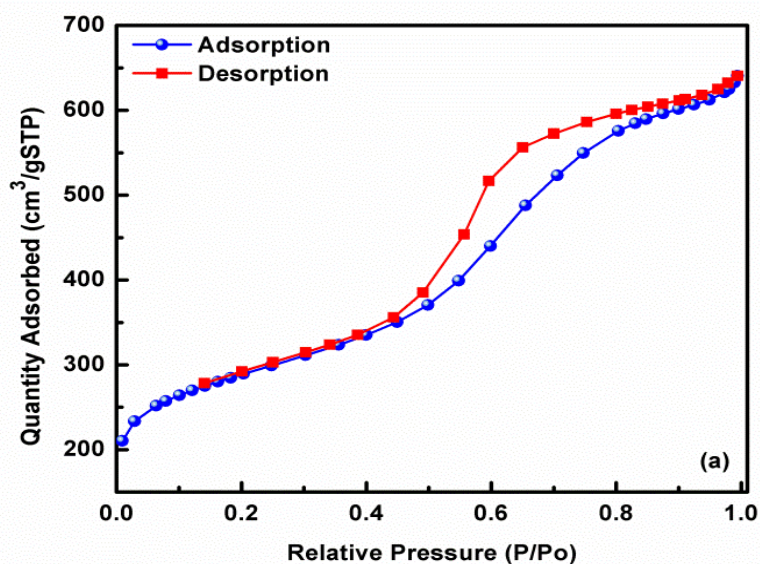


Figure 7-2 FT-IR spectra of (a) CMK-3 and (b) O-CMK-3

The effect of NA exposure on the surface chemistry of the sorbent studied to see if the interactions of the functionalized groups with the analytes are reversible or irreversible. Mixtures of NAs at concentration of 500 ppbs were prepared and extractions were carried out. After desorption of analytes, the sorbent was taken out from the  $\mu$ -SPE device and FT-IR spectrum of the sorbent was recorded. Interestingly,

FT-IR pattern observed was same as seen for sorbent before exposure with NAs. This observation has two potential benefits: 1) sorbent exposure to NAs has no effect on the functionalized groups of the surface, suggesting that the adsorption process was reversible. 2) The sorbent remained intact. Hence, it can be used for subsequent extractions, thereby saving time and making the process cost-effective.

Adsorption of  $N_2$  gas is the most popular method to determine the surface area and pore size of porous materials. Figure 7-3 shows the  $N_2$  adsorption-desorption isotherm of CMK-3 and O-CMK-3. Both samples show IV adsorption isotherm, consistent with that for uniform mesoporous structure [154, 155]. Nearly same isotherm for both CMK-3 and O-CMK-3 indicates that modification had no effect on the uniform mesoporous structure of the CMK-3 and the ordered mesoporous structure was resistant to modification.



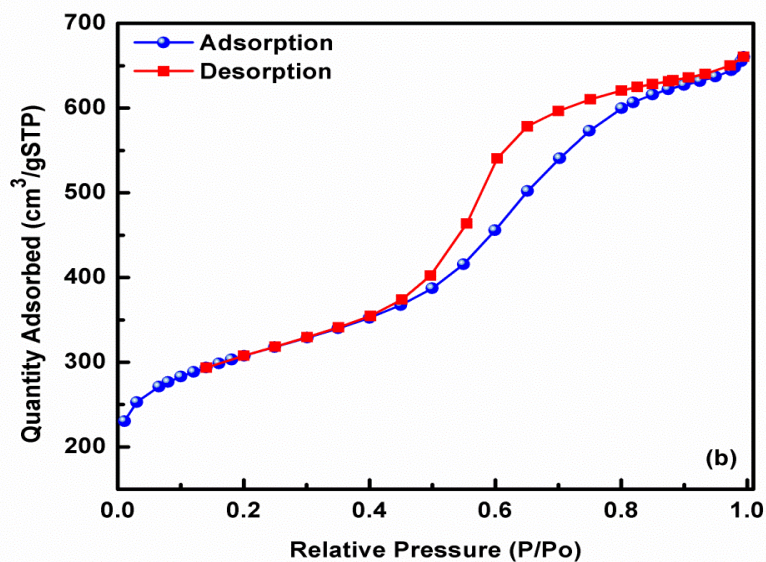


Figure 7-3 Nitrogen adsorption-desorption isotherm of (a) CMK-3, (b) O-CMK-3

Using BJH, the most widely used method to analyze PSD in the mesopore materials, the pore-size distribution curves were calculated from the adsorption branch. The results clearly confirmed a narrow pore-size distribution centered at about 4.8 nm, which interestingly was not affected by surface modification (Figure 7-4).

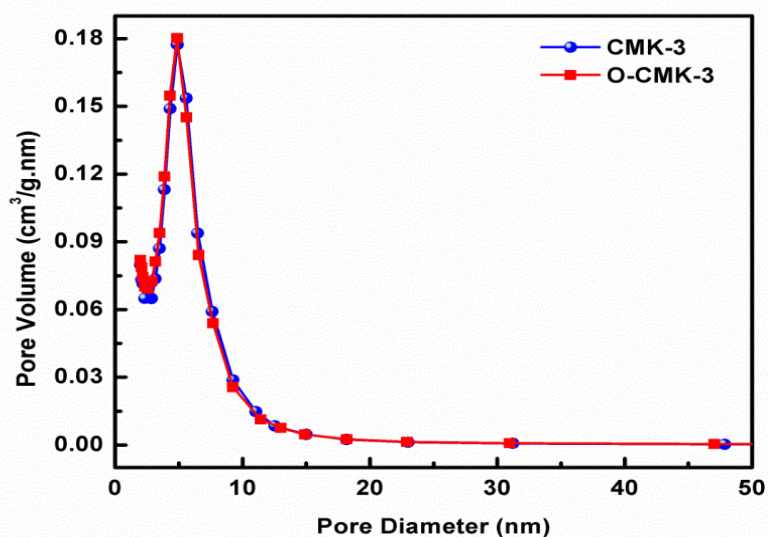


Figure 7-4 Pore size distribution of CMK-3 and O-CMK-3

Table 7-2 summarizes the BET-specific surface area, total pore volume, micropore volume, and mesopore size for CMK-3 and O-CMK-3. These results show that both CMK-3 and O-CMK-3 exhibit high BET-specific surface area, high pore volume, and proper pore size thereby making them potentially favorable sorbents that can meet primary requirements (refer Chapter 1, section 1.4.3) of an ideal sorbent.

Table 7-2 Adsorption isotherm parameters for CMK-3 and O-CMK-3

Sample	BET surface area(m <sup>2</sup> /g)	V <sub>total</sub> (cm <sup>3</sup> /g)	Average pore width (nm)
CMK-3	1061.65	0.996	3.84
O-CMK-3	999.942	0.960	375

SEM is an effective technique used to assess particle size and morphology. SEM images of sorbents shown in Figure 7-5 revealed that both SBA-15 and CMK-3 consist of rope-like parts of exactly same morphology. It confirmed that CMK-3 had ordered structure nearly same as that of SBA-3 because it was the exact inverse of SBA-15 [36]. Moreover, it was confirmed that oxidative treatment did not change the rope-like morphology of O-CMK-3 and that it had the same SEM image as that of CMK-3. This evidence confirmed that the pore structures were unaffected by modification and were not damaged during oxidative treatment. Same observations have been reported in wet oxidative treatment of the carbonic mesostructure [35, 36].



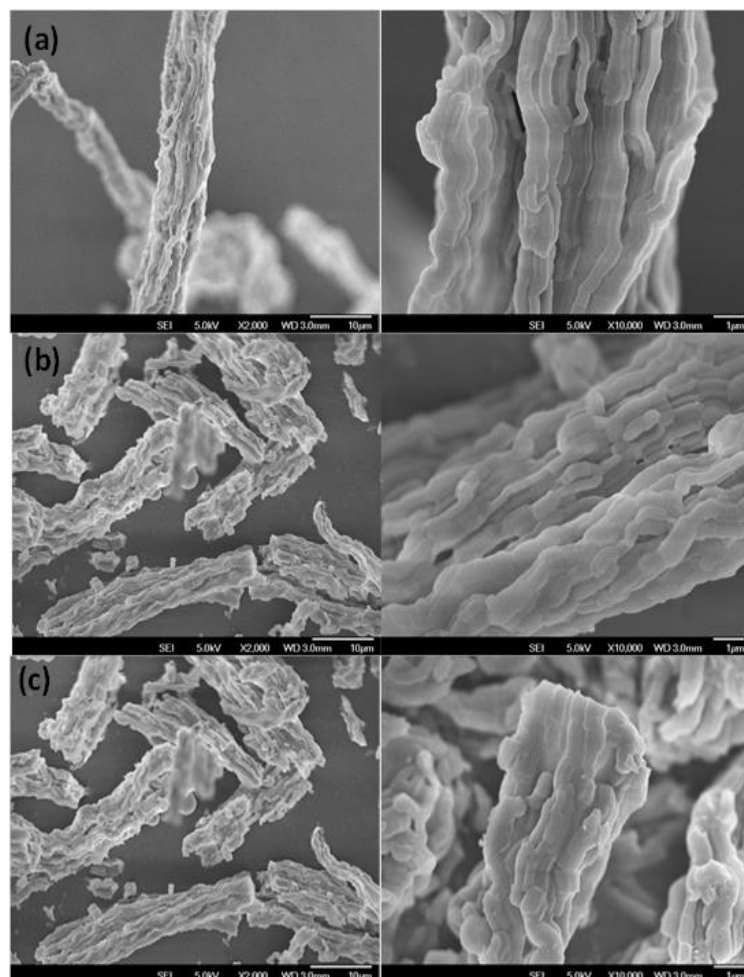


Figure 7-5 SEM images of (a) SBA-15, (B) CMK-3, and (C) O-CMK-3

### 7.3.2. Evaluation of the extraction behaviour of sorbents

Figure 7-6 shows the results (peak area) obtained for each analyte after extraction by using different sorbents. Name of the sorbents used and their characterization have been presented in Table 7-3.

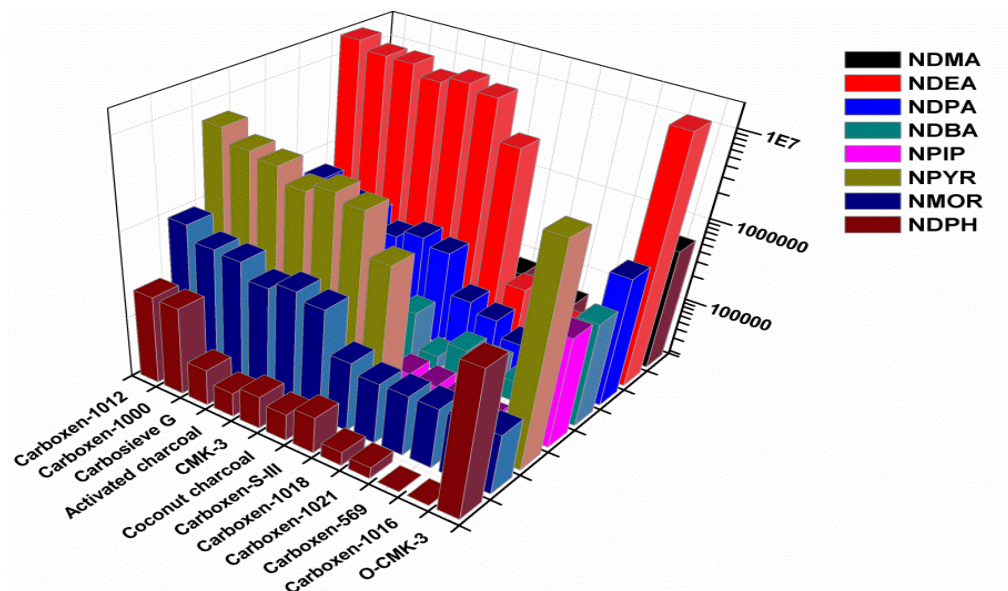


Figure 7-6 Efficiency of the different carbonaceous sorbents in the extraction of NAs.

Table 7-3 Name and the surface area of used carbonaceous sorbents

Sorbent	BET surface area (m <sup>2</sup> /g)
O-CMK-3	999
CMK-3	1061
Coconut charcoal	970
Activated charcoal	985
Carboxen-1016	75
Carboxen-569	485
Carboxen-1021	600
Carboxen-1018	675
Carboxen-1000	1200
Carboxen-1012	1500
Carboxen-S-III	975
Carbosieve G	1160

In general, O-CMK-3 showed best results for all NAs (including polar and non-polar). From the observations, we draw the following conclusions:

- 1) O-CMK-3 showed better results for all analytes (although it had similar surface area, spatial structure, and PSD as CMK-3). This observation was associated to surface modification.
- 2) Improved in extraction for polar and hydrophilic analytes can be explained by below: As mentioned before (Chapter 1 Section 1.5.3), the inert and

hydrophobic nature of OMC with poor wettability may limit its application for some analytes, since the entire surface and all pores of the sorbent may not be involved in the adsorption process. Through surface modification, molecular oxygen can dissociate into atoms that react chemically with those of carbon lead to the introduction of carboxylic functional groups to the surface. In fact, numerous hydrophilic groups were created on the mesoporous surface through oxidative treatment of CMK-3 and without destroying the ordered mesostructure (Figure 1-5) [36]. The hydrophilicity of the surface is increased and it is more desirable for hydrophilic analytes. Moreover, it enhances the wettability of polar solvents and makes the surface active for immobilization of hydrophilic compounds via adsorption. Hence, it improves the results for polar and hydrophilic analytes.

- 3) Improved in extraction for non-polar and hydrophobic analyte might be explained by bellows: Surface modification by carboxylic groups is also advantageous for the extraction of the less polar and non-polar analytes. In general, carbon surface is hydrophobic. However, the presence of the polar oxygen-containing groups (carboxylic group) may increase the hydrophilicity at the surface. Meanwhile water molecules can form hydrogen bonds with the oxygen atoms at the surface. These molecules may in turn form new hydrogen bonds with new water molecules (Figure 7-7). Moisture (water molecules) may limit the access of the hydrophobic adsorbate to the surface, thereby the adsorption of hydrophobic and non-polar analytes will not be as strong as before and the analytes may elute easily during desorption step. Hence a

hydrophobic/hydrophilic balance at the surface of carbonaceous sorbents is created.



Figure 7-7 Increase in the hydrophilic character of a carbon surface as a consequence of the presence of oxygen-containing surface groups.

- 4) The results indicate that the effect of modification was more significant for non-polar analytes than polar analytes. For instance, the observed peak area for the NDPhA increased 23 times when O-CKM-3 was used rather than CMK-3; however, this increase for NDMA was about twice.
- 5) The surface area of the sorbent is the second important factor for efficient extraction. Lowest results were obtained by Carboxen-1016 with surface area of 75 m<sup>2</sup>/g, and increasing the surface area improved the extraction results.
- 6) Carbosieve S-III with a surface area approximately same as coconut charcoal and activated charcoal showed poorer results than the latter two. This may be attributed to the fact that Carbosieve S-III has a closed pore structure and hence not enough pores may be available for the entrapment and adsorption of the analyte. Hence, not only the surface area and surface chemistry of the adsorbent but also the pores structure and their availability play an important role in entrapment and adsorption of analytes.

From all the above conclusions, O-CMK-3 with high surface area and moderated hydrophilicity/hydrophobicity surface could be considered as a promising sorbent for the simultaneous extraction of groups of NAs with a wide range of hydrophilicity and hydrophobicity.

#### **7.4. Conclusion**

There is an unmet need for simultaneous extraction of group of NAs with a wide range of polarity. Due to high polarity of some of NAs such as NADMA—the most well defined NA— their extraction is difficult and is mainly achieved by carbonaceous sorbent. However, non-polar or less polar NAs are strongly absorbed on the carbonic surface of the sorbent, leading to low extraction recoveries for less polar and non-polar analytes. To overcome this problem, for the first time surface-modified CMK-3 as OMC was used to extract groups of NAs. CMK-3 surface was modified by oxidative treatment and different carboxylic groups were attached on the carbonic surface of the sorbent, resulting in a hydrophilic/hydrophobic balance at the inert surface of carbonaceous sorbent. Following this modification, an acceptable extraction recovery was obtained for all analytes. Our results show that the proposed surfaced-modified sorbent was potentially able to extract and cover various NAs in a wide ranges of polarity. It was also confirmed that the oxidative process not only attached the oxygen-containing groups at the surface of the sorbent and moderate surface hydrophobicity but also maintained the ordered structure of carbonaceous sorbent.

## **CHAPTER 8: Analysis and determination of N-nitrosamines in wastewater and swimming pool water**

### **8.1. Introduction**

The US EPA Method 521, and some minor variations of it, is the most commonly cited instrumental analysis for trace analysis of NAs [145]. This method is based on GC-MS/MS, using large volume of injection on an ion trap mass spectrometer and chemical ionization (CI) with methanol or acetonitrile. Hence, CI has been adopted for practically all GC-MS methods reported for trace analysis of NAs. Regulations require many organizations and laboratories to routinely monitor NAs. However, few laboratories are equipped with GC-CI-MS/MS instruments with ion trap mass spectrometer. Instead, triple quadrupole with electron ionization (EI) is more affordable and cost-effective for many environmental and water quality control laboratories around the world.

As discussed in Chapter 7, carbonaceous sorbents by surface modification of CMK-3 (O-CMK-3) for simultaneous extraction of NAs was successfully developed. Consequently in this chapter a sensitive, practical, and reliable extraction method using O-CMK-3 as a sorbent for extraction of NAs from environmental water samples with subsequent analysis by using triple quadrupole GC-EI-MS/MS is developed.

### **8.2. Experimental**

#### **8.2.1. Chemicals and solutions**

NA reagents are same as those mentioned in Chapter 7 (section 7.2.2). In addition, isotopically labeled standards [6-2H] N-nitrosodimethylamine (NDMA-d6, 98%, 1 mg/L in

methylene chloride-d<sub>2</sub>) and [8-2H] N-nitrosopyrrolidine (NPYR-d<sub>8</sub>, 98%, 1 mg/mL in methylene chloride-d<sub>2</sub>) were purchased from Cambridge Isotope Laboratories (Tewksbury, MA, USA) and used as internal standard (IS) and surrogate standard (SS), respectively.

Stock standard solutions of individual NA (10 mg/L concentration) were prepared with extreme care during weighing (solid or liquid) and dissolving in methanol (LC-MS grade). The secondary stock standard solutions were prepared by diluting each stock solution in methanol to obtain a mixture of standards in concentration range of 100–1000 µg/L. All stock solutions were stored at –23°C and re-prepared freshly every month. Working standard mixture solutions were prepared daily in desirable concentration range by spiking secondary standard solutions in ultrapure water. Some NAs degrade when exposed to UV light, hence their prolonged exposure to fluorescent light was avoided by covering with foil. Standards and extracts were stored in freezer in amber-colored bottles or foiled-covered containers.

O-CMK-3 was synthesized as explained before (Chapter 7, Section 7.2.3) using same materials and procedure. Whatman filter paper (grade 1, 11 µm, cellulose filters, Maidstone, England) was used to filter real samples. All organic solvents purchased from Fisher Scientific (Fair Lawn, NJ, USA) were LC graded and included methanol (MEOH), acetonitrile, acetone, dichloromethane, chloroform (CHCl<sub>3</sub>), and carbon tetrachloride (CCl<sub>4</sub>). Ultrapure water was used for all experiments.

### **8.2.2. Sample collection**

Water samples were collected in disposable 500 mL polypropylene bottles (covered with aluminum foil to avoid exposure to light). Bottles were pre-cleaned with ultrapure water and methanol and baked at 110 °C for 3 h prior to use. Domestic wastewater samples (from

the primary clarifier of the Ulu Pandan Reclamation Plant, Singapore), and swimming pool water samples (from three different outdoor pools in the campus of National University of Singapore) were collected between August and September 2014. Bottles were filled completely up to rim. In order to quench any residual chlorine (that might be used for disinfection),  $\text{Na}_2\text{S}_2\text{O}_3$  as a preservative was added to bottles (50 mg per bottle) before samples collection. Samples filtered using Whatman filter paper and were stored at 4 °C prior to analysis. Analyses were carried out within 2 weeks of sample collection. Blank samples containing ultrapure water and preservative reagent were maintained at same conditions for blank control analysis. Samples were used in their original conditions without any pH adjustment or dilution.

### **8.2.3. Safety considerations and pollution prevention**

All conditions mentioned in Chapter 7 (Section 7.2.1) were carefully followed for this study as well and any contact with the standard and working solutions was strictly avoided. We optimized the experimental design, thereby reducing the numbers of primary experiments.

### **8.2.4. Instrumental analysis**

Instrumental conditions for the analysis have been described in detail in Chapter 7 (Section 7.2.6). In the current study, instrumental analysis for two isotopic IS and SS were also carried out using procedure same as that for other NAs. The general separation of the eight NAs, IS, and SS was performed in less than 18 min.



### 8.2.5. Identification and quantitation

MRM transition data acquisition mode was used to enhance the selectivity and sensitivity for simultaneous detection of eight volatile and semi-volatile NAs. In order to obtain product ions with highest sensitivity and minimum interference, a suitable MRM transition was chosen carefully. GC-MS/MS analysis was performed by data acquisition of two simultaneous MS/MS transition per compound. The most suitable transitions for MRM were identified by initially analyzing each analyte in scan mode, with a scan range of 50 m/z to M+10 m/z (M is the mass of the compound of interest), to determine the most suitable precursor ions in the first MS. Following this, the product ion scan was assessed to perform fragmentation of the precursor ions in the collision cell (using the same mass range and scan time). Quantitation and confirmation of precursor ions was chosen from the mass spectrum and product ion scan. Samples were run with a solvent cut time of 4 min. All the analytes were separated into seven discrete time segments for MRM monitoring with event time ranging from 0.086 to 0.3 seconds, depending on the time segment to achieve maximum cycles across each peak for good quantification. This allowed collection of a sufficient number of data points across the peak while retaining the signal intensity. In order to obtain the most intense fragmentation as well as to enhance detection sensitivity in EI mode, the collision energy was optimized in the range of 5–45 KV. Information related to analytes and isotopic standards, monitoring of ion transitions, specific dwell times, and collision energies is presented in Table 8-1. Confirmation of the analytes was carried out by accomplishment of two transitions and retention times. Chromatograms showing peaks of eight analytes on the column from an injection of 500 pg are presented in Appendix 4.

Table 8-1 Information on the analytes, standards and their MS/MS optimized conditions

No.	N-nitrosamines	Abbr.	CAS number	Molecular weight	RT. (min)	Quantitative ion		Qualitative ion		Event time (sec)
						Transition	CE	Transition	CE	
1	N-Nitrosodimethylamine	NDMA	62-75-9	74.08	6.25	74.10>42.00	11	74.10>30.00	11	0.150
2	N-Nitrosodiethylamine	NDEA	55-18-5	102.14	6.79	102.1>85.1	4	102.1>56.0	14	0.300
3	N-Nitroso-di-n-propylamine	NDPA	621-64-7	130.19	7.74	130.2>113	4	130.20>88.1	4	0.300
4	N-Nitroso-di-n-butylamine	NDBA	924-16-3	158.28	8.88	158.2>99.1	8	-	-	0.300
5	N-Nitrosopiperidine	NPIP	100-57-4	114.17	9.16	114.10>97.10	27	114.10>84.10	28	0.300
6	N-Nitrosopyrrolidine	NPYR	930-55-2	100.12	9.36	100.10>70.0	7	100.10>55.0	8	0.086
7	N-Nitrosomorpholine	NMOR	59-89-2	116.12	9.63	116.10>86.0	8	116.10>56.0	8	0.086
8	N-Nitroso-di-phenylamine	NDPhA	86-30-6	198.22	17.81	168.00>141.00	6	168.00>128.0	11	0.300
9	[6-2H] N-Nitrosodimethylamine	NDMA-D <sub>6</sub>	DLM-2130-S	80.08	6.25	80.00>50.00	7	80.00>62.00	17	0.150
10	[8-2H] N-Nitrosopyrrolidine	NPYR-D <sub>8</sub>	DLM-8252-1.2	108.12	9.36	108.00>708.	8	108.00>62.0	8	0.128

### 8.2.6. Extraction procedure

The  $\mu$ -SPE device (bag) with polypropylene membrane envelope ( $2 \times 2.5$  cm) was enclosed with O-CMK-3. The edges of the bag were heat sealed to secure the contents. As described in Chapter 1 (Section 1.4.1), different steps involved in  $\mu$ -SPE extraction were as given below: Conditioning: The bag was sonicated in pure methanol for 10 min followed by drying with lint-free tissue. Extraction: The bag was placed in the sample solution and maintained under shaker conditions of 300 revolutions per minute (rpm; KS 4000i control orbital shaker incubator, IKA, Germany) at 30 °C for a specified extraction time. Desorption: After extraction, the bag was taken out of the sample solution using a pair of tweezers, dried thoroughly with lint-free tissue, and placed in a vial for desorption. The analytes were desorbed by ultra-sonication with 200  $\mu$ L of desorption solvent, and 1  $\mu$ L of the extract was injected into the GC-MS/MS system. Studies have reported the use of nitrogen flow for solvent drying after desorption to concentrate the analyte, especially when the sensitivity of the instrument is not high enough for trace analysis [12]. We avoided this step, as our analytes were volatile and semi-volatile and there was a risk of analyte losses. Moreover, GC-MS/MS was sensitive enough for analysis of low level concentration.

The bag could be reused at least five times after ultra-sonication in methanol after every use (15 min, twice, each time in 5 mL fresh methanol). Carry-over effect after each extraction was checked in the highest concentration of analytes solution (100 ppb); no carry-over effect was observed.

### 8.2.7. Extraction optimization

The extraction optimization procedure was applied to find the best and optimum responses for all analytes. Finding simultaneous optimum conditions is more efficient and reliable, as it evaluates the effects of all the variations at the same time while taking into account the effect of each variation on the other. Hence, it was advantageous to use a multivariate statistical technique that could significantly save experiments, and hence cost and time. As mentioned in Chapter 4 (Section 4.2.5), to perform this task experimental designs such as RSM were employed in many of extraction studies [95, 156].

Evidently, there are many factors and parameters which are important for sorption-based extraction methodology. The sorbent type and the desorption solvent were qualitative parameters, while extraction and desorption time, amount of sorbent and sample, and salt concentration were most effective numeric parameters in determining the efficiency of  $\mu$ -SPE that we optimized them. Here, we separately evaluated the effect of different desorption solvent types on extraction. Following this, we systematically optimized the numeric parameters by RSM. A CCD with five independent variables was chosen for carrying out RSM. This is an effective statistical approach for responses which are influenced by different factors. All experiments were performed in random order to minimize the effects of uncontrolled parameters. ANOVA was used for data analysis. The software package design expert (version 9.0.1.0, Stat-Ease, Minneapolis, Minnesota, USA) was used for design generation and statistical analysis.

### 8.3. Results and discussion

#### 8.3.1. Optimization of the extraction

Optimization of desorption solvent: Given that NAs have a wide range of polarity, different organic solvents with varying polarity were used to examine the performance of desorption process (some important properties of solvents used have been summarized in the Appendix 1). Extraction was carried out on ultrapure water sample spike with 100 ng/mL mixture of analytes. The results of the extraction are presented in Figure 8-1. Evidently, DCM showed the best chromatographic signal and hence was deemed acceptable for the subsequent experiments. This was in line with the reported sorption-based extraction of NAs [121, 126, 140].

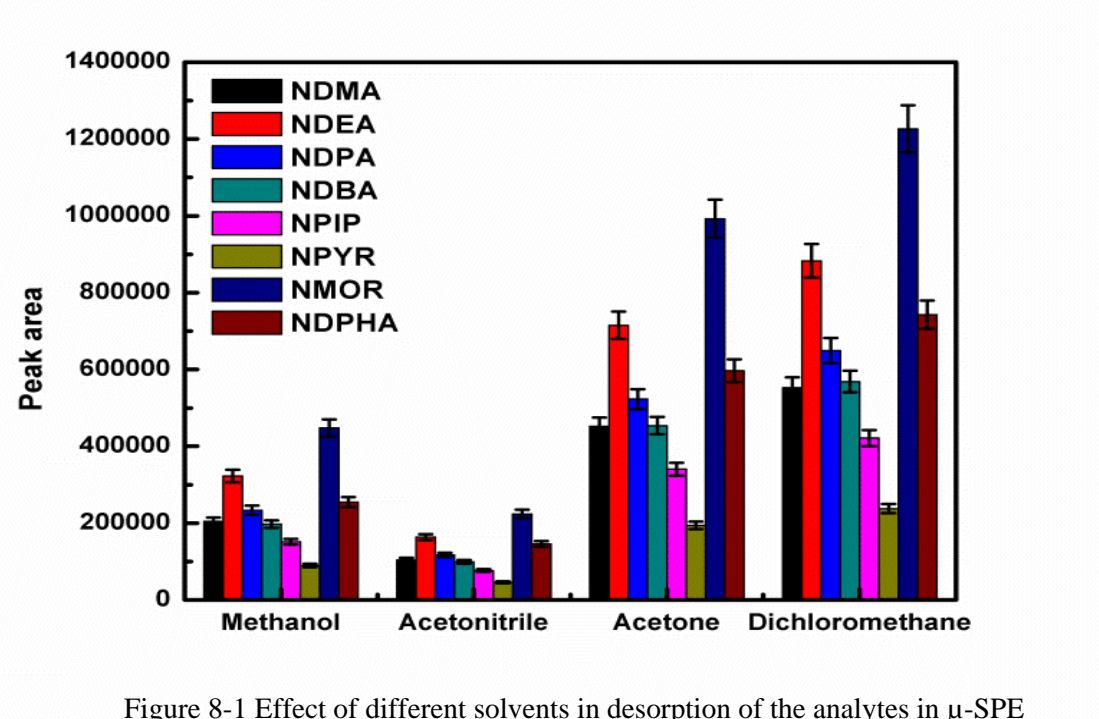


Figure 8-1 Effect of different solvents in desorption of the analytes in  $\mu$ -SPE

Optimization of numeric parameters: Numeric parameters were optimized simultaneously by CCD. The factors and their symbols and levels are shown in Table 8-2.

Table 8-2 Factors, their symbols and levels for CCD

Factor	Symbol	Level				
		- $\alpha$	-1	0	+1	+ $\alpha$
Amount of sorbent (mg)	A	7.5	15	22.5	30	37.5
Volume of sample (ml)	B	7.5	15	22.5	30	37.5
Extraction time (min)	C	0	5	10	15	20
Desorption time (min)	D	0	5	10	15	20
Salt concentration (w/v%)	E	0	10	20	30	40

Details of CCD have been described in Chapter 4 (Section 4.3.1). The total number of experiments was equal to 32 and all were performed based on Table 8-3.

Table 8-3 Design matrix (actual) with responses

Run	A	B	C	D	E	Response
1	30.00	15.00	5.00	5.000	10.00	6.35465
2	30.00	15.00	15.00	5.000	30.00	3.22281
3	22.50	22.50	10.00	20.00	20.00	4.10191
4	15.00	15.00	5.000	5.000	30.00	1.11239
5	22.50	37.50	10.00	10.00	20.00	4.91537
6	30.00	30.00	15.00	5.000	10.00	8.00000
7	22.50	22.50	0.000	10.00	20.00	0.76354
8	15.00	30.00	5.000	5.000	10.00	1.55599
9	15.00	15.00	15.00	15.00	30.00	1.57689
10	15.00	15.00	5.000	15.00	10.00	1.58056
11	37.50	22.50	10.00	10.00	20.00	6.46225
12	7.500	22.50	10.00	10.00	20.00	0.27203
13	22.50	22.50	10.00	10.00	20.00	5.08173
14	15.00	15.00	15.00	5.00	10.00	2.34522
15	22.50	22.50	10.00	10.00	20.00	4.09165
16	15.00	30.00	5.000	15.00	30.00	1.13257
17	22.50	22.50	10.00	10.00	0.000	0.76327
18	30.00	15.00	5.000	15.00	30.00	3.24542
19	30.00	30.00	5.000	5.000	30.00	3.20795
20	22.50	22.50	10.00	10.00	20.00	4.08596
21	22.50	22.50	10.00	0.000	20.00	3.29142
22	30.00	30.00	5.000	15.00	10.00	6.43139
23	15.00	30.00	15.00	5.000	30.00	1.57695
24	15.00	30.00	15.00	15.00	10.00	2.36479
25	30.00	15.00	15.00	15.00	10.00	7.99017
26	22.50	22.50	20.00	10.00	20.00	4.05153
27	22.50	7.500	10.00	10.00	20.00	0.36874
28	30.00	30.00	15.00	15.00	30.00	3.25505
29	22.50	22.50	10.00	10.00	20.00	5.09221
30	22.50	22.50	10.00	10.00	20.00	3.09405
31	22.50	22.50	10.00	10.00	20.00	4.08202
32	22.50	22.50	10.00	10.00	40.00	0.53507

In this study, normalized extraction efficiency (extraction efficiency being defined as a ratio of concentration after and before extraction)—an approach widely used for simultaneous optimization of several response variable—was chosen as an experimental response [91 ,90]. Responses were obtained by a procedure described in Chapter 4 (Section 4.3.1) [90]. ANOVA was used to evaluate data (Table 8-4). A F value of 13.92 indicated that the model was significant. A lack of fit (LOF) F-value of 2.45 implied that the model was insignificant relative to the pure error. Adeq Precision measured the signal to noise ratio; a ratio greater than 4 was desirable. In our study, the ratio was 13.89, indicating an adequate signal. Therefore, the suggested model could be used to navigate the designed space.

Table 8-4 ANOVA for CCD

Source	Sum of Squares	d.f. <sup>a</sup>	Mean Square	F-Value <sup>b</sup>	p-value <sup>c</sup> Prob > F	
Model	117.81	7	16.83	13.92	< 0.0001	significant
A-Amount of sorbent	69.50	1	69.50	57.50	< 0.0001	
B-Volume of sample	3.52	1	3.52	2.91	0.1009	
C-Extraction time	6.29	1	6.29	5.20	0.0317	
D-Desorption time	0.14	1	0.14	0.11	0.7381	
E-Salt effect	14.65	1	14.65	12.12	0.0019	
AE	11.22	1	11.22	9.28	0.0056	
E <sup>2</sup>	12.49	1	12.49	10.33	0.0037	
Residual	29.01	24	1.21			
Lack of Fit <sup>d</sup>	26.20	19	1.38	2.45	0.1632	not significant
Pure Error	2.82	5	0.56			

<sup>a</sup> Degrees of freedom.

<sup>b</sup> Test for comparing model variance with residual (error) variance.

<sup>c</sup> Probability of seeing the observed F-value if the null hypothesis is true.

<sup>d</sup> The variation of the data around the fitted model.

F-value less than 0.0500 indicated statistical significance of the effect at 95% confidence level. Hence, based on the results A, E, E<sup>2</sup>, AE are the most effective factors. In this study, CCD was expressed as the following second order model for the most effective independent variables:

$$\sqrt{\text{Normalized peak area}} = -9.67576 + 0.45019 A + 0.051055 B + 0.10239 C + 0.015182 D + 0.43118 E - 0.011164 AE - 0.011164E - 0.00645267 E^2 \quad (8-1)$$

Thus, the quadratic model was considered as appropriate response surface model for CCD. Graphs related to the effect of each factor in the desirability (maximum normalized peak area), in addition to interactions between variables have been submitted in the Appendix 5 and 6 respectively.

Eventually, in order to achieve maximum efficiency, optimization mode of Design-Expert 9.0.7.1 was used to obtain optimum values for all parameters. These values were 30 mg of sorbent, 30 mL of sample, 10% concentration of salt in the sample, extraction time of 15 min, and desorption time of 15 min. These conditions were chosen for subsequent experiments.

### **8.3.2. Study of the $\mu$ -SPE mechanism**

For better understanding of the mechanism of  $\mu$ -SPE, following experiments were conducted. Solutions containing 10 and 100 ng/mL of all analytes were prepared and extraction process was performed twice consecutively on the same solution. Each experiment was repeated thrice. The relative response parameter (RRP) was calculated based on the percentage of ratio of peak area of analytes in the second extraction to that found in the first extraction. An average of RRP obtained for all analytes ( $n = 3$ ) was 28.05 and 45.30 for 10 and 100 ng/mL, respectively (Table 8-5).

The results revealed that  $\mu$ -SPE had an equilibrium-based mechanism and was not exhaustive as like some of the sorption-based methods such as SPE. Moreover, mass transfer with  $\mu$ -SPE was not as effective when compared with SPE. Some reasons for



this observation can be speculated: Firstly, in SPE the sample solution is in close and direct contact with sorbent for longer time and the sample is passed through the column (driven by pumping mechanism, whether by gravity or applied pressure). In contrast, the only driving force for mass transfer in  $\mu$ -SPE is stirring of the sample. Secondly, SPE requires almost 1000 times more sorbent as compared to  $\mu$ -SPE (25 g versus 25 mg). The low amount of sorbent in  $\mu$ -SPE might be an obstacle in exhaustive and comprehensive extraction of analytes. This can be proved from the following observation: It is evident that RRP (representative of mass transfer) depends upon the concentration of the sample and by increasing the concentration of the sample, the active sites on the sorbent might start losing their availability [the ratio of the number of analyte molecules to the available surface area (active site) of the adsorbent] for the analytes, thereby increasing the RRP. Moreover, absorption of the analytes on the sorbent surface would change the chemical properties of the diffusion layer or the surface of the sorbent, which in turn would reduce the diffusion rate of the target analyte into the sorbent. This could be attributed to the fact that formation of a layer of analyte over the adsorbent surface hinders the formation of further layers; due to the interaction between analytes present at the surface and in the solution.

Table 8-5 Evaluation of the mechanism of the  $\mu$ -SPE

Compound	RRP (%) (at 10 ng/ml)	RRP (at 100 ng/ml)
NDMA	30.31	46.47
NDEA	28.77	45.81
NDPA	28.30	45.25
NDBA	28.64	44.22
NPIP	20.27	44.76
NPYR	31.14	45.83
NMOR	28.35	44.98
NDPhA	28.65	45.06
Avg.	28.05	45.30

### 8.3.3. Method validation

After establishing the best instrumental conditions, instrumental quality parameters were evaluated as below:

Instrument stability was assessed on an intra-day and inter-day analysis. RSDs of five consecutive injections of 500 pg of mixture of analytes at the same day (run-to-run injection) were considered as intra-day assay of instrument. Day-to-day (inter-day) assay for the instrument was evaluated by injecting 500 pg mixture of compounds in 3 consecutive days. The average RSDs for retention times were 0.01 and 0.02 for the intra-day and inter-day assay, respectively. It means the instrument conditions had a great stability for the detection of analytes at same days and different days. The average RSDs for the peaks area were 11.46 and 1.66 for the inter-day and intra-day assay, respectively. Increase in the RSDs for the inter-day assay is probably due to the thermal instability of these compounds. Hence, instrumental analysis of the samples at the same day of experiment was recommended. Instrumental detection limit (IDL), and instrumental quantification limits (IQLs) were determined using 1  $\mu$ L injection of compounds as a mass (pg) of analyte that produced an MS signal 3 and 10 times greater than the signal to noise ratio for IDL and IQL, respectively. All results related to instrumental quality parameters were presented in Table 8-6. As can see from these figures of merit, GC-EI-MS/MS is sensitive enough for our aim.

Table 8-6 Instrumental quality parameters

Compound	IDL (ng/ml)	IQL (ng/ml)	RSD (%) run-to-run (n=5)		RSD (%) day-to-day (n=3)	
			RT	Peak area	RT	Peak area
NDMA	0.347	1.157	0.03	1.38	0.03	11.60
NDEA	0.032	0.108	0.01	1.58	0.01	12.54
NDPA	0.030	0.097	0.01	1.63	0.01	12.74
NDBA	0.070	0.230	0.01	1.8	0.02	12.47
NPIP	0.300	0.998	0.01	1.72	0.01	9.35
NPYR	1.260	4.202	0.00	1.87	0.01	10.71
NMOR	0.119	0.395	0.00	1.59	0.01	11.11
NDPhA	0.438	1.462	0.01	1.66	0.03	11.15
Avg.	0.3245	1.081	0.01	1.65	0.02	11.46

The method quality parameters was evaluated and validated by a series of factors such as linearity range and correlation coefficient of the calibration curves, LODs, LOQs, and precision (RSDs). The results have been summarized in Table 8-7.

The linearity range of the method was obtained by analysis of ultrapure water samples which were spiked at a concentration range of 0.1–100 ng/mL. Calibration curves were obtained by plotting the relative response ratio (peak area) versus relative concentration ratio of the analyte to internal standard. Each calibration standard solution included 20 ng/mL of isotopically labeled internal standard. The use of isotopic dilution ensure accurate quantification by accounting all varieties and uncertainties that may be introduced during the whole process (sampling, extraction, ionization, mass fragmentation, etc) [157]. Approximately 13 calibration points were used for each analyte separately. All calibration curves showed correlation coefficient of minimum 0.999. Graphs related to calibration curves for each analyte have been reported in the Appendix 7. LODs and LOQs of the method were calculated based on the mass of analyte that produced a response 3 and 10 times greater than the signal to noise ratio for LODs and LOQs, respectively. The RSD% of the method was calculated at a concentration of 50 ng/mL (n = 8). The obtained values for LODs and LOQs were higher than those reported by the others studies using SPE as an extraction

methodology (LODs less than ng/L have been reported for them). In our study, we could not produce such a low LOD value. This is attributable to the limitation of the  $\mu$ -SPE in mass transfer compared to SPE. Mass transfer in the  $\mu$ -SPE is not exhaustive and as efficient as that in SPE. The limited amount of sorbent used in  $\mu$ -SPE is considered as one of the advantages of  $\mu$ -SPE; however, it may pose certain limitations for specific applications.

Table 8-7 Method quality parameters

Compound	Linear range (ng/ml)	Calibration equation	R <sup>2</sup>	LOD (ng/ml)	LOQ (ng/ml)	RSD (%) (n=8) (50ng/ml)
NDMA	0.1-100	Y = 0.1252113x - 6.854739e-003	0.9995	0.051	0.172	3.09
NDEA	0.1-100	Y = 0.1981883x - 1.272771e-002	0.9995	0.005	0.018	4.80
NDPA	0.1-100	Y = 0.1455687x - 1.089966e-002	0.9994	0.004	0.016	4.92
NDBA	0.1-100	Y = 0.1270689x - 1.062884e-00	0.9990	0.016	0.055	4.90
NPIP	0.1-100	Y = 0.1638663x - 6.310227e-003	0.9996	0.084	0.282	5.20
NPYR	0.1-100	Y = 5.384861e-002x - 2.076047e-003	0.9996	0.283	0.943	6.22
NMOR	0.1-100	Y = 9.478164e-002x - 6.475003e-003	0.9994	0.067	0.226	4.53
NDPhA	0.1-100	Y = 0.2721248x - 1.748773e-002	0.9995	0.039	0.131	4.50
Avg.			0.9994	0.056	0.187	4.77

#### 8.3.4. Analysis of the real samples

Once optimization of  $\mu$ -SPE-GC-MS/MS for the analysis of NAs was achieved, the method was extended to monitor NAs in environmental water samples. The occurrence and distribution pattern of NAs vary with different water samples and depend on the geographical locations and sources. Hence, there is a need for monitoring various real water samples to evaluate the occurrence and levels of NAs in water. To our best knowledge, there is no such monitoring carried out for water matrices in Singapore. The obtained figures of merit Table 8-7 confirm that the current method could not be employed for analysis of drinking water; however, it is suitable for other real water samples. These figures of merit are within the applicable and acceptable range for analysis of river water, wastewater, and swimming pool water. For instance Ji-Hyun Lee and co-workers reported analysis of river water and wastewater with a total

concentration of target NAs ranging from 3.061 to 28.268 ng/mL [141]. In addition, Krauss and co-workers reported higher levels of different NAs in Switzerland domestic wastewater than the concentration range obtained from the figures of merit of this study [147]. In this direction, we chose two water sample types for determination of NA levels and most importantly for evaluation of the performance of the proposed method using different complex aqueous matrices—swimming pool water and domestic wastewater. The importance of the analysis of NAs in wastewater has been described in Chapter 6 (section 6.4). With respect to swimming pool water, it must be emphasized that DBPs in swimming pool water have become a topic of interest, as epidemiologic research has shown increased incidence of asthma and bladder cancer with an exposure to DBPs in indoor pools. As mentioned before, swimming pools have additional precursors (including components of human sweat, urine, sunscreens, etc.) for the formation of NAs [158]. Moreover, the awareness for the analysis of NAs in swimming pool water increased when it was revealed that swimming can actively increase the dermal adsorption and inhalation of these compounds. Studies show that swimming contribute to equivalent, or even greater, exposure to NAs than ingestion of disinfected drinking water [159]. As mentioned before, NDMA has the same skin permeability as hydrocortisone ( $10^{-4}$  cm/h), an active ingredient of topical ointments used for treatment of skin illness [158, 160]. Hence, the analysis and determination of NAs in swimming pool waters has significant importance in public health.

Samples were collected as described before (Section 8.2.2). They were spiked at a concentration of 100 ng/mL of mixture of analytes and 20 ng/mL of IS and SS.

Relative recoveries (RR%): RR% were calculated as follows. Extraction was carried out on the spiked samples (100ng/ml) and 1  $\mu$ L of the extract was injected on GC-MS/MS.  $A_i$  was the peak area obtained for each analyte. Following this, parallel non-spiked sample was extracted and the extract was spiked with a mixture of analytes at concentration of 100ng/mL. Then 1  $\mu$ L of mixture was injected.  $B_i$  was the peak area obtained for each analyte. Recovery for each analyte was assumed as a percentage of the ratio of  $A_i$  to  $B_i$ . As seen from the results, a recovery of more than 60% was obtained for all analytes and all samples (regardless of the polarity of the analytes). As described in Chapter 6 (Section 6-7), achieving such high recovery (simultaneously for all the analytes) was needed and this could be considered as the best achievement of this work.

Matrix effect: Post-extraction addition strategy was chosen to evaluate the matrix effect [161]. Matrix effect was estimated for each analyte by calculating the ratio of the peak area in presence of the matrix (spiked extract) to that in absence of the matrix (spiked solvent). As seen in Table 8-8 and Table 8-9, the matrix effect obtained for all samples (both swimming pool and wastewater) was close to 1 and no significant variation from the unit was observed. To conclude, the results are about free of matrix effects and interferences that may affect the result are negligible. This might be attributed to the combination of two phenomena: First, the potential interference source had less chance to compete with the analyte in the extraction due to higher affinity of the sorbent for the analyte or the protective effect of the polypropylene membrane in removing interference source from the sorbent. Second, the use of MRM methodology in the instrumental analysis; MRM made the analysis very sensitive and specific to

fragmentations resulted from NAs than other probable species producing same fragmentation. (Although matrix effect can affect the results in other ways, some species may be present in the sample that would influence the ionization process, either by suppression or enhancement).

NAs in swimming pool water samples: The concentration of NAs in swimming pool water samples are reported in Table 8-8. Evidently, all samples were contaminated with relatively high concentration of NDMA, potentially due to the reaction between chlorinating <sup>1</sup> agents and dimethylamine contributed from urine and sweat. The amount of urine and sweat depends on many factors such as bad personal habits, numbers of swimmers, and hours of practice. Furthermore, a direct relation between temperature and formation of NDMA in water has been reported [162]. In our study, samples were collected from outdoor swimming pool. Singapore is a tropical country with high temperature during sampling time (August-September). Hence, this could be considered as one of the reasons for high level of NDMA. NDEA, NDBA, and NDPhA were also detected in all samples at less than LODs. Jurado-Sanchez and co-workers reported the presence of NDMA, NDEA, and NPYR [163]. Pozzi and co-workers reported the presence of NPYR in swimming pool samples. Fu and co-workers reported different concentration of NDMA in different swimming pool samples [140]. Hence, similar results for the specific amount of each NA have not been reported and it depends on many factors which have been described before.

---

<sup>1</sup> Based on our enquiry chlorination had been used for the disinfection of the swimming pools from where samples had been taken.

NAs in wastewater samples: The concentration of NAs determined in wastewater samples are reported in Table 8-9 and Figure 8-2 displays the chromatograms of non-spiked and spiked samples of the wastewater samples. Samples were contaminated with high concentration of most of the NAs included in the analysis. NDPA and NDPIP were undetected either due to their absence or concentration below LODs. As stated before, NA occurrence and distribution pattern differs from country to country and source to source [164]. For instance, the concentration of nitrosamines detected was as high as 2.5 mg/L for NDMA and 0.17 mg/L for NDEA in Russian industrial effluents. NDMA and NDEA concentrations were 9.040 and 0.132 g/L, respectively, in German wastewaters. More recently, NDMA level ranged from 160 to 834 ng/L in chlorinated wastewater effluents from USA. NDMA and NMOR levels of 8–400 and 56–1390 ng/L, respectively, were recorded for wastewater effluents from USA [134]. The highest concentration was reported for NPYR, NDMA, NDEA, NMOR, NDPA, NPYR, NPIP, and NDBA in the wastewater [135, 165]. Yoon and co-workers reported the presence of NDMA in wastewater [135]. Lee and co-workers reported high and varying concentration of different NAs (except NDPhA) in wastewater [141].

#### **8.4. Conclusion**

Analysis of NAs in water samples is challenging, yet demanding. In this study, we have devised a simple, reliable, and practical methodology for the quantitative determination of eight NAs considered important by the US-EPA from swimming pool water and wastewater samples. The method was based on  $\mu$ -SPE followed by gas chromatography coupled to tandem mass spectrometry electron ionization (GC-EI-MS/MS) with the triple quadrupole analyzer (QqQ). The combination of these two



approaches, used for extraction and instrumental analysis, makes the whole process very cost-effective for the routine analysis of NAs as compared to the previously reported methodologies.

For quantitative instrumental analysis of each compound, simultaneous acquisition of two MS/MS transitions in selected reaction monitoring mode along with the evaluation of its relative intensity was used to allow simultaneous reliable quantification and identification. The instrument showed satisfactory stability over inter-day and intra-day analysis, with average RSDs of 11.46 and 1.66, respectively.

We used a porous polypropylene membrane bag containing 30 mg surface-modified CMK-3— as an oxidative-treated carbonaceous sorbent in a  $\mu$ -SPE extraction strategy. Moreover, CCD has been used for simultaneous optimization of the extraction process.

The optimized method was validated at a concentration range of 0.1–100 ng/mL. The precision of method was evaluated and an average RSDs of 4.77 ( $n = 8$ ) for 50 ng/mL was obtained. For accurate quantification, the isotope labeled NA (NDMA-d6) was added as internal standard to the samples. LODs were found to be in the range of 0.005–0.283 ng/mL.

Domestic wastewater and swimming pool water were used to evaluate the applicability of the method and to monitor NAs. All samples were contaminated by NAs. The concentrations were less than 2 ng/mL for swimming pool waters and less than 11 ng/mL for wastewaters. Satisfactory recovery was obtained for all the samples.

The mechanism of the  $\mu$ -SPE was also studied. It has been revealed that the  $\mu$ -SPE is an equilibrium-based extraction process and does not have an exhaustive mechanism as SPE. This might be related to the low amount of the sorbents used and/or to the way that analyte and sorbent make contact with each other (in comparison to SPE). This could be one of the drawbacks of  $\mu$ -SPE which can limit its applicability for some applications.

Table 8-8 Analytical parameters of NAs in swimming pool water samples

Analyte	Swimming pool water 1			Swimming pool water 2			Swimming pool water 3		
	ME	Rec. (%)	Conc.	ME	Rec. (%)	Conc.	ME	Rec. (%)	Conc.
NDMA	1.05	74.03	1.812	1.05	74.58	1.829	1.11	71.66	1.85
NDEA	1.05	70.30	<LOD	1.12	66.16	<LOD	1.06	72.20	<LOD
NDPA	1.06	70.92	n.d.	1.12	66.42	n.d.	0.95	80.096	n.d.
NDBA	0.98	76.90	<LOD	1.05	71.35	<LOD	0.97	60.413	<LOD
NPIP	0.96	78.03	n.d.	1.02	73.28	n.d.	0.95	60.422	n.d.
NPYR	1.05	70.55	n.d.	1.12	66.31	n.d.	1.05	72.86	n.d.
NMOR	0.99	69.63	n.d.	1.13	61.70	n.d.	1.01	71.88	n.d.
NDPhA	1.06	68.26	<LOD	1.13	63.51	<LOD	1.10	56.164	<LOD

Table 8-9 Analytical parameters of NAs in wastewater samples

	Wastewater 1			Wastewater 2			Wastewater 3		
	ME	Rec. (%)	Conc.	ME	Rec. (%)	Conc.	ME	Rec. (%)	Conc.
NDMA	1.12	67.13	2.052	1.08	66.27	<LOD	1.10	69.17	2.032
NDEA	0.98	72.5	<LOD	1.01	66.70	<LOD	1.04	68.66	1.298
NDPA	0.95	75.76	2.315	0.99	68.45	<LOD	1.05	68.49	<LOD
NDBA	0.98	57.24	<LOD	0.93	56.37	<LOD	1.05	68.42	<LOD
NPIP	0.93	76.30	n.d.	0.99	69.10	<LOD	1.05	68.60	<LOD
NPYR	1.02	70.69	10.165	0.99	51.68	10.249	1.04	68.23	10.4135
NMOR	1.03	56.20	2.126	1.00	64.95	1.595	1.04	62.99	2.0755
NDPhA	1.02	66.74	1.51	0.99	56.66	1.558	1.04	65.71	1.526

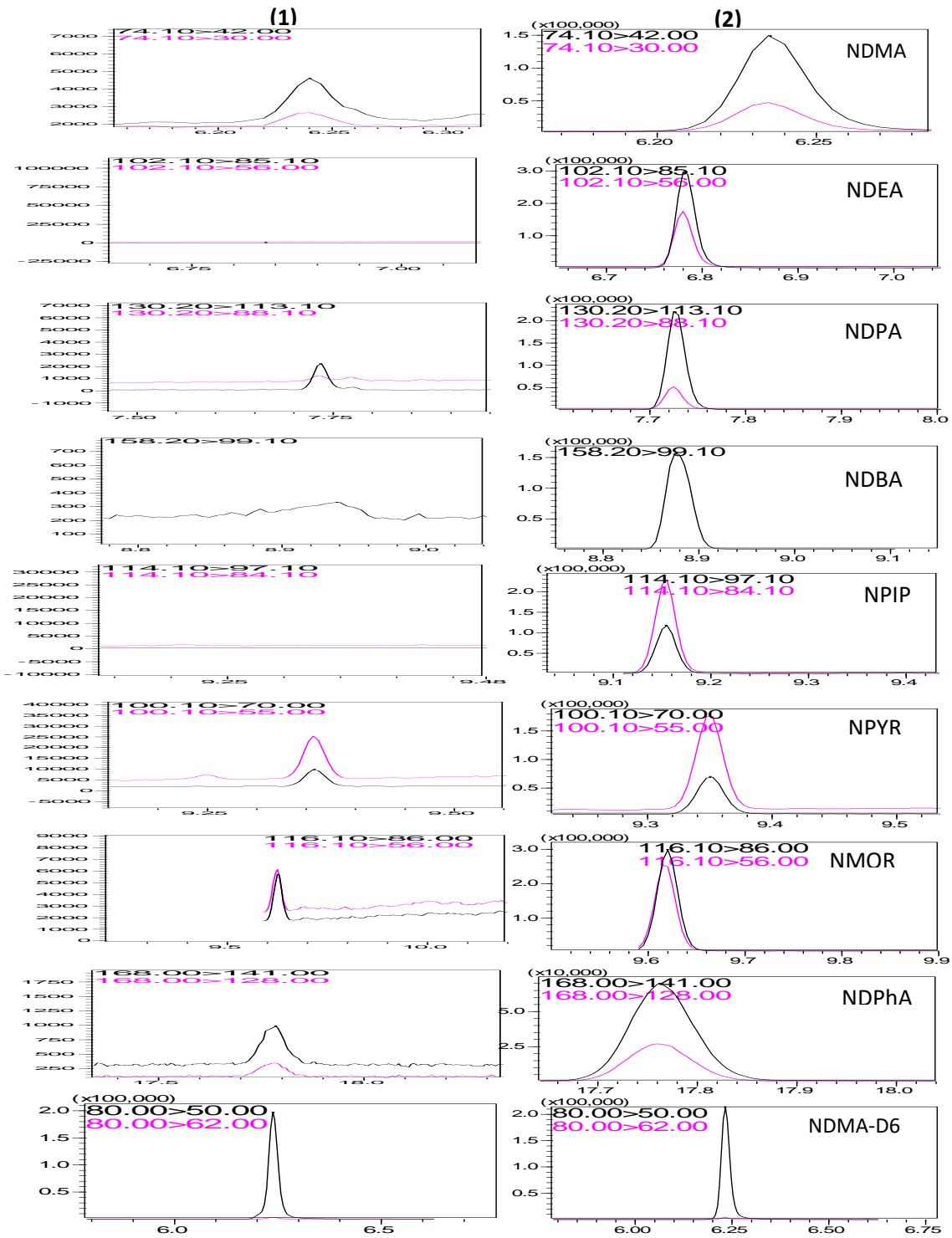


Figure 8-2 GC-EI-MS/MS of analytes extracted from wastewater by the developed method: (1)

Unspiked sample, (2) spiked sample at 100 ng/ml.  $^{13}\text{H}$  mass labelled NDMA (NDMA-D6) was used as internal standard

## **CHAPTER 9: Analysis and determination of N-nitrosamines in beverages**

### **9.1. Introduction**

The sources of NA in food matrices and beverages have been described in Chapter 6 (Section 6.4). Controlling NA levels in beverages is important not only for trade purposes but also for ensuring safety of humans. Historically, there are many extraction and clean-up procedures for the determination of NAs in food, including LLE [136], solvent extraction methods using dry Celite column [166, 167], and AOAC official method 982.11 using low temperature vacuum distillation [168]. These methods are time consuming, labor intensive (resulting in loss of some analyte), and require the use of large volumes of toxic solvents. More recently, SPME employing various fiber materials, including polydimethylsiloxane–divinylbenzene (PDMS–DVB), and divinylbenzene/carboxen/polydimethylsiloxane (DVB/CAR/PDMS) was used for the determination of volatile NAs in beer and some food samples [169, 170]. SPME required careful optimization of various parameters (such as the sampling and desorption time and temperature) in order to achieve repeatability and equilibration of NAs between sample and headspace. However, it was confirmed that despite the use of lengthy extraction times, equilibrium of NAs between the sample and the fiber was not always achieved. Moreover, SPME extraction efficiency was too low for most important NAs [114, 171]. Eventually, sample preparation methods for beverages employed SPE using carbonaceous sorbent. It provided fairly clean extracts and reduced the use of environmentally toxic solvents. However, the current challenges as described in Chapter 6 (Sections 6.6. and 6.7) still remain unsolved.

In this direction, in the current chapter we develop the improved version of our presented method (described in Chapter 8) as an elegant alternative to the existing procedures for the determination of NAs in beverages. This method was used for a range of beverages, including soft drinks (juice), beers, wines, vodka, and whiskey. The results of this study could be useful to develop a reliable and practical methodology for routine monitoring of NAs in beverages.

## **9.2. Experimental**

### **9.2.1. Chemicals and materials**

Chemicals and materials same as those described in Chapter 8 (Section 8.2.1.) were used. In addition, ethanol was used for the evaluation of the effect of alcohol on the analysis. HPLC-graded ethanol was purchased from Fisher Scientific (Loughborough, UK). O-CMK-3 was synthesized using the procedure as described in Chapter 7 (Section 7.2.3.) and used as  $\mu$ -SPE sorbent.

### **9.2.2. Instrumental analysis**

In the present study, the conditions for instrumental analysis were same as those described in Chapter 7 (Section 7.2.6). The same optimization approach as described in Chapter 8 (Section 8.2.5) was used for the identification and quantitation of the analytes.

### **9.2.3. Sample preparation and extraction**

Seven samples (alcoholic and non-alcoholic, bottles and cans from different brands, different countries), were purchased from the local supermarket (Singapore,

August- September 2014). These were stored in their sealed containers at 4°C until analysis. Some samples which required filtering (grape juice and wine) were passed through Whatman filter paper (Maidstone, England) (grade 1, 11 µm, cellulose filters). In order to estimate the performance of the method, the samples were used in their original state without any pH adjustment or dilution. Samples (30 mL) were degassed by vigorous shaking and spiked with different concentrations of NAs and 20 ng/mL of IS. Extraction was carried out using the protocol described in Chapter 8 (Section 8.3.1.).

#### **9.2.4. Effect of alcohol concentration on the extraction process**

We aimed to investigate the applicability of this study for alcoholic beverages. The alcohol (ethanol) content might affect the retention of the analytes on the sorbent or surface chemistry of the sorbent, leading to variation in results or overall performance of the extraction methodology.

The samples we evaluated contained ethanol concentration ranging from 0% for juice to 40% for whiskey. Alcohol effect was evaluated as following: Water-ethanol solutions from NAs in a 100 ng/L concentration were prepared (with ethanol concentration ranging from 0% to 40%). Extraction and analysis were carried out accordingly and results were obtained for each analyte separately.

### **9.3. Results and discussion**

#### **9.3.1. Effect of ethanol concentration on the extraction process**

Results have been summarized in Figure 9-1. As shown in the figure, the concentration of alcohol had no significant effect (positive or negative) on the



extraction process and the results were independent of the ethanol content (in the evaluated range). Our observations are in line with those recorded previously [136].

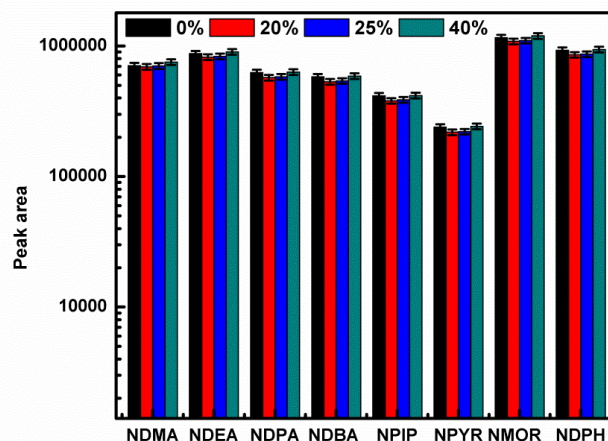


Figure 9-1 Effect of the alcohol content in the sample media on the extraction process

We are convinced that the change in the surface chemistry of the sorbent is the most important factor that might change the results of the extraction. Hence seems the alcohol content of the solution did not interfere with the surface chemistry of the sorbent. This can be explained by the pH of the media in relation to the point of zero charge ( $pH_{pzc}$ ) of the sorbent; that is, if the  $pH > pH_{pzc}$ , acidic functionalities would dissociate, releasing protons into the medium and leaving negative charge at carbon surface. On the other hand, if the  $pH < pH_{pzc}$ , basic sites would combine with protons from the medium to leave positive charge at carbon surface [172]. Hence, based on the above description the surface of the sorbents will be highly affected by the pH of the media. Notably, basic carbons are preferred for adsorbing acidic molecules while acidic carbons will perform better for the adsorption of basic compounds. Hence interactions of each analyte with surface, changes significantly at different pH. When the medium contains alcohol (ethanol), there is no significant change in the pH of the media because

ethanol is a neutral molecule and the acidity of water and ethanol is nearly the same as indicated by their pKa. Eventually, the changes in the surface chemistry of the sorbent due to change in pH are not significant and thus the results are not affected by the alcohol content (at least in the surveyed concentration rate).

### **9.3.2. Method validation**

The analytical features of the optimized  $\mu$ -SPE coupled with GC-EI-MS/MS were investigated in terms of linear response ranges, reproducibility (RSDs), MEs, LODs, and LOQs for each analyte. Three replicated analyses were carried out for each concentration level. The blank analysis was carried out in parallel with every analysis. Isotopically-labeled internal standards were used. The results have been summarized in Table 9-1.

Separate calibration curves for each analyte were obtained by the analysis of spiked sample at concentration ranging from 0.1 to 100 ng/mL. Each calibration standard included 20 ng /mL of isotopically-labeled IS. Calibration curves comprised 13 points (0.1, 0.5, 1, 5, 10, 15, 20, 30, 40, 50, 60, 80, and 100 ng/mL) and were plotted as relative response ratio versus relative concentration ratio of the analyte to internal standard for each analyte separately. All calibration curves had a minimum correlation coefficient of 0.99.

RSD for samples containing 50 ng/mL of each NA was considered as repeatability of the proposed method (n = 5, within day). An average RSDs of 13.72 was obtained for all analytes.

Matrix effect was assessed as described in Chapter 8 (Section 8.3.4). Matrix effect value of about 1 was obtained for all analytes, indicating that the interference of the matrix with the results was negligible. Thus, the method was successful in significantly decreasing the ME and interferences.

As described previously in Chapter 8 (Section 8.3.3.), LODs and LOQs of the method were calculated from the analysis and extraction of red wine sample spiked with mixtures of analytes. An average LOD of 0.44 ng/mL (can be equal to  $\mu\text{g}/\text{kg}$  of sample if the density of the samples is considered to be 1 g/L) was obtained. We found that LODs obtained were within the range reported in previous studies [136].

Table 9-1 Method quality parameters for analysis of NAs in beverages

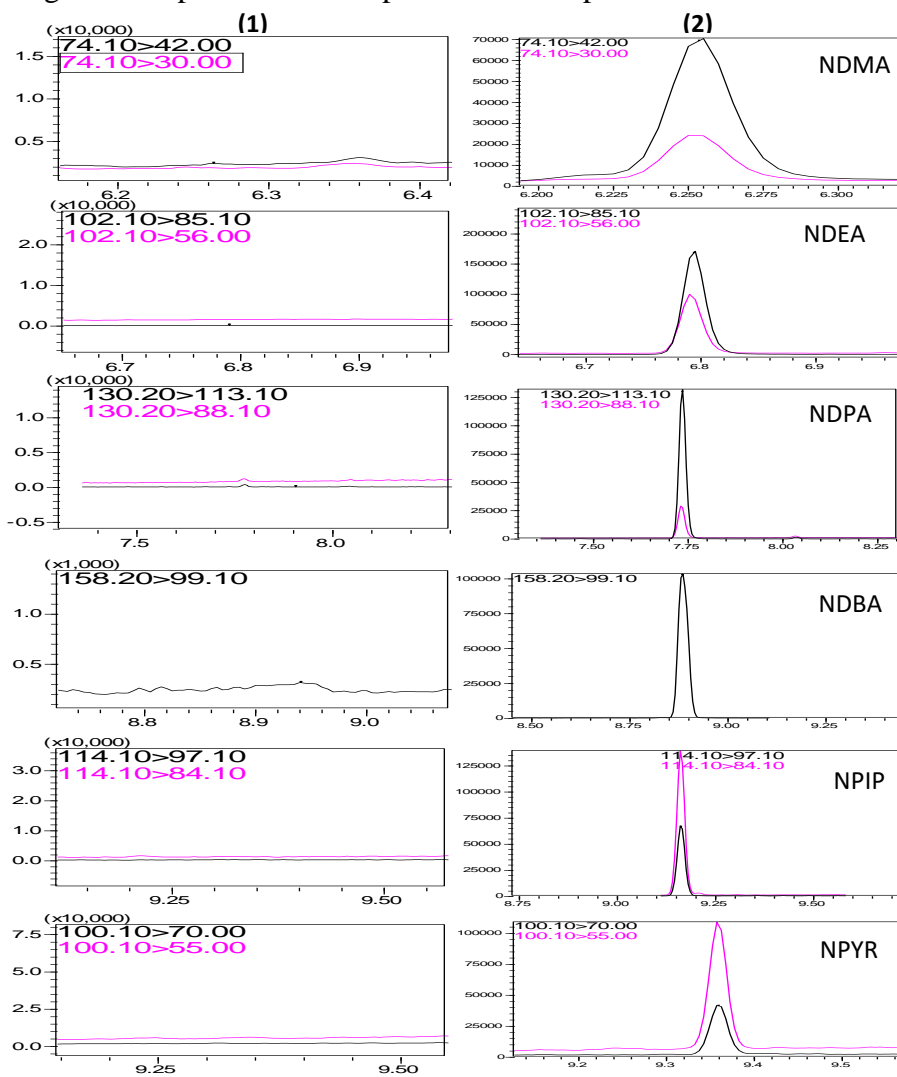
Compound	Linear range (ng/ml)	Calibration equation	R <sup>2</sup>	LOD (ng/ml)	LOQ (ng/ml)	RSD (%) (n=8) (50ng/ml)	Matrix effect
NDMA	0.1-100	Y = 0.1542065X - 9.064084e-003	0.9989	0.060	0.197	13.86	1.00
NDEA	0.1-100	Y = 0.1810248X - 1.328306e-002	0.9988	0.007	0.023	13.9	0.99
NDPA	0.1-100	Y = 0.126283X - 1.002178e-002	0.9986	0.008	0.026	14.27	0.99
NDBA	0.1-100	Y = 0.1172994X - 9.777834e-003	0.9984	0.026	0.088	13.33	0.99
NPIP	0.1-100	Y = 8.38291e-002X - 6.371566e-003	0.9985	0.084	0.279	13.02	0.99
NPYR	0.1-100	Y = 4.784117e-002X - 1.870728e-003	0.9989	0.094	0.314	14.36	1.00
NMOR	0.1-100	Y = 0.238134X - 1.817007e-002	0.9981	0.050	0.167	13.42	1.00
NDPH	0.1-100	Y = 0.1876731X - 1.086407e-002	0.9962	0.023	0.077	13.60	0.96
Avg.			0.9983	0.044	0.146	13.72	0.99

Table 9-2 Detected concentration and spiked recovery (in percent) of the eight NAs in different beverages

Sample (Ethanol %)	NDMA		NDEA		NDPA		NDBA		NPIP		NPYR		NMOR		NDPH	
	Rec.	Conc.	Rec.	Conc.	Rec.	Conc.	Rec.	Conc.	Rec.	Conc.	Rec.	Conc.	Rec.	Conc.	Rec.	Conc.
Red grape juice (0%)	66.67	<LOD	98.58	<LOD	97.586	<LOD	103.69	<LOD	89.41	n.d.	92.50	n.d.	79.65	<LOD	75.02	<LOD
Red wine (13.5%)	75.49	<LOD	70.47	<LOD	69.58	n.d.	66.03	<LOD	69.25	<LOD	68.56	n.d.	72.65	n.d.	54.97	<LOD
White wine (12.5%)	73.22	<LOD	79.798	<LOD	82.91	n.d.	80.73	<LOD	80.21	<LOD	133.67	n.d.	71.91	<LOD	98.11	<LOD
Supper dry bear (5%)	77.29	<LOQ	85.04	<LOQ	87.53	<LOD	86.27	<LOQ	85.78	<LOQ	85.75	<LOQ	79.78	<LOQ	101.44	1.17
Bear (8.8%)	76.82	<LOD	78.12	<LOD	77.95	<LOD	77.94	<LOD	76.96	<LOD	77.04	<LOD	72.22	<LOD	83.61	<LOD
Whiskey (40%)	53.84	<LOD	67.11	<LOD	70.43	<LOD	80.84	<LOD	70.50	<LOD	70.29	<LOD	70.68	<LOD	99.18	<LOD
Vodka (35.5%)	89.75	<LOD	92.93	n.d.	93.77	<LOD	93.19	<LOD	91.78	n.d.	90.76	n.d.	88.55	<LOD	71.09	<LOD

### 9.3.3. Analysis of real samples

The proposed method was used for the analysis of eight NAs in alcoholic and non-alcoholic beverages, including non-alcoholic grape juice, beers (with different alcohol concentration), red wine, white wine, vodka, and whiskey. The preparation of beverages is described in Section 9.2.3. Results have been summarized in Table 9-2. The average recoveries were in a range of 55% for NDMA to 101% for NDPhA. Low concentration of NDPhA was detected in beer samples; all other species were either absent or undetected due to their levels being below the LODs. Figure 9-2 displays chromatograms of spiked and non-spiked wine samples after extraction.



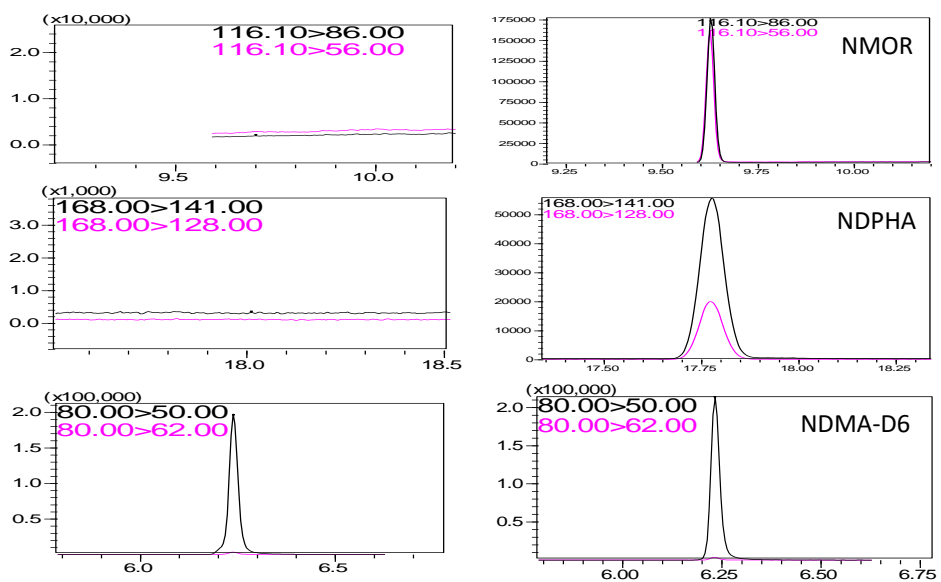


Figure 9-2 GC-EI-MS/MS of analytes extracted from wine by the developed method. (1)

Unspiked sample, (2) spiked sample at 100 ng/ml.  $^2\text{H}$  mass labelled NDMA (NDMA-D6) was used as internal standard.

#### 9.4. Conclusion

In the present work,  $\mu$ -SPE method coupled with triple quadrupole GC-EI-MS/MS analysis was developed and validated for the simultaneous analysis of eight NAs in six representative juice, beers, wine, vodka, and whiskey using oxidative surface-modified OMC as a sorbent. Only one beer sample showed contamination with NDPhA, while the rest of the samples were either not contaminated with NAs or had NA concentration below LOD. The obtained LOD values (averages amount 0.044 ng/mL) were low enough to meet the requirements of the regulatory organizations. The method has an acceptable precision and reproducibility, with an RSD of 13.72 (n = 8) at a concentration of 50 ng/mL. Matrix effect was evaluated and showed negligible effect on the analysis. We also evaluated the effect of alcohol content in the samples and confirmed that alcohol in the concentration range of 0%–40% did not interfere with the analysis. Hence, due to its simplicity, affordability (both in extraction and instrumental part), and reliability in obtaining data, this method could be suitable for alternative routine analysis of NAs in beverages. Most published studies have developed analytical methods for the analysis of NAs in beverages could only determine one or two NAs. In contrast, we analyzed eight important NAs simultaneously with average acceptable recoveries for all.

## **CHAPTER 10: Conclusions and future work**

In this thesis, we aimed to develop and design new approaches for determination and monitoring of two important groups of emerging contaminants consist of PFCAs and NAs from different environmental matrices. The main achievements of this thesis are highlighted as below.

In the first chapter, an overview on importance of emerging contaminants was described. The importance of monitoring and determination of emerging contaminants and significant roles of sample preparation in their monitoring were explained. Thereafter, the thesis structure was divided into two broad parts.

The first part has been devoted to PFCAs in chapters 2, 3, 4 and 5. Chapter 2 introduced these compounds and comprehensively described the current challenges in their monitoring. Subsequently, chapters 3, 4, and 5 reported simple, fast, and efficient approaches to determine the PFCAs in water samples, human plasma, and fish fillet, respectively.

In chapter 3, the usage of CTAB-MCM-41 as a sorbent in  $\mu$ -SPE for determination of PFCAs at trace levels (ng/L) in aqueous media was reported for the first time. We have been convinced that PFCAs with both anionic and hydrophobic characteristic can be trapped by the hydrophobic and positively charged surface of CTAB. The values of LODs, LOQs and %RSDs were obtained in the satisfactory ranges. Moreover, the developed method was demonstrated to be useful in reduction of matrix interferences (which has been mentioned in chapter 2 as the most important



challenges in determination of PFCs). The method was easy to use in comparison to previously reported approaches.

In chapter 4, the most significant effective parameters on  $\mu$ -SPE have been optimized simultaneously by using CCD for the first time. Protein precipitation, followed by  $\mu$ -SPE and LC-MS/MS were successfully utilized to determine the trace levels of PFCAs in human plasma.

Chapter 5 described the development of  $\mu$ -SPE as a potential and feasible strategy for simultaneous monitoring and determination of ten types of PFCAs in fish fillet. This efficient combination of protein precipitation with sorption-assisted extraction method could reduce significantly the matrix effects and interferences. The recovery amount of real samples proved the feasibility and reliability of the proposed method. The method should be suitable to determine PFCAs in these samples at ng/g concentration range.

The second part of this thesis (Chapters 6-9) is devoted to NAs. Chapter 6 described the important aspects of NAs and explained the basic issue associated with simultaneous monitoring and determination of NAs as a group of compounds. NAs exist in a wide range of polarity and hydrophobicity/hydrophilicity, hence it is difficult to make simultaneous extraction of NAs by conventional approaches.

Therefore in Chapter 7, we described the application of OMC as a carbonaceous sorbents for the extraction of NAs. This application provided us useful information about the role of mesoporous structure in the adsorption of NAs. Moreover, we modified the OMC surface by oxidative treatment and attached different carboxylic groups at the carbonic surface of the sorbent. This resulted a hydrophilic/hydrophobic

balance on the inert surface of carbonaceous sorbent. Furthermore, the acceptable extraction recoveries were obtained for all analytes (polar and non-polar). To the best of our knowledge, this was the first attempt to modify the surface chemistry of the carbonaceous sorbents to enhance the efficiency of the surface for the non-polar and hydrophobic analytes as well as the polar and hydrophilic analytes. Until now, only pure carbonaceous sorbents sorbent without any modification or regeneration of the carbon chemistry had been used. This study opened up more opportunities for functionalization of potential sorbents in commercial production.

In Chapter 8, we described the optimization of  $\mu$ -SPE using surface-modified CMK-3 and GC-EI-MS/MS for the quantitative determination of eight NAs from water samples. Regulations require many organizations and laboratories to routinely monitor NAs. However, few laboratories are equipped with high resolution GC systems such as GC-CI-MS/MS instruments with ion trap mass spectrometer. Instead, GC-EI-MS/MS is more affordable and cost-effective for many of the laboratories. Hence, here we attempted to utilize a triple quadrupole GC-EI-MS/MS in our methodology. This was one of the significant achievements of our work which might be promising for the routine analysis of NAs. The proposed approaches, presented a sensitive and reliable results for the analysis. It provided a good precision and a wide linear range. The LODs were at ng/mL level. Although this range of LODs limited the method application for drinking water analysis, it could be used for samples with higher level of NAs. Subsequently, the method was successfully used for determination of NAs from domestic wastewater and swimming pool water. The extraction recovery and matrix

effects were calculated and assessed for each same separately. Despite the complex and non-clean nature of the matrices, negligible matrix effects were observed.

In Chapter 9,  $\mu$ -SPE-GC-EI-MS/MS was used for the quantitative determination of NAs in different beverages. The developed method was naturally easy to use. Contrary to the previous sample preparation methods reported for the analysis of NAs from beverages, this method did not need any special setup or even high-cost instruments. Hence, it could be applied easily for the routine monitoring in quality control laboratories and it could be considered as an efficient alternative to the existing procedures. Although, the LODs were a barrier in determination of exact value of the contaminants, this method is sensitive enough to fulfill the established requirements for the monitoring of NAs in beverages. We evaluated this method in different types of beverages (juice, wine, beer, vodka, and whiskey) and found that the method could be used for different textures and matrices of beverages. We also evaluated the effect of alcohol content of the samples and confirmed that alcohol in the concentration range of 0%–40% had no significant influence on the performance of the methodology. Most of published studies on analytical methods for the analysis of NAs in beverages could only determine one or two NAs. In contrast, we simultaneously analyzed eight important NAs and obtained average acceptable recovery for all of them.

Our study also had some shortcomings and limitations. We would like to address these and come up with potential alternatives and solutions to overcome them in future studies.

In the present thesis, because of the lack of availability of suitable isotopic internal standard and cost issue, we limited these to  $^{13}\text{C}$ -PFOA for PFCAs and NAMA- $\text{d}_6$  for NAs. The usage of separate isotopic label internal standard for each analyte is recommended. In the developed methods for the determination of PFCAs, we only covered PFCAs. However, future researches should attempt to cover more members of these analytes, especially PFOS which is of significant concern. For the determination of NAs in water samples (Chapter 8), we used only domestic wastewater and swimming pool water sample because of the unavailability of other sample types. However, sampling from different types of wastewater such as different industrial wastewater, and samples from wastewater treatment plants (WWTPs) such as effluent and influent could be considered for future studies. We point out the values of LODs in determination of NAs were not as low as those reported using SPE. Amendments in the current methodology might help us to decrease the LODs. Moreover optimization of pH and temperature in the process could be considered for future studies. The application of same sorbent in higher amount could be suggested for future works. One possible avenue for future work is to harness the ideal properties of ordered mesoporous materials as sorbent. Therefore, evaluation and applicability of other members of this type of materials could be considered.

Last but not least, we emphasize that determination of NAs and PFCs in environmental samples is still an ongoing research area in analytical Chemistry. Therefore more studies and investigations are needed for establishment of a method that meets most of the requirements, if not all, of an ideal analytical method.

## BIBLIOGRAPHY

- [1] J.W.A. Charrois, *Ency. Anal. Chem.* 2010, DOI: 10.1002/9780470027318.a9057.
- [2] S.D. Richardson, *Anal. Chem.* 84 (2012) 747.
- [3] E. Baltussen, C.A. Cramers, P.J. Sandra, *Anal. Bioanal. Chem.* 373 (2002) 3.
- [4] J.M. Nogueira, *Anal. Chim. Acta*, 757 (2012) 1.
- [5] C.L. Arthur, J. Pawliszyn, *Anal. Chem.* 62 (1990) 2145.
- [6] G. Ouyang, J. Pawliszyn, *Trends Anal. Chem.* 25 (2006) 692.
- [7] Y. Gou, J. Pawliszyn, *Anal. Chem.* 72 (2000) 2774.
- [8] H.L. Lord, *J. Chromatogr. A*, 1152 (2007) 2.
- [9] C. Basheer, A.A. Alnedhary, B.S.M. Rao, S. Valliyaveetil, H.K. Lee, *Anal. Chem.* 78 (2006) 2853.
- [10] W.S. Khayoon, B. Saad, B. Salleh, N.H. Manaf, A.A. Latiff, *Food. Chem.* 147 (2014) 287.
- [11] H. Bagheri, F. Khalilian, M. Naderi, E. Babanezhad, *J. Sep. Sci.* 33 (2010) 1132.
- [12] J. Huang, J. Liu, C. Zhang, J. Wei, L. Mei, S. Yu, G. Li, L. Xu, *J. Chromatogr. A*, 1219 (2012) 66.
- [13] C. Basheer, W. Wong, A. Makahleh, A.A. Tameem, A. Salhin, B. Saad, H.K. Lee, *J. Chromatogr. A*, 1218(2011) 4332
- [14] *Activated Carbon Surfaces in Environmental Remediation*. T.J. Bandosz, 2006 Elsevier Ltd.
- [15] G.Q. Lu, X.S. Zhao, *Nanoporous Materials: Science and Engineering*, Imperial College Press, Vol. 4 (2004).
- [16] X.S. Zhao, G.Q. Lu, G.J. Millar, *Ind. Eng. Chem. Res.* 35 (1996) 2075.
- [17] Z. Alothman, *Mater.* 5 (2012) 2874.
- [18] P.A. Mangrulkar, S.P. Kamble, J. Meshram, S.S. Rayalu, *J. Hazard. Mater.* 160 (2008) 414.
- [19] Y. Han, D. Zhang, *Curr. Opin. Chem. Engin.* 1 (2012) 129.
- [20] K.H. Knox, B. Kaur, *J. Chromatogr. A*, 352 (1986) 3.
- [21] C.T. Kresge, M.E. Leonowicz, W.J. Roth, J.C. Vartuli, J.S. Beck, *Nature*, 359 (1992) 710.
- [22] Z.A. Alothman, A.W. Apblett, *J. Hazard. Mater.* 182 (2010) 581.

- [23] X. Yang, S. Zhang, Z. Qiu, G. Tian, Y. Feng, F.S. Xiao, *J. Phys. Chem. B*, 108 (2004) 4696.
- [24] J.S. Beck, J.C. Vartuli, W.J. Roth, M.E. Leonowicz, C.T. Kresge, K.D. Schmitt, C.T.W. Chu, D.H. Olson, E.W. Sheppard, S.B. McCullen, J.B. Higgins, J.L. Schlenkert, *J. Am. Chem. Soc.* 114 (1992) 10834.
- [25] Y.X. Zhao, M.Y. Ding, D.P. Chen, *Anal. Chim. Acta*, 542 (2005) 193.
- [26] M. Ghiaci, A. Abbaspur, R. Kia, F. Seyedeyn-Azad, *Sep. Purif. Technol.* 40 (2004) 217.
- [27] C. Zamani, X. Illa, S. Abdollahzadeh-Ghom, J.R. Morante, A. Romano Rodriguez, *Nanoscale Res. Lett.* 4 (2009) 1303.
- [28] M.C. Bruzzoniti, C. Sarzanini, B. Onida, B. Bonelli, E. Garrone, *Anal. Chim. Acta*, 422 (2000) 231.
- [29] R. Denoyel, E. Sabio-Rey, *Langmuir*, 14 (1998) 7321.
- [30] H. Zhao, K. Nagy, J. Waples, G. Vance, *Environ. Sci. Technol.* 2 34 (2000) 4822.
- [31] J. Lee, J. Kim, T. Hyeon, *Adv. Mater.* 18 (2006) 2073.
- [32] R. Ryoo, S.H. Joo, S. Jun, *J. Phys. Chem. B*, 103 (1999) 7743.
- [33] S. Oh, K. Kim, *Chem. Commun.* (1999) 2177.
- [34] S. Jun, S.H. Joo, R. Ryoo, M. Kruk, M. Jaroniec, Z. Liu, T. Ohsuna, O. Terasaki, *J. Am. Chem. Soc.* 122 (2000) 10712.
- [35] C. Liang, Z. Li, S. Dai, *Angew. Chem. Int. Ed.* 47 (2008) 3696.
- [36] Y. Chi, W. Geng, L. Zhao, X. Yan, Q. Yuan, N. Li, X. Li, *J. Colloid Interface Sci.* 369 (2012) 366.
- [37] R.C. Bansal, M. Goyal, *Activated Carbon Adsorption*, Taylor & Francis, 2005.
- [38] D.J. Kim, H.I. Lee, J.E. Yie, S.J. Kim, J.M. Kim, *Carbon*, 43 (2005) 1868.
- [39] Z. Wu, P.A. Webley, D. Zhao, *Langmuir*, 26 (2010) 10277.
- [40] B. Jurado-Sanchez, E. Ballesteros, M. Gallego, *Talanta*, 79 (2009) 613.
- [41] Z. Kuklenyik, L.L. Needham, A.M. Calafat, *Anal. Chem.* 77 (2005) 6085.
- [42] K. Saito, E. Uemura, A. Ishizaki, H. Kataoka, *Anal. Chim. Acta*, 658 (2010) 141.
- [43] S. Ullah, T. Alsberg, U. Berger, *J. Chromatogr. A*, 1218 (2011) 6388.
- [44] B.S. Larsen, M.A. Kaiser, *Anal. Chem.* (2007) 3966.

- [45] A.B. Lindstrom, M.J. Strynar, E.L. Libelo, *Environ. Sci. Technol.* 45 (2011) 7954.
- [46] A. Karrman, B. van Bavel, U. Jarnberg, L. Hardell, G. Lindstrom, *Chemosphere*, 64 (2006) 1582.
- [47] J.L. Domingo, *Environ. Int.* 40 (2012) 187.
- [48] E. Corsini, A. Avogadro, V. Galbiati, M. dell'Agli, M. Marinovich, C.L. Galli, D.R. Germolec, *Toxicol. Appl. Pharmacol.* 250 (2011) 108.
- [49] Y. Pico, M. Farre, M. Llorca, D. Barcelo, *Crit. Rev. Food. Sci.* 51 (2011) 605.
- [50] G.W. Lien, T.W. Wen, W.S. Hsieh, K.Y. Wu, C.Y. Chen, P.C. Chen, *J. Chromatogr. B*, 879 (2011) 641.
- [51] L. Maestri, S. Negri, M. Ferrari, S. Ghittori, F. Fabris, P. Danesino, M. Imbriani, *Rapid. Commun. Mass Spectrom.* 20 (2006) 2728.
- [52] F. Gosetti, U. Chiuminatto, D. Zampieri, E. Mazzucco, E. Robotti, G. Calabrese, M.C. Gennaro, E. Marengo, *J. Chromatogr. A*, 1217 (2010) 7864.
- [53] F. Guo, Y. Zhong, Y. Wang, J. Li, J. Zhang, J. Liu, Y. Zhao, Y. Wu, *Chemosphere*, 85 (2011) 156.
- [54] S. Valsecchi, M. Rusconi, S. Polesello, *Anal. Bioanal. Chem.* 405 (2013) 143.
- [55] C.R. Powley, S.W. George, T.W. Ryan, R.C. Buck, *Anal. Chem.* 77 (2005) 6353.
- [56] F. Gosetti, E. Mazzucco, D. Zampieri, M.C. Gennaro, *J. Chromatogr. A*, 1217 (2010) 3929.
- [57] L.W. Yeung, S. Taniyasu, K. Kannan, D.Z. Xu, K.S. Guruge, P.K. Lam, N. Yamashita, *J. Chromatogr. A*, 1216 (2009) 4950.
- [58] S.P.J. Leeuwen, J. Boer, *J. Chromatogr. A*, 1153 (2007) 172.
- [59] H. Nakata, K. Kannan, T. Nasu, H.S. Cho, E. Sinclair, A. Takemura, *Environ. Sci. Technol.* 40 (2006) 4916.
- [60] M. Llorcaa, M. Farrea, Y. Picob, D. Barcelo, *J. Chromatogr. A*, 1216 (2009) 7195.
- [61] G.W. Olsen, *Environ. Health Perspect.* 111 (2003) 1892.
- [62] S. Takagi, F. Adachi, K. Miyano, Y. Koizumi, H. Tanaka, M. Mimura, I. Watanabe, S. Tanabe, K. Kannan, *Chemosphere*, 72 (2008) 1409.

- [63] M. Onghena, Y. Moliner-Martinez, Y. Pico, P. Campins-Falco, D. Barcelo, J. Chromatogr. A, 1244 (2012) 88.
- [64] S. Taniyasu, K. Kannan, L.W. Yeung, K.Y. Kwok, P.K. Lam, N. Yamashita, Anal. Chim. Acta, 619 (2008) 221.
- [65] S. Taniyasu, K. Kannan, M.K. So, A. Gulkowska, E. Sinclair, T. Okazawa, N. Yamashita, J. Chromatogr. A, 1093 (2005) 89.
- [66] H. Trufelli, P. Palma, G. Famigliani, A. Cappiello, Mass Spectrom. Rev. 30 (2011) 491.
- [67] R. Vestergren, S. Ullah, I.T. Cousins, U. Berger, J. Chromatogr. A, 1237 (2012).64.
- [68] S. Taniyasu, P.K.S. Lam, G.J. Zheng, J.P. Giesy, N.Yamashita. Arch. Environ. Contam. Toxicol. 50 (2006) 240.
- [69] N. Luquea, A. Ballesteros-Gomez, S.V. Leeuwenb, S. Rubio. J Chromatogr A, 1217 (2010) 3774.
- [70] A. Ballesteros-Gomez, S. Rubio, S.Van. Leeuwen, J. Chromatogr. A, 1217 (2010) 5913.
- [71] L. Wanga, H. Suna, L. Yanga, C. Hea, W. Wua, S. Sunb, J. Chromatogr. A, 1217 (2010) 436.
- [72] U. Berger, M. Haukas, J. Chromatogr. A, 1081 (2005) 210.
- [73] H. Chen, Y. Wang, Ceram. Intern. 28 (2002) 541.
- [74] M. Lashgari, C. Basheer, H.K. Lee, Talanta, 141 (2015). 200.
- [75] D. Cao, Z. Wang, C. Han, L. Cui, M. Hu, J. Wu, Y. Liu, Y. Cai, H. Wang, Y. Kang, Talanta, 85 (2011) 345.
- [76] S.G.S. Samanta, P.U. Sastry, N.K. Mal, A. Manna, A. Bhaumik, Ind. Eng. Chem. Res. 42 (2003) 3012.
- [77] X. Zhang, H. Niu, Y.Pan, Y. Shi, Y. Cai, Anal. Chem. 82 (2010) 2363.
- [78] X. Zhao, Y. Cai, F. Wu, Y. Pan, H. Liao, B. Xu, Microchem. J. 98 (2011) 207.
- [79] X. Zhao, J. Li, Y. Shi, Y. Cai, S. Mou, G. Jiang, J. Chromatogr. A, 1154 (2007) 52.
- [80] D. Ge, H.K. Lee, J. Chromatogr. A, 1218 (2011) 8490.



- [81] S. Kanimozhia, C. Basheer, K. Narasimhan, L. Liuc, S. Kohc, F. Xuea, M. Choolanic, H. K. Lee, *Anal. Chim. Acta.* 687(2011) 56.
- [82] L. Guo, H.K. Lee, *J. Chromatogr. A*, 1218 (2011) 9321.
- [83] H.H. See, M. Marsin Sanagi, W.A.W. Ibrahim, A.A. Naim. *J. Chromatogr. A*, 1217 (2010). 1767.
- [84] N.N. Naing, S.F. Li, H.K. Lee, *J. Chromatogr. A*, 1426 (2015) 69.
- [85] T. Wen, F. Qu, N.B. Li, H.Q. Luo, *Anal. Chim. Acta*, 749 (2012) 56.
- [86] L. Jin, L. Shang, S. Guo, Y. Fang, D. Wen, L. Wang, J. Yin, S. Dong, *Biosens. Bioelectron.* 26 (2011) 1965.
- [87] X. Zhang, H. Niu, Y.Pan, Y. Shi, Y. Cai, *Anal. Chem.* 82 (2010) 2363.
- [88] M. D. Malinsky, C. B. Jacoby, W. K. Reagen, *Anal. Chim. Acta*, 683 (2011) 248.
- [89] M. Rezazadeh, Y. Yamini, S. Seidi, E. Tahmasebi, F. Rezaei, *J. Agric. Food Chem*, 62 (2014) 3134.
- [90] S. Seidia, Y. Yaminia, T. Baherib, R. Feizbakhsha, *J. Chromatogr. A*, 1218 (2011) 3958.
- [91] M. Rezazadeh, Y. Yamini, S. Seidi, B. Ebrahimpour. *J. Chromatogr. A*, 1280 (2013) 16.
- [92] A. Stein, Z. Wang, M. A. Fierke, *Adv. Mater.* 21 (2009) 265.
- [93] L.S. Haug, C. Thomsen, G. Becher, *J. Chromatogr. A*, 1216 (2009) 385.
- [94] M. Karimi, H. Sereshti, S. Samadi, H. Parastar, *J. Chromatogr. A*, 1217 (2010) 7017.
- [95] H. Sereshti, M. Karimi, S. Samadi, *J. Chromatogr. A*, 1216 (2009) 198.
- [96] C. Basheer, K. Narasimhan, M. Yin, C. Zhao, M. Choolani, H.K. Lee, *J. Chromatogr. A*, 1186 (2008) 358.
- [97] C. Basheer, T.M. Hii, H.K. Lee, *Anal. Chem.* 79 (2007) 6845.
- [98] L. Xu, H.K. Lee, *J. Chromatogr. A*, 1192 (2008) 203.
- [99] H.K. Bagheri, F. Naderi, M. Babanezhad, *J. Sep. Sci.* 33 (2010) 1132.
- [100] FDA-US. Department of Health and Human Services, Center for Drug Evaluation and Research (CDER) 2001.
- [101] A. Karrman, B. Bavel, U. Jarnberg, L. Hardell, G. Lindstrom, *Anal. Chem.* 77 (2005) 864.

- [102] J.W.A. Charrois, M.W. Arend, K.L. Froese, S.E. Hrudey, *Environ. Sci. Technol* 38 (2004) 4489.
- [103] Z. Kuklennyik, L.L. Needham, A.M. Calafat, *Anal. Chem.* 77 (2005) 6085.
- [104] European commission (2011) proposal for a directive of the european parliament and of the council amending directives 2000/60/EC and 2008/105/EC as regards priority substances in the field of water policy, COM(2011) 876, Brussels, 31.01.2012
- [105] C.R. Powley, S.W. George, M.H. Russell, R.A. Hoke, R.C. Buck, *Chemosphere*, 70 (2008) 664.
- [106] M. Fernandez-Sanjuan, J. Meyer, J. Damasio, M. Faria, C. Barata, S. Lacorte, *Anal. Bioanal. Chem.* 398 (2010) 1447.
- [107] World Health Organization, *Progress on sanitation and drinking water*: New York, 2012.
- [108] G.A Boorman, *Environ Health Perspect.* 107 (1999) 207.
- [109] S.D. Richardson, M.J. Plewa, E.D. Wagner, R. Schoeny, D.M. Demarini, *Mutat. Res.* 636 (2007) 178.
- [110] A.E. Poste, M. Grung, R.F. Wright, *Sci. Total Environ.* 481 (2014) 274.
- [111] G.A. Kim, H.J. Son, C.W. Kim, S.H. Kim, *Environ. Monit. Assess.* 185 (2013) 1657.
- [112] J.M. Boyd, S.D. Richardson, X.F. Li, *Trends. Anal. Chem.* 30 (2011) 1410.
- [113] J. Nawrocki, P. Andrzejewski, *J. Hazard. Mater.* 189 (2011) 1.
- [114] C. Crews, *Quality Assurance and Safety of Crops & Foods*, 2 (2010) 2.
- [115] M.C. Huang, H.C. Chen, S.C. Fu, W.H. Ding, *Food Chem.* 138 (2013) 227.
- [116] I.J. Brisson, P. Levallois, H. Tremblay, J. Serodes, C. Deblois, J. Charrois, V. Taguchi, J. Boyd, X. Li, M.J. Rodriguez, *Environ. Monit. Assess.* 185 (2013) 7693.
- [117] W.A. Mitch, J.O. Sharp, R.R. Trussell, R.L. Valentine, L. Alvarez-Cohen, D.L. Sedlak, *J. Environ. Eng. Sci.* 20 (2003) 389.
- [118] M.R. Templeton, Z. Chen, *J. Water Supply Res. Technol. Aqua*, 59 (2010)
- [119] J.H. Wang, J. Yu, M. Yang, *J. Environ. Sci.* 22 (2010) 1508.
- [120] M. Asami, M. Oya, K. Kosaka, *Sci. Total Environ.* 407 (2009) 3540.
- [121] J.W.A. Charrois, M.W. Arend, K.L. Froese, S.E. Hrudey, *Environ. Sci. Technol.* 40 (2006) 7636.

- [122] W.A. Mitch, A.C. Gerecke, D.L. Sedlak, *Water Res.* 37 (2003) 3733.
- [123] J.W.A. Charrois, S.E. Hrudey, K.L. Froese, J.M. Boyd, *J. Environ. Engin. Sci.* 6 (2007) 103.
- [124] W.H. Chen, T.M. Young, *Water Res.* 43 (2009) 3047.
- [125] J.L. Roux, H. Gallard, J.P. Croue, *Water Res.* 45 (2011) 3164.
- [126] C. Ripolles, E. Pitarch, J.V. Sancho, F.J. Lopez, F. Hernandez, *Anal. Chim. Acta*, 702 (2011) 62.
- [127] F. Ma, Y. Wan, G. Yuan, L. Meng, Z. Dong, J. Hu, *Environ. Sci. Technol.* 46 (2012) 3236.
- [128] L. Fishbein, *Environ. Health Perspec.* 27 (1978) 125.
- [129] Concise international chemical assessment document 38, World health organization, International programme on chemical safety, Geneva, 2002.
- [130] S.D. Richardson, *Anal. Chem.* 80 (2008) 4373.
- [131] US Environmental Protection Agency (US EPA), Basic information, Unregulated Contaminant Monitoring Rule-2 (UCMR 2), 2010.
- [132] US Environmental Protection Agency (US EPA), Occurrence, Unregulated Contaminant Monitoring Rule-2 (UCMR 2), 2008-2010.
- [133] California Environmental Protection Agency (CA EPA). (2006). Public health goals for chemicals in drinking water, N-nitrosodimethylamine.
- [134] C. Planas, O. Palacios, F. Ventura, J. Rivera, J. Caixach, *Talanta*, 76 (2008) 906.
- [135] S. Yoon, N. Nakada, H. Tanaka, *Talanta*, 97 (2012) 256.
- [136] B.J. Sanchez, M. Gallego, *J. Agric. Food Chem.* 55 (2007) 9758.
- [137] W.A. Mitch, *Environ. Sci. Technol.* 36 (2002) 588.
- [138] J.E. Grebel, C.C. Young, I.H. Suffet, *J. Chromatogr. A*, 1117 (2006) 11.
- [139] H.W. Hung, T.F. Lin, C.H. Chiu, Y.C. Chang, T.Y. Hsieh, *Water Air Soil Poll.* 213 (2010) 459.
- [140] S.C. Fu, S.H. Tzing, H.C. Chen, Y.C. Wang, W.H. Ding, *Anal. Bioanal. Chem.* 402 (2012) 2209.
- [141] J.H. Lee, S.U. Lee, J.E. Oh, *Int. J. Environ. Anal. Chem.* 93 (2013) 1261.
- [142] J.H.M. Krauss, *Anal. Chem.* 2 80 (2008) 834.
- [143] J. Kim, T.E. Clevenger, *J. Hazard. Mater.* 145 (2007) 270.

- [144] M.H. Plumlee, M. Lopez-Mesas, A. Heidlberger, K.P. Ishida, M. Reinhard, *Water Res.* 42 (2008) 347.
- [145] EPA/600/R-05/054, Determination of nitrosamines in drinking water by solid phase extraction and capillary column gas chromatography with large volume injection and chemical ionization tandem mass spectrometry (MS/MS), Version 1, 2004
- [146] K.Y. Foo, B.H. Hameed, *J. Hazard. Mater.* 175 (2010) 1.
- [147] M. Krauss, P. Longree, F. Dorusch, C. Ort, J. Hollender, *Water Res.* 43 (2009) 4381.
- [148] M.H. Plumlee, M. Reinhard, *Environ. Sci. Technol.* 41 (2007) 6170.
- [149] S. Mitragotri, *J. Control. Release*, 86 (2003) 69.
- [150] D.Y. Zhao, J.L. Feng, Q.S. Huo, N. Melosh, G.H. Fredrickson, B.F. Chmelka, G.D. Stucky, *Science*, 279 (1998) 548.
- [151] N.A. Melosh, P. Lipic, F.S. Bates, F. Wudl, G.D. Stucky, G.H. Fredrickson, B.F. Chmelka, *Macromolecules*, 32 (1999) 4332.
- [152] C.Z. Yu, J. Fan, B.Z. Tian, D.Y. Zhao, G.D. Stucky, *Adv. Mater.* 14 (2002) 1742.
- [153] J.S. Lettow, Y.J. Han, P. Schmidt-Winkel, P.D. Yang, D.Y. Zhao, G.D. Stucky, J.Y. Ying, *Langmuir*, 16 (2000) 8291.
- [154] S. Jun, S.H. Joo, R. Ryoo, M. Kruk, M. Jaroniec, Z. Liu, T. Ohsuna, *J. Am. Chem. Soc.* 122 (2000) 10712.
- [155] Z. Wu, W. Li, P.A. Webley, D. Zhao, *Adv. Mater.* 24 (2012) 485.
- [156] J.S. Ribeiro, R.F. Teofilo, F. Augusto, M.M.C. Ferreira, *Chemometr. Intell. Lab.* 102 (2010) 45.
- [157] J.A. McDonald, N.B. Harden, L.D. Nghiem, S.J. Khan, *Talanta*, 99 (2012) 146.
- [158] S.D. Richardson, *Anal. Chem.* 81 (2009) 4645.
- [159] R. Pozzi, P. Bocchini, F. Pinelli, G.C. Galletti, *J. Chromatogr. A*, 1218 (2011) 1808.
- [160] S. Mitragotri, *J. Control. Release*, 86 (2003) 69.
- [161] F. Gosetti, E. Mazzucco, D. Zampieri, M.C. Gennaro, *J. Chromatogr. A*, 1217 (2010) 3929.
- [162] S.W.S. Spencer, W.A. Mitch, *Environ. Sci. Technol.* 42 (2008) 1032.
- [163] B. Jurado-Sanchez, E. Ballesteros, M. Gallego, *J. Sep. Sci.* 33 (2010) 610.

- [164] A. Llop, F. Borrull, E. Pocurull, *J. Sep. Sci.* 33 (2010) 3692.
- [165] U.T.L. Padhye, W.A. Mitch, S.G. Pavlostathis, C.H. Huang, *Environ. Sci. Technol.* 43 (2009) 3087.
- [166] M. Izquierdo-Pulido, J.F. Barbour, R.S. Scanlan, *Food Chem. Toxicol.* 34 (1996) 297.
- [167] M.B. Gloria, J.F. Barbour, R.A. Scanlan, *J. Agric. Food Chem.* 45 (1997) 814.
- [168] AOAC official method 982.11, N-Nitrosodimethylamine in beer.
- [169] D.M. Perez, G.G. Alatorre, E.B. Alvarez, E.E. Silva, J.F.J. Alvarado, *Food Chem.* 107 (2008) 1348.
- [170] R. Andrade, F.G.R. Reyes, S. Rath, *Food Chem.* 91 (2005) 173.
- [171] S. Ventanas, D. Martin, M. Estevez, J. Ruiz, *Food Chem.* 99 (2006) 842.
- [172] Nanoporous materials: science and engineering. series on chemical engineering: G.Q Lu, X.S Zhao, 2004

## APPENDICES

### Appendix 1

Properties of common solvents used. The solvents are grouped into non-polar, polar aprotic, and polar protic solvents and ordered by increasing polarity. The polarity is given as the dielectric constant.

Solvent	Chemical formula	Boiling point	Dielectric constant	Density	Dipole moment
<b>Non-polar solvents</b>					
Hexane	CH <sub>3</sub> -CH <sub>2</sub> -CH <sub>2</sub> -CH <sub>2</sub> -CH <sub>2</sub> -CH <sub>3</sub>	69 °C	1.88	0.655 g/ml	0.00 D
Chloroform	CHCl <sub>3</sub>	61 °C	4.81	1.498 g/ml	1.04 D
Diethyl ether	CH <sub>3</sub> -CH <sub>2</sub> -O-CH <sub>2</sub> -CH <sub>3</sub>	35 °C	4.3	0.713 g/ml	1.15 D
Dichloromethane	CH <sub>2</sub> Cl <sub>2</sub>	40 °C	9.1	1.3266 g/ml	1.60 D
<b>Polar aprotic solvents</b>					
Acetone	CH <sub>3</sub> -C(=O)-CH <sub>3</sub>	56 °C	21	0.786 g/ml	2.88 D
Acetonitrile	CH <sub>3</sub> -C≡N	82 °C	37.5	0.786 g/ml	3.92 D
<b>Polar protic solvents</b>					
Ethanol	CH <sub>3</sub> -CH <sub>2</sub> -OH	79 °C	24.55	0.789 g/ml	1.69 D
Methanol	CH <sub>3</sub> -OH	65 °C	33	0.791 g/ml	1.70 D
Acetic acid	CH <sub>3</sub> C(=O)OH	118 °C	6.2	1.049 g/ml	1.74 D
Water	H-O-H	100 °C	80	1.000 g/ml	1.85 D

## Appendix 2

Descriptive calculations evaluating the dependence of recovery to concentration. Groups 1, 2, 3 are representative of concentration levels of 40, 80, and 100 ng/ml respectively. Statistical tests were used for the analysis of the data by IBM SPSS Statistics (version 20) software.

Descriptives									
		N	Mean	Std. Deviation	Std. Error	95% Confidence Interval for Mean		Minimum	Maximum
						Lower Bound	Upper Bound		
C9	1.00	3	94.2849	2.94601	1.70088	86.9666	101.6032	91.85	97.56
	2.00	3	96.0526	2.64160	1.52513	89.4905	102.6147	93.06	98.06
	3.00	3	94.0746	1.78045	1.02794	89.6517	98.4974	92.82	96.11
	Total	9	94.8040	2.36473	.78824	92.9863	96.6217	91.85	98.06
C8	1.00	3	84.3654	30.46456	17.58872	8.6872	160.0436	49.25	103.74
	2.00	3	103.6119	5.91062	3.41250	88.9291	118.2947	98.05	109.82
	3.00	3	97.2406	4.19740	2.42337	86.8136	107.6675	92.99	101.38
	Total	9	95.0726	17.81178	5.93726	81.3813	108.7640	49.25	109.82
C7	1.00	3	96.9985	6.76564	3.90614	80.1918	113.8053	92.77	104.80
	2.00	3	97.7481	3.92533	2.26629	87.9970	107.4992	93.50	101.24
	3.00	3	96.5766	.82687	.47740	94.5225	98.6307	95.67	97.29
	Total	9	97.1077	3.96617	1.32206	94.0591	100.1564	92.77	104.80
C10	1.00	3	96.4971	1.43523	.82863	92.9318	100.0624	95.26	98.07
	2.00	3	102.1920	3.70687	2.14016	92.9836	111.4004	97.92	104.60
	3.00	3	97.2972	1.13984	.65809	94.4656	100.1287	96.34	98.56
	Total	9	98.6621	3.37696	1.12565	96.0663	101.2579	95.26	104.60
C5	1.00	3	77.2508	5.09312	2.94052	64.5988	89.9029	73.71	83.09
	2.00	3	78.2036	2.79953	1.61631	71.2492	85.1580	75.69	81.22
	3.00	3	75.9613	2.89254	1.67001	68.7759	83.1468	72.76	78.39
	Total	9	77.1386	3.38907	1.12969	74.5335	79.7437	72.76	83.09
C12	1.00	3	97.0832	16.02118	9.24983	57.2844	136.8820	81.02	113.06
	2.00	3	90.5885	3.72790	2.15230	81.3278	99.8491	87.27	94.62
	3.00	3	87.8540	1.08882	.62863	85.1492	90.5588	87.17	89.11
	Total	9	91.8419	9.20841	3.06947	84.7637	98.9201	81.02	113.06
C11	1.00	3	100.9182	7.10421	4.10162	83.2704	118.5660	94.37	108.47
	2.00	3	99.7759	2.76556	1.59670	92.9058	106.6459	96.59	101.50
	3.00	3	98.3152	3.26624	1.88576	90.2014	106.4290	95.75	101.99
	Total	9	99.6698	4.29806	1.43269	96.3660	102.9735	94.37	108.47
C6	1.00	3	87.8976	6.62387	3.82429	71.4430	104.3523	82.17	95.15
	2.00	3	88.5805	4.86005	2.80595	76.5075	100.6536	83.57	93.27
	3.00	3	86.1169	.72218	.41695	84.3229	87.9109	85.32	86.72
	Total	9	87.5317	4.26822	1.42274	84.2509	90.8125	82.17	95.15
C13	1.00	3	130.4471	4.17658	2.41135	120.0719	140.8223	127.92	135.27
	2.00	3	130.4932	6.34096	3.66095	114.7413	146.2450	123.43	135.71
	3.00	3	90.7519	61.19436	35.33058	-61.2633	242.7671	20.23	129.84
	Total	9	117.2307	36.67405	12.22468	89.0406	145.4209	20.23	135.71
C14	1.00	3	119.6062	8.64989	4.99402	98.1186	141.0937	109.65	125.29
	2.00	3	125.1533	2.46881	1.42537	119.0204	131.2862	122.40	127.18
	3.00	3	117.9843	5.64867	3.26126	103.9522	132.0164	112.37	123.66
	Total	9	120.9146	6.22938	2.07646	116.1263	125.7029	109.65	127.18

### Appendix 3

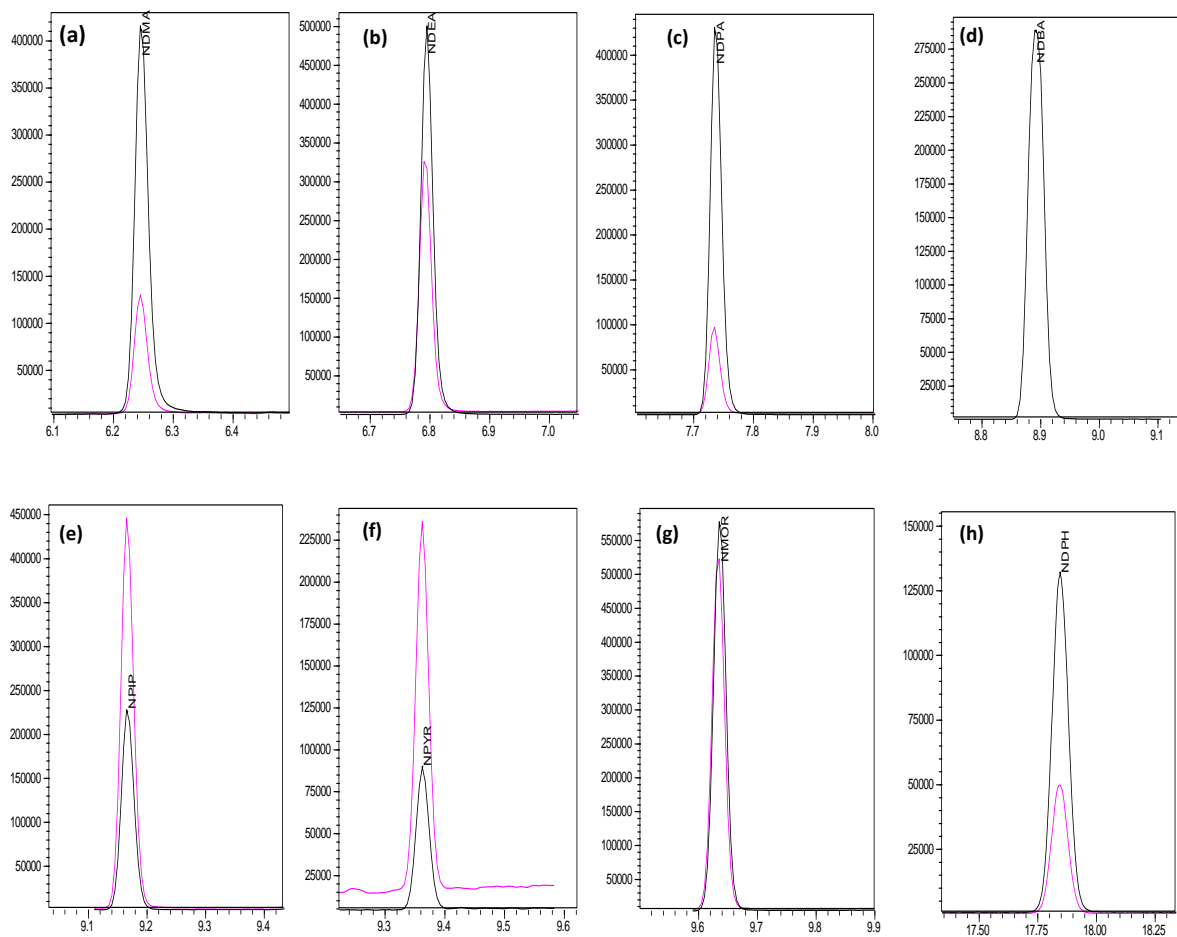
ANOVA results for the evaluation of the dependence of recovery to concentration. Groups relay on concentration levels of 40, 80, and 100 ng/ml. The results were obtained by IBM SPSS Statistics (version 20) software.

		<b>Sum of Squares</b>	<b>df</b>	<b>Mean Square</b>	<b>F</b>	<b>Sig.</b>
9	Between Groups	7.081	2	3.541	0.564	0.596
	Within Groups	37.654	6	6.276		
	Total	44.735	8			
C8	Between Groups	576.791	2	288.395	0.882	0.461
	Within Groups	1961.286	6	326.881		
	Total	2538.077	8			
C7	Between Groups	2.112	2	1.056	0.051	0.950
	Within Groups	123.732	6	20.622		
	Total	125.844	8			
C10	Between Groups	57.031	2	28.516	5.003	0.053
	Within Groups	34.200	6	5.700		
	Total	91.231	8			
C5	Between Groups	7.598	2	3.799	0.270	0.772
	Within Groups	84.288	6	14.048		
	Total	91.886	8			
C12	Between Groups	134.837	2	67.419	0.744	0.514
	Within Groups	543.522	6	90.587		
	Total	678.359	8			
C11	Between Groups	10.214	2	5.107	0.223	0.807
	Within Groups	137.573	6	22.929		
	Total	147.787	8			
C6	Between Groups	9.707	2	4.853	0.214	0.813
	Within Groups	136.035	6	22.672		
	Total	145.741	8			
C13	Between Groups	3155.083	2	1577.542	1.245	0.353
	Within Groups	7604.803	6	1267.467		
	Total	10759.886	8			
C14	Between Groups	84.795	2	42.398	1.127	0.384
	Within Groups	225.646	6	37.608		
	Total	310.442	8			



## Appendix 4

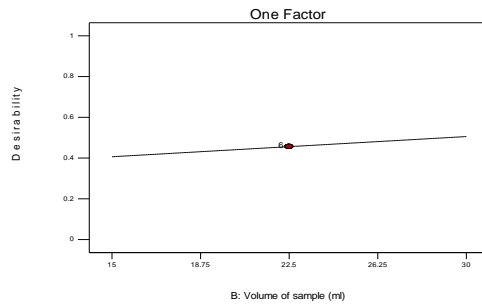
Mass chromatograms of MRM data of NAs (500pg), (a) NDMA, (b) NDEA, (c) NDPA, (d) NDBA, (e) NPIP, (f) NPYR, (g) NMOR, and (h) NDPhA



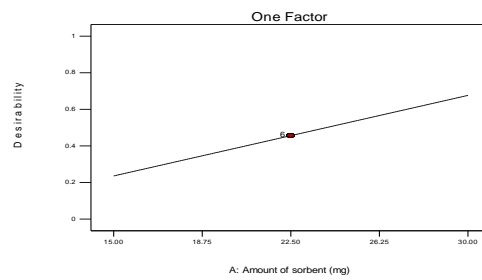
# Appendix 5

## Linear effect of changing of each variable on the extraction efficiency

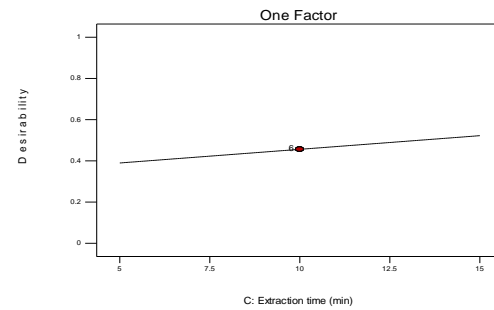
Design-Expert® Software  
 Factor Coding: Actual  
 Desirability  
 ● Design Points  
 X1 = B: Volume of sample



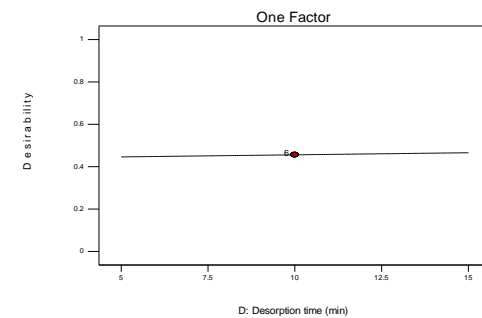
Design-Expert® Software  
 Factor Coding: Actual  
 Desirability  
 ● Design Points  
 X1 = A: Amount of sorbent



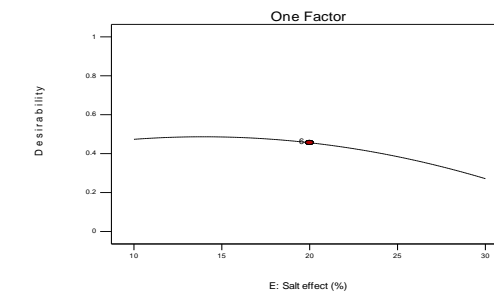
Design-Expert® Software  
 Factor Coding: Actual  
 Desirability  
 ● Design Points  
 X1 = C: Extraction time



Design-Expert® Software  
 Factor Coding: Actual  
 Desirability  
 ● Design Points  
 X1 = D: Desorption time



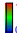
Design-Expert® Software  
 Factor Coding: Actual  
 Desirability  
 ● Design Points  
 X1 = E: Salt effect



## Appendix 6

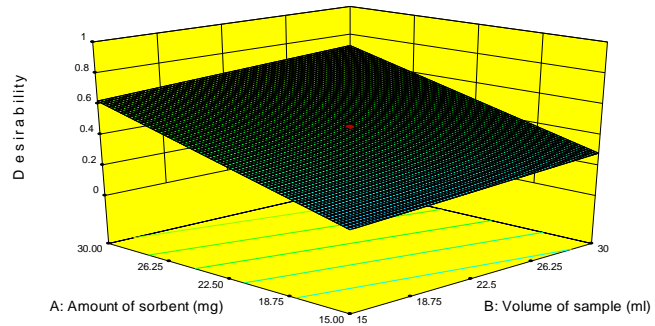
3D response surfaces against different operating variables.

Design-Expert® Software  
 Factor Coding: Actual  
 Desirability

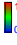


X1 = B: Volume of sample  
 X2 = A: Amount of sorbent

Actual Factors  
 C: Extraction time = 10.00  
 D: Desorption time = 10.00  
 E: Salt effect = 20.00

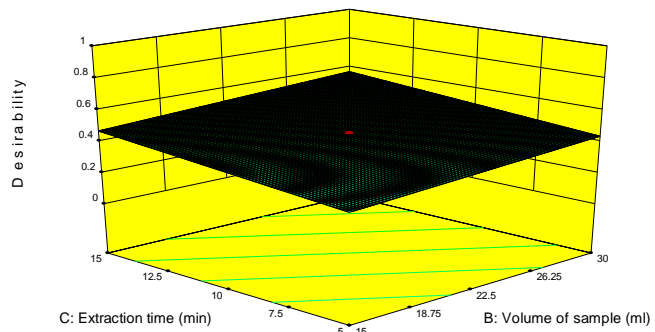


Design-Expert® Software  
 Factor Coding: Actual  
 Desirability

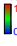


X1 = B: Volume of sample  
 X2 = C: Extraction time

Actual Factors  
 A: Amount of sorbent = 22.50  
 D: Desorption time = 10.00  
 E: Salt effect = 20.00

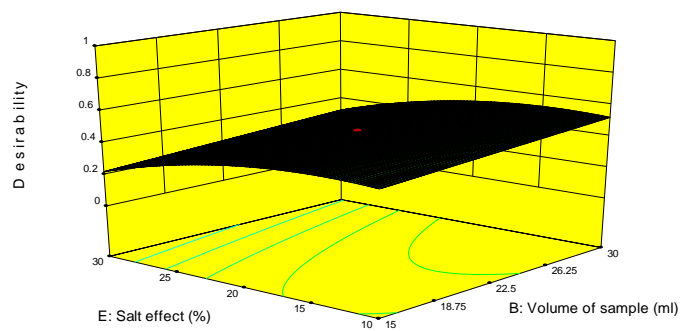


Design-Expert® Software  
 Factor Coding: Actual  
 Desirability



X1 = B: Volume of sample  
 X2 = E: Salt effect

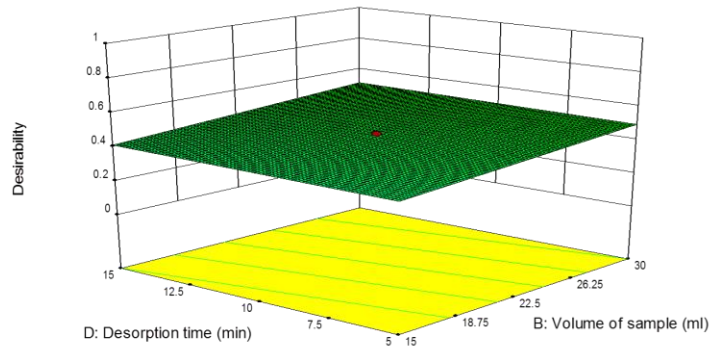
Actual Factors  
 A: Amount of sorbent = 22.50  
 C: Extraction time = 10.00  
 D: Desorption time = 10.00



Design-Expert® Software  
 Factor Coding: Actual  
 Desirability

X1 = B: Volume of sample  
 X2 = D: Desorption time

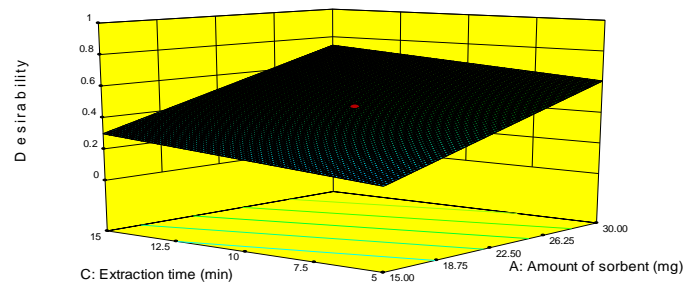
Actual Factors  
 A: Amount of sorbent = 22.50  
 C: Extraction time = 10.00  
 E: Salt effect = 20.00



Design-Expert® Software  
 Factor Coding: Actual  
 Desirability

X1 = A: Amount of sorbent  
 X2 = C: Extraction time

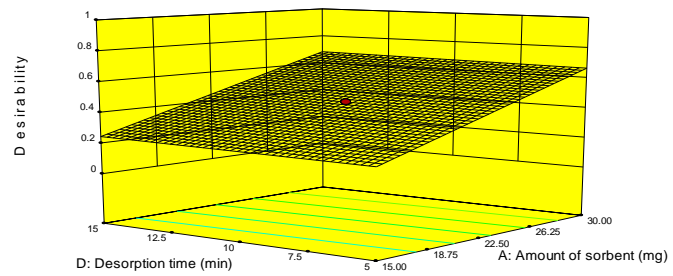
Actual Factors  
 B: Volume of sample = 22.50  
 D: Desorption time = 10.00  
 E: Salt effect = 20.00



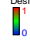
Design-Expert® Software  
 Factor Coding: Actual  
 Desirability

X1 = A: Amount of sorbent  
 X2 = D: Desorption time

Actual Factors  
 B: Volume of sample = 22.50  
 C: Extraction time = 10.00  
 E: Salt effect = 20.00

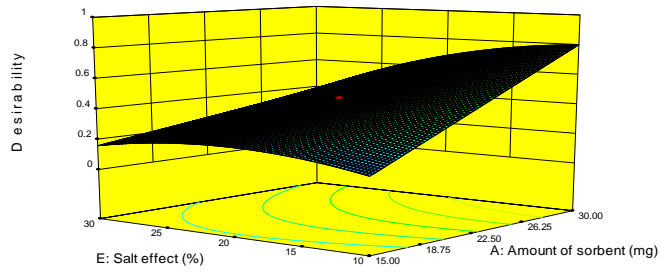


Design-Expert® Software  
 Factor Coding: Actual  
 Desirability

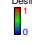


X1 = A: Amount of sorbent  
 X2 = E: Salt effect

Actual Factors  
 B: Volume of sample = 22.50  
 C: Extraction time = 10.00  
 D: Desorption time = 10.00

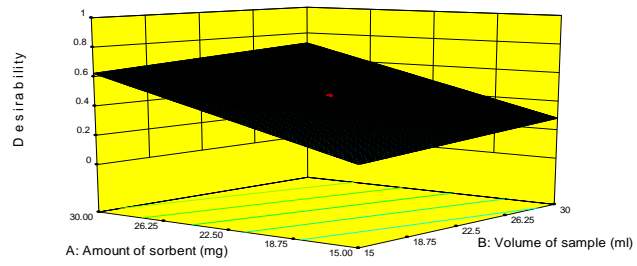


Design-Expert® Software  
 Factor Coding: Actual  
 Desirability

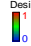


X1 = B: Volume of sample  
 X2 = A: Amount of sorbent

Actual Factors  
 C: Extraction time = 10.00  
 D: Desorption time = 10.00  
 E: Salt effect = 20.00

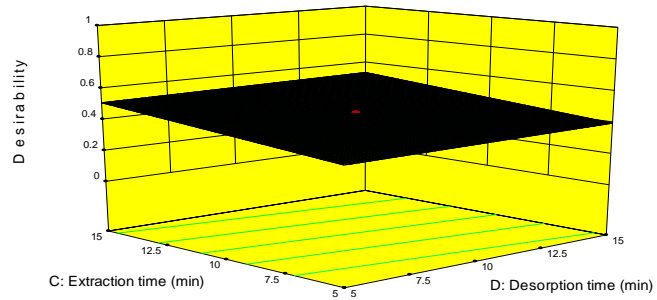


Design-Expert® Software  
 Factor Coding: Actual  
 Desirability



X1 = D: Desorption time  
 X2 = C: Extraction time

Actual Factors  
 A: Amount of sorbent = 22.50  
 B: Volume of sample = 22.50  
 E: Salt effect = 20.00

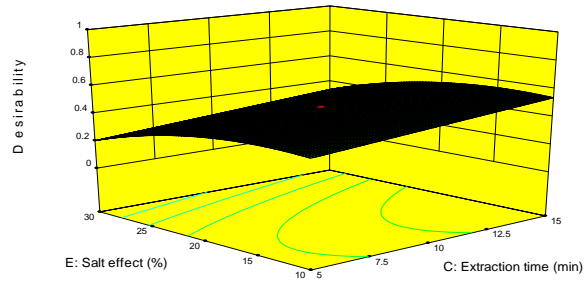


Design-Expert® Software  
Factor Coding: Actual  
Desirability



X1 = C: Extraction time  
X2 = E: Salt effect

Actual Factors  
A: Amount of sorbent = 22.50  
B: Volume of sample = 22.50  
D: Desorption time = 10.00

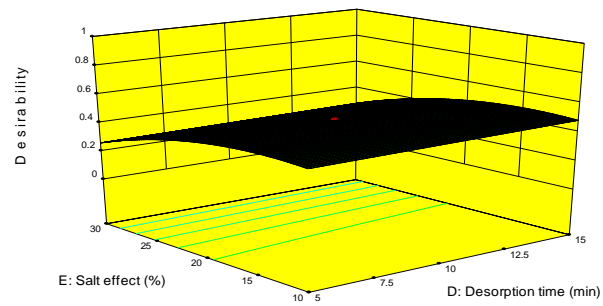


Design-Expert® Software  
Factor Coding: Actual  
Desirability



X1 = D: Desorption time  
X2 = E: Salt effect

Actual Factors  
A: Amount of sorbent = 22.50  
B: Volume of sample = 22.50  
C: Extraction time = 10.00



## Appendix 7

Calibrations curves of NAs in the ranges of 0.1-100 ng/ml and 20 ng/ml IS. (a) NDMA, (b) NDEA, (c) NDPA, (d) NDPA, (e) NDPA, (f) NDPA, (g) NDPA, and (h) NDPA.

